

Ben-Gurion University of the Negev
Faculty of Engineering Sciences
Department of Industrial Engineering and
Management

**Olive Oil Content Prediction Models
based on Image Processing**

Submitted in partial fulfillment of the requirements for the degree of M.Sc. in
Industrial Engineering

By: Tomer Ram

June 2009

Advisors: Prof. Y. Edan, Prof. Z. Wiesman

Ben-Gurion University of the Negev
Faculty of Engineering Sciences
Department of Industrial Engineering and
Management

Olive Oil Content Prediction Models
based on Image Processing

Submitted in partial fulfillment of the requirements for the degree of M.Sc. in
Industrial Engineering

By: Tomer Ram

June 2009

Advisors: Prof. Y. Edan, Prof. Z. Wiesman

Author	<hr/>	Date	<hr/>
Advisor	<hr/>	Date	<hr/>
Advisor	<hr/>	Date	<hr/>
Chairman of Graduate Studies Committee	<hr/>	Date	<hr/>

Acknowledgements

Prof. Yael Edan

Prof. Zeev Weisman

Shahar Laykin

Shahar Nizri

Maxim Spivakovsky

Peer Shoval

Shirly Berman

Yossi Zahavi

Nissim Abuhazira

Abstract

An increase in olive oil content can be achieved by optimizing the harvesting time of the olives in an orchard. In order to determine optimal harvest time, prediction models were developed to determine oil content based on quality features derived from known image processing algorithms.

Digital color photographs were taken of opposing sides of large samples of olives of two varieties – *Picual* and *Souri* – on a weekly basis during the ripening season. In addition, the fallout was collected and weighed weekly during the same period. Quality features such as size, shape, color, and texture were derived from the photographic images of the olives. Low resolution-nuclear magnetic resonance was used for rapid and accurate determination the oil content of each photographed olive. The correlations between the various quality features and oil content were determined. Two prediction models based on linear regressions and artificial neural networks were developed to predict the quantity of oil in individual olives. The sensitivity of the models to different proportions between training and testing sets, the topologies of the networks, and various transfer functions was analyzed. The neural network models were more accurate compared to linear regression, resulting in average linear correlations of 0.81 and 0.87 to the oil quantity in *Picual* and *Souri* olives, respectively.

Keywords: Olive oil, Olive harvesting date, maturity index, prediction models, artificial neural network, image processing

Table of Contents

1. Introduction	12
1.1 Description of the problem	12
1.2 Objectives	13
1.3 Thesis structure	14
2. Literature Review.....	15
2.1 Olive oil industry	15
2.2 Prediction models in agriculture	20
2.3 Artificial Neural Networks	23
2.4 Dimension reduction.....	27
2.5 Machine Vision.....	28
2.6 Low Resolution Nuclear Magnetic Resonance (LR-NMR).....	31
3. Methodology.....	34
3.1 Data collection	34
3.2 Data analysis	36
3.3 Prediction Models	37
3.4 Sensitivity analyses.....	38
4. Results	40
4.1 Data analysis	40
4.2 Prediction models.....	61
4.3 Sensitivity analysis.....	72
4.4 Best prediction model	79
5. Discussion	83
6. Summary and Future Work.....	86
6.1 Summary	86
6.2 Future Work	87
7 .References	89
8. Appendices	95
Appendix A. MLR results.....	95
Appendix B. ANN results	95
Appendix C. ANN software.....	116
Appendix D. Statistical Analysis software	116

Appendix E. Raw data – example.....	117
Appendix F. Abbreviation	118
Appendix G. Weights and biases of best networks.....	119

List of Figures

Figure 1 – Experiment's and analyses' structure	14
Figure 2 - Classes of olives by MI (Mailler et al., 2005).....	17
Figure 3– Olive oil percentage vs. number growing weeks (Vossen, 2004)	18
Figure 4– Color and polyphenol level during growing season (Vossen, 2004).....	19
Figure 5– Structure of a neural network (Kaul et al., 2005)	24
Figure 6– Fixed illumination photo cell.....	34
Figure 7– Picture of one sample - a group of 10 olives	35
Figure 8– Average oil content and average Oil percent vs. sampling time – <i>Picual</i> ...	41
Figure 9– Average weight vs. sampling time - <i>Picual</i>	41
Figure 10– Average oil content and avearge oil percent vs. sampling time – <i>Souri</i> ...	42
Figure 11 - Average weight vs. sampling time – <i>Souri</i>	42
Figure 12– Fallout and oil content vs. sampling time – <i>Souri</i>	43
Figure 13 - Fallout vs. color distribution – <i>Souri</i>	43
Figure 14– Eigenvalues of extracted components - <i>Picual</i>	58
Figure 15– Eigenvalues of extracted components - <i>Souri</i>	58
Figure 16 - Results of MLR with different proportions between training and testing - <i>Picual</i>	72
Figure 17- Results of MLR with different proportions between training and testing - <i>Souri</i>	73
Figure 18 – Results of ANNs with different proportion between trainnig validation and testing – <i>Picual</i>	74
Figure 19 – Results of ANNs with different proportion between trainnig validation and testing – <i>Souri</i>	75
Figure 20 - Results of ANNs in different topologies (Input, Hidden and Output) - <i>Picual</i>	76
Figure 21 - Results of ANNs in different topologies (Input, Hidden and Output) - <i>Souri</i>	77
Figure 22 – Results of different transfer functions – <i>Picual</i>	78
Figure 23 – Results of different transfer functions – <i>Souri</i>	79
Figure 24 – Structure of best model - <i>Picual</i>	80
Figure 25 – Structure of best model - <i>Souri</i>	81
Figure 26 – Regression between best model prediction and actual values - <i>Picual</i>	82

Figure 27 – Regression between best model prediction and actual values - *Souri*.....82

List of Tables

Table 1 - Characteristics of the primary world olive oil cultivars (Vossen, 2004).....	16
Table 2 - Examples of features extracted by imaging and NIR sensors	22
Table 3- Examples of food science ANN applications.....	26
Table 4 – Examples of application of NMR in food and agriculture.....	32
Table 5–Features derived by the image processing algorithms	36
Table 6 - Results of paired T test of the difference between <i>Picual</i> image features of opposite sides.....	45
Table 7 - Results of paired T test of the difference between <i>Souri</i> image features of opposite sides	46
Table 8 – R values of regression models	47
Table 9 – Descriptive statistic of oil amount	47
Table 10 – ANOVA variance analysis of oil amount table	47
Table 11 - MLR results of models for each variety separately & together.....	48
Table 12- Descriptive statistics of image features – <i>Picual</i>	49
Table 13 – Descriptive statistics of image features - <i>Souri</i>	50
Table 14 – Coefficients table of MLR model of <i>Picual</i> variety	51
Table 15 – Coefficients table of MLR model <i>Souri</i> variety	52
Table 16 – Correlation table - Picual	53
Table 17 – Correlation table - Souri	54
Table 18 – Variance explained by extracted component – <i>Picual</i>	56
Table 19 – Variance explained by extracted component t – <i>Souri</i>	57
Table 20 – Significance of extracted factors – <i>Picual</i>	59
Table 21 – Significance of extracted factors – <i>Souri</i>	60
Table 22- Original data set MLR results - <i>Picual</i>	61
Table 23- Stepwise MLR results - <i>Picual</i>	62
Table 24– Selected model by stepwise – <i>Picual</i>	64
Table 25 - FA set MLR results - <i>Picual</i>	64
Table 26– Best FA MLR model – <i>Picual</i>	64
Table 27 - Original data set MLR results - <i>Souri</i>	65
Table 28- Stepwise MLR results - <i>Souri</i>	66
Table 29– Selected model by stepwise – <i>Souri</i>	68
Table 30- FA set MLR results - <i>Souri</i>	68

Table 31– Best FA MLR model – <i>Souri</i>	69
Table 32- Original data set ANN results - <i>Picual</i>	69
Table 33- Results of ANN model based on stepwise selected features - <i>Picual</i>	69
Table 34- FA set ANN results - <i>Picual</i>	70
Table 35 - Original data set ANN results - <i>Souri</i>	70
Table 36- Results of ANN model based on stepwise selected features - <i>Souri</i>	70
Table 37- FA set ANN results - <i>Souri</i>	71
Table 38 - Average standard errors.....	71

List of Abbreviations

- ANN – Artificial Neural Network
- NIR – Analysis of variance
- MLR – Multiple Linear Regression
- PCA – Principal Component Analysis
- LR-NMR – Low Resolution Nuclear Magnetic Resonance
- ANOVA – Analysis of Variance
- MI – Maturity Index
- FW – Fresh Weight
- FRF – Fruit Removal Force
- IOOC – International Olive Oil Council
- FA - Factor Analysis
- MSE – Mean Root Square

1. Introduction

1.1 Description of the problem

The world olive oil production grew from 1,828,200 tons in 1990 to 2,314,200 tons in 2000, which reflects an annual growth of 2.3% (Luchetti, 2002). Assuming a price of 5 Euro per KG, the total revenue in the olive industry is over 10 billion Euros annually. This fact creates a significant economic drive for more efficient production. Over 95% of the olive oil is produced in the Mediterranean basin, with Spain the world biggest producer with a market share of 33% (Luchetti, 2002). The health related attributes of the olive oil together with the healthy nutrition trend of the last decade creates demand all over the world, even in nontraditional consumer countries such as Japan and U.S.A (Morello et al., 2006). The consumption of olive oil in the U.S. grew in 65% from 1996 to 2003 which made it the fourth biggest consumer in the world (Mili, 2004). However, the average consumption is only 0.7 Liter/person which is relatively low compare to 13-15 Liter/person in Italy and Spain, the world biggest consumers (Vossen, 2007). This fact can imply on the growth potential in the consumption in the coming years.

More efficient production of the olive oil will generate significant extra income for producers. One of the options to improve efficiency is by increasing the amount of oil extracted from the fruit per land unit. The amount of oil in the fruit is determined by many characteristics like cultivar, irrigation, soil and climate (Vossen, 2004). Most of these factors are hard to change once the trees are planted. However, harvest time can be easily adjusted to meet the optimal point and by that improving the olive oil quality and quantity significantly (Mailer et al., 2005).

Vossen (2004) reviewed the development of oil in olives along the ripening season. He mentions that oil starts to accumulate in the fruit after 10 weeks from the beginning of the season. The increase is very rapid in the first 12 weeks, until it reaches a certain level which remains constant until the fruit rotten or drop from the tree. He also refers to the common deception of increasing in the oil percent while the fruits become shriveled due to loss of moisture, but the total amount of oil does not change. Moreover, there are oil quality changes along the ripening season, and in particular the level of polyphenols might have major influence on the oxidation rate

level of the oil. This component reaches its maximum level when the fruit starts to change its color from yellow to purple and from then on rapidly decreases. Olive oil rich with polyphenols has a longer shelf life and higher nutrition quality (Vossen, 2007).

Experiments have shown correlation between the appearance of the fruit to the amount and quality of oil that can be extracted from it (Salvador et al., 2001). The color of the fruit can be used as an indicator for the fruit ripeness which has significant influence on the oil content and quality of the olive (Vossen, 2004). To estimate the best harvest time growers use the Maturation Index (MI) published by the International Olive Oil Council (IOOC) (Mailer et al., 2005). This index is calculated by classifying 100 randomly picked olives into 7 groups by their color, from green to black with 1 corresponding to green olives and 7 to black. The sum of the values of all olives divided by 100 will generate the MI (Mailer et al., 2005). The MI appeared to be inaccurate in many cases and changed dramatically between cultivars and between seasons (Mailer et al., 2005; Salvador et al., 2001). Another problem of this technique is inconsistency of humans in the classification of olives by color due to physical related factors like fatigue (Diaz et al., 2000). A better technique to determine the optimal harvest time will probably lead to improvement in the olive oil yield.

Computer vision holds great potential and benefits for the agriculture industry because of its simplicity, low cost, rapid inspection rate and broad range of applications (Chen et al., 2002). It provides accurate, consistent information and has been applied successfully in agriculture (Diaz et al., 2000). Zheng et al. (2006) divided the information that can be achieved by machine vision to 4 categories: color, size, shape and texture. Each category is used for different applications but the combination of some categories can reveal quality attributes that cannot be identified by any single one of them. Color is the most important category employed frequently in quality evaluation in food industry (Cheng et al., 2006). Computer vision was successfully used to classify table olives by different quality parameters, and presented better results as compared to human performances (Diaz et al., 2000; Laykin et al., 2008).

1.2 Objectives

This study is a part of a larger research which aims to develop a tool for finding the optimal harvesting time of olive groves. Such a tool if developed successfully can be

used as a decision making supporting tool for olive growers all over the world and can have a major economic potential.

The purpose of this research is to develop prediction models to determine accurately and repetitively the oil content of intact olives based on quality features derived from computer vision system. The specific objectives are to:

- (a) Develop a prediction model for the oil content based on features extracted from images of *Souri* and *Picual* olives.
- (b) Analyze models' compatibility to different varieties.
- (c) Analyze models' compatibility to different conditions.

1.3 Thesis structure

The thesis starts with a literature review (chapter 2) which contains a description of: (2.1) olive oil industry, (2.2) prediction models in agricultures, (2.3) Machine vision and its applications in agriculture, (2.4) LR-NMR and its applications in agriculture and (2.5) ANN and its applications in agriculture. The methodology of the research is described in chapter 3 and is illustrated in Figure 1. The results can be found in chapter 4 followed by discussion and summary in chapter 5 and chapter 6 respectively.

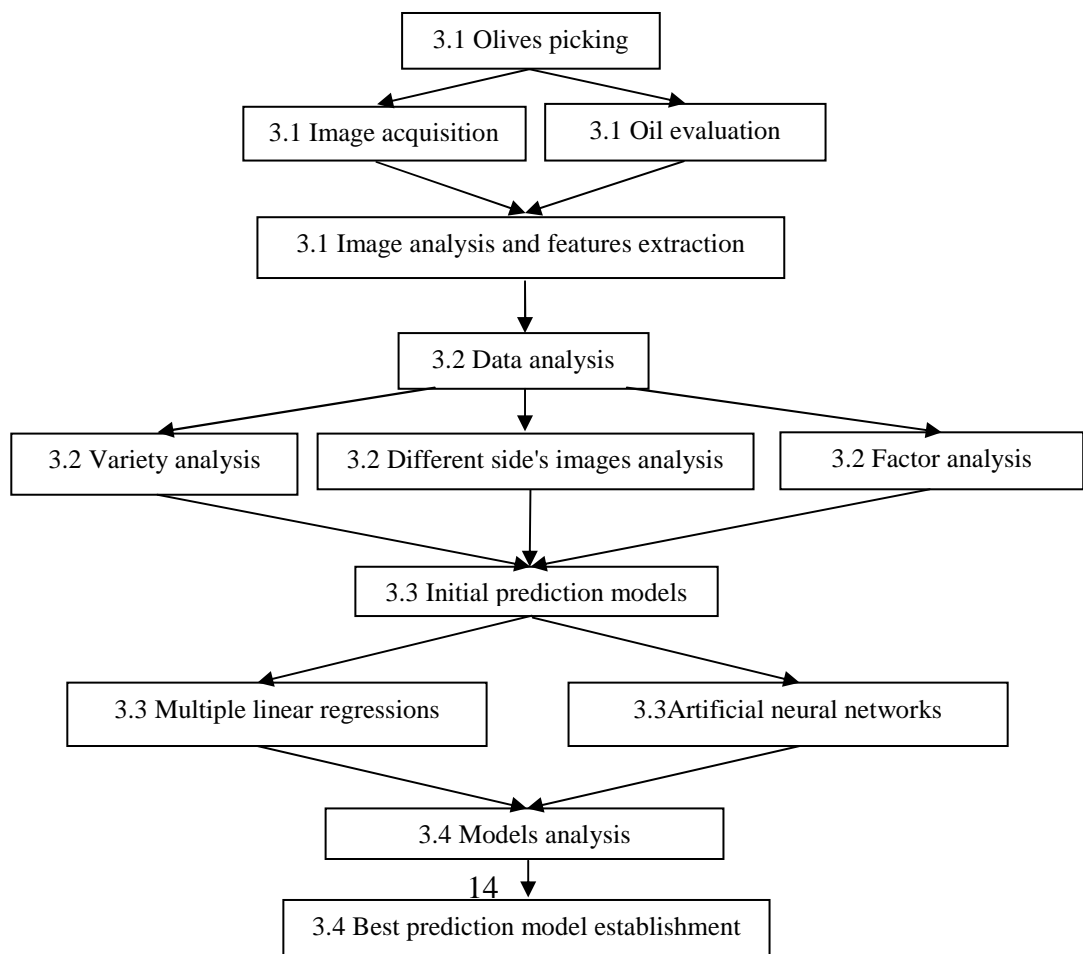


Figure 1 – Experiment's and analyses' structure

2. Literature Review

2.1 Olive oil industry

The olive oil industry is estimated in over 10 billion Euros per year, where about 95% of the production produces is in the Mediterranean basin (Luchetti, 2002). Almost all of the olive oil in the world is produced on about 24 million acres in the countries surrounding the Mediterranean (Morello et al., 2006). The big three producers, Spain, Italy, and Greece, produce about 75% of the world's olive oil (Mili, 2004). The other European, North African, and Middle Eastern countries produce about 20%, and the new world countries of Argentina, Australia, Chile, South Africa, New Zealand, and the USA produce the remaining 5% (Mili, 2004). "A counting interest in Mediterranean cuisine and promotion by the controlling body of the industry and the international Olive Oil Council have stimulated market demand for olive oil particularly in countries not traditionally associated with this oil, such as United States and Japan" (Morello et al., 2006).

"There are six olive oil Appellations of Controlled Origin (ACO) in Spain: *Barnea*, *Les Garrigues*, *Priego de C'ordoba*, *Sierra M'agina*, *Sierra de Segura* and *Siurana*" (Rial, 2003). The predominant variety of olive is *Picual*, with average annual yields of 142,000 t of olives producing 30,000 t of olive oil (Rial, 2003). This ACO has the highest rate of production and covers the largest area in Spain (Rial, 2003).

"Virgin olive oils are oils obtained from the fruit of the olive tree solely by mechanical or other physical means under conditions, particularly thermal, that do not lead alterations in the oil, and furthermore, these oils have not undergone any treatment other than washing decantation, centrifugation and filtration" (Morello et al., 2006).

The flavor of the olive oil changes dramatically according to the color at the time the olives were harvested (Vossen, 2004). Olives harvested early when they are still green or just turning yellow to red are characterized as having herbaceous flavor characteristics such as fresh grass, herbal, artichoke, nettle, mint, tomato leaf, etc (Vossen, 2004). Early harvested fruit is also much more bitter and pungent, because it is higher in polyphenols (Vossen, 2004). Later harvested fruits that when the colors are changing from red to black yeild oils that are much less bitter and pungent (Vossen, 2004). Fully mature olives yield oils in flavors that are often described as floral, buttery, nutty, apple, banana, berry, or tropical (Vossen, 2004).

Table 1 - Characteristics of the primary world olive oil cultivars (Vossen, 2004)

CULTIVAR	-% OIL	COLD HARDINESS	FRUIT SIZE	POLYPHENOL CONTENT	POLLINIZER VARIETIES
Aglandau	23-27	Hardy	Medium	Medium	Self compatible
Arbequina	22-27	Hardy	Small	Low	Self compatible
Arbosana	22-27	Hardy	Small	Medium	Self compatible
Barnea	16-26	-	Medium	Medium	Self - Manzanillo - Picholine
Bosana	18-28	-	Medium	High	T de Cagliari - Pizzé Carroga
Chemlali	26-28	-	V Small	High	Self compatible
Coratina	23-27	Hardy	Medium	Very High	Self - Ogliarola
Cornicabra	23-27	Hardy	Medium	Very High	Self compatible
Empeltre	18-25	Sensitive	Medium	Medium	Self - Arbequina
Frantoio	23-26	Sensitive	Medium	Medium-High	Pendolino - Leccino
Hojiblanca	18-26	Hardy	Large	Medium	Self compatible
Koroneiki	24-28	Sensitive	V Small	Very High	Mastoides
Lechin Sevilla	22-23	-	Medium	Medium	Hojiblanca - Picual
Leccino	22-27	Hardy	Medium	Medium	Frantoio - Pendolino
Manzanillo	15-26	Sensitive	Large	High	Sevillano - Ascolano
Moraiolo	18-28	Sensitive	Small	Very High	Pendolino - Maurino
Picudo	22-24	Hardy	Large	Low	Hojiblanca - Picual
Picual	24-27	Hardy	Medium	Very High	Self - Picudo
Picholine	22-25	Moderate	Medium	High	Self - Aglandau
P. Marocaine	22-25	Hardy	Medium	High	Self - P. Languedoc
Taggiasca	22-27	Sensitive	Medium	Low	Self compatible
Verdal Huevar	24-26	Hardy	Medium	High	Manzanilla - Gordal

The maturation of olive fruits last several months, and development varies according to the growing area, olive variety, temperature and cultural practices (Salvador et al., 2001). In order to obtain a “characteristically fragrant and delicately flavored olive oil, it is therefore imperative that it is properly extracted from undamaged fruits at its best degree of ripeness” (Salvador et al., 2001).

Various methods have been proposed for expressing the stage of maturity of olives. Among them the International Olive Oil Council (IOOC) has suggested a simple technique which is based on the assessment of colour of skins of 100 olives which are randomly drawn from 1 Kg of the sample (Mailer et al., 2005). The drawn olives are manually classified into 7 groups by the colour of their flesh and skin (Figure 2). Then a Maturity Index (MI) is calculated (Mailer et al., 2005). The MI appeared to be inaccurate in many cases and changed dramatically between cultivars and between seasons (Mailer et al., 2005; Mailer et al., 2005). Another problem of this technique is inconsistency of humans in the classification of olives by colour due to physical related factors like fatigue (Diaz et al., 2000). A better technique to determine the optimum harvest will probably lead to yield improvement.

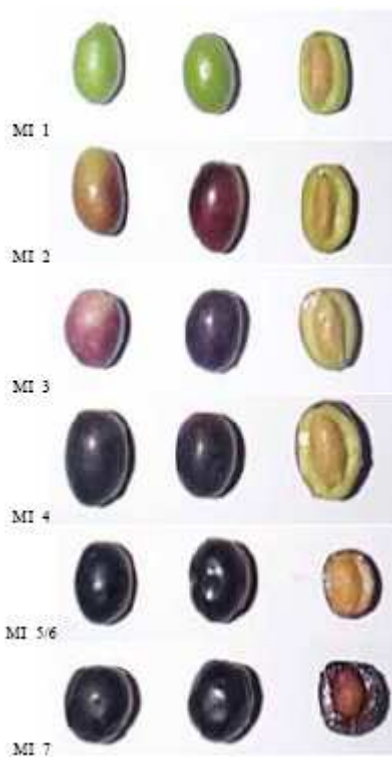


Figure 2 - Classes of olives by MI (Mailler et al., 2005)

Salvador et al. (2001) studied several analytical parameters which have significant influence on the oil's quality such as free acidity, peroxide value, stability and sensory of 'Cornicabra' olives. They found that the best ripeness stage would be when the MI is from 3 to 4.5. They also found out that the olive oil industry of Castilla-La Mancha usually harvests 'Cornicabra' olives when the MI is greater than 5, assuming traditionally that the oil extraction yield always increases with maturity (Salvador et al, 2001).

Mailer et al (2005) and *Bertlan et al.* (2004) studied the optimal harvesting time of several olive varieties in relation to the MI. They found significant changes in optimal MI between cultivars between and between seasons. These studies emphasize the necessity of accurate analytical tools for harvest time determination.

"Oil synthesis and accumulation in the olive fruit occurs over about 34 weeks (Figure 3), begins about 10 weeks into the growing season, increases steeply up until fruit maturity (color change and softening) then, the rate of accumulation reduces, but still continues" (Vossen, 2004). "It seems like there is a much larger increase than there really is late in the fruit-ripening season due to the loss of moisture in the fruit" (Vossen, 2004). "When the fruit becomes very over-ripe, oil synthesis stops completely" (Vossen, 2004).

The first stage of ripening is called the 'green stage' corresponding to green mature fruits that have reached their final size, afterwards, chlorophyll pigments in the olive skin are progressively replaced by anthocyanines during fruit ripening (Morello et al., 2006). This process causes the fruit to change its color and makes it possible to identify a 'spotted stage', a 'purple stage' and a 'black stage' according to the skin color of the fruits (Morello et al., 2006)

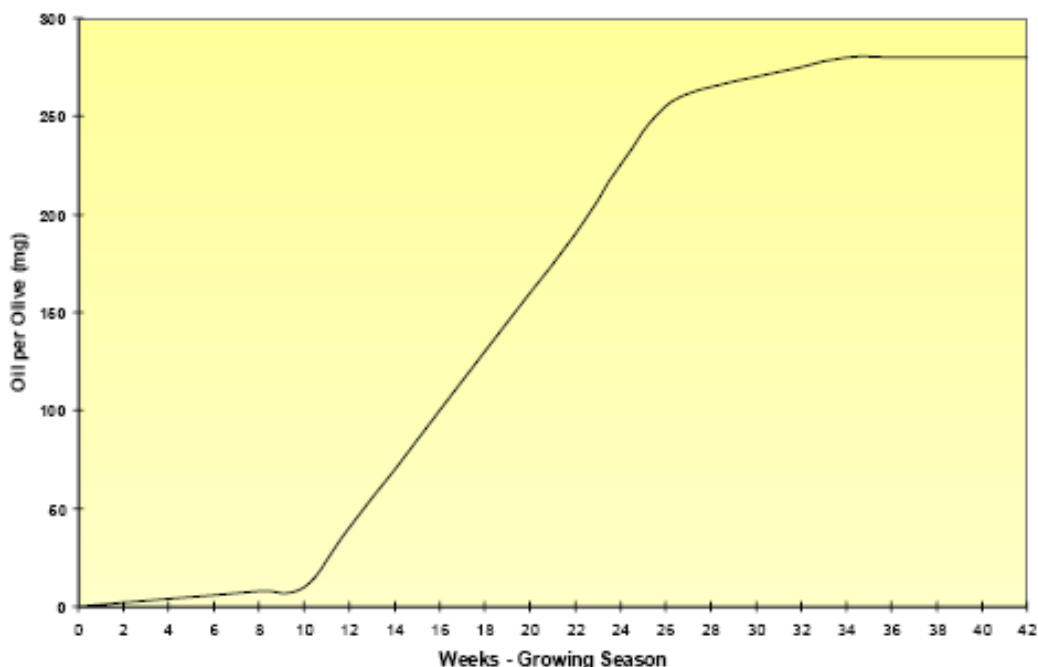


Figure 3– Olive oil percentage vs. number growing weeks (Vossen, 2004)

Polyphenol is a component that significantly decreases the oxidation rate of the olive oil (Vossen, 2004). Olive oil rich in polyphenols have longer shelf life and higher nutrition quality (Vossen, 2007). During the growth of the olive fruits along the season, the content of polyphenols gradually increases and reaches a maximum level when the fruit skin begins to change its color from light green to yellow and purple (Figure 4) (Vossen, 2004). When the fruit is completely ripened and the color spread all the way to the pit the content of polyphenols and most of the other flavor components of the fruit decline within 2-5 weeks (Vossen, 2004). These facts can imply on the strong connection between the color of the olive and maturity level.

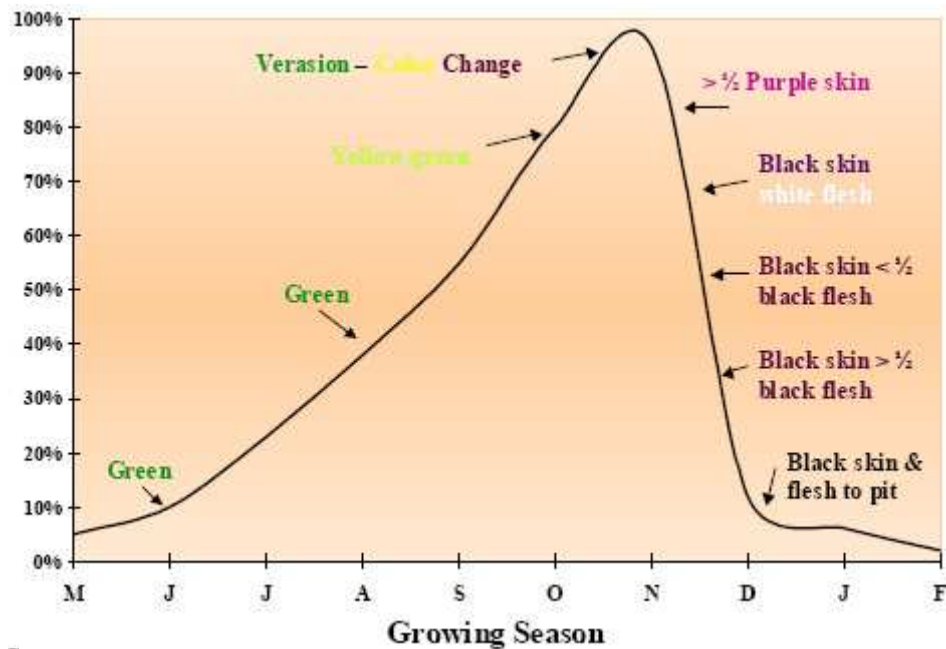


Figure 4– Color and polyphenol level during growing season (Vossen, 2004)

Studies have shown that olive oil quality of any variety can be completely changed by either harvesting the fruit green (unripe) or mature (ripe) (Slavador et al., 2001; Mailer et al., 2005; Beltran et al., 2004)). The range in between those two extremes still can have a big influence on the style of oil produced (Slavador et al., 2001). Some producers believe that maturity can even have a greater influence on quality than the variety itself (Slavador et al., 2001).

For any given variety there is probably no more than about two to three weeks of ideal harvest period to capture its maximum oil potential (Slavador et al., 2001). An increase of 5 g of oil per 100 g of dry olive could easily be obtained by choosing an appropriate maturation stage before processing (Slavador et al., 2001).

Romero et al. (2002) studied the evolution of oil content and quality in Arbequina olives along the ripening period. They investigated the changes in fruit removal force (FRF), fresh weight (FW), maturity index (MI) and color distribution. Results indicated that the MI was not a suitable indicator for oil quality and quantity assessment, while color distribution was a better indicator for the beginning of harvest period. While FRF alone showed no relation with the oil content, the FRF/W was significantly correlating with it.

Undoubtedly the content of the oil in the olive fruits is influenced by many factors such as variety, climate, soil mineral content, sunlight intensity, rainfall, and irrigation

(Mailer et al., 2005). But, among all the harvest time is probably the easiest and the cheapest to adjust in order to maximize the oil potential.

2.2 Prediction models in agriculture

Predicting the optimal action time is a great challenge in different agricultural fields (Machado el al., 2004, Lotze & Bergh, 2004) due to the complexity embedded in biological systems because of the inherent variability and unknown external conditions. There are usually several influencing factors with mutual effects (Kominakis et al., 2002; Carvajal & Nebot, 1998). This combined with changing external conditions (Kominakis et al., 2002) makes it hard to implement prediction techniques used in other known industries.

Prediction models are used in several agriculture applications. *Carvajal* (1998) built a growth model of white shrimps based on Fuzzy Inductive Reasoning (FIR) which showed major advantaged over linear regression. *Salehi* (1998) improved the prediction of dairy yield by using record classifier combined with artificial neural network.

Lotze & Bergh (2004) developed a model to predict the size of apples at harvest time. They were able to predict the final fruits size distribution by linear regression based model. They developed different model for each cultivar in each area due to differences in climates conditions.

2.2.1 Quality and yield prediction models - The market shows an increasing demand for accurate predictions of yield and quality (Marcelis & Gijzen, 1998). Moreover, yield predictions can be used to estimate the labor requirement for the harvest (Marcelis & Gijzen, 1998). The increasing need to lower cost of production and the growing complexity of commercial competition increases the value and benefit of research and development related to precision agriculture and automation (Abdullah & Guan, 2002).

Abdullah & Guan (2002) determined the degree of ripeness of oil palm fruits, using machine vision. In their experiment, they used multivariate discriminant analysis to classify the fruits into 4 degrees of ripeness. The results showed 90% matching with human experts' classification. Difficulty in assigning colors for samples whose discriminant scores located near discrimination boundaries was the main source of error.

Machado et al. (2004) investigated the optimal harvest time of tomatoes. They found out that the yield of tomatoes field in relation to weight of marketable fruits is bell shaped, when in the beginning of season the weight of unripe fruits is high then more and more fruits are becoming marketable, but also some fruit becoming over ripe and cannot be sold. In their research, they developed a model that can predict the maximum point of the bell shaped curve based on the maximum day temperature over the growing season. The model was based on polynomial regression of each group of fruits (i.e. unripe, ripe and over ripe). The results varied between different regions of tomatoes fields, and the average R^2 of the regressions was 0.886.

Schmilovich et al. (1999) developed a method to predict the optimal harvest time of fresh dates by using Near Infra Red spectroscopy. The results of the NIR spectroscopy were analyzed to determine the content of sugar and water in the fruit which known to have major influence on the ripening of the dates. Each of the dates was scanned for its NIR spectrum and then its level of sugar and water were evaluated by conventional means (which are destructive and time consuming). Finally, a model was obtained based on the first derivative of the spectrum that represented in the best way the correlation between the NIR spectroscopy results and the actual results. The standard error was less than 1%.

2.2.2 Sensors used in agriculture applications - Sensors are widely used in agricultural technologies. There are simple and known sensors such as thermometers, rainfall meters and humidity sensors which are used to sense the external conditions. *Hueso et al.* (2006) used a thermometer to measure the daily air temperature and developed a prediction model for loquat harvest time. *Marcelis & Gijzen* (1998) used the temperature and the humidity values in the greenhouse as one of many inputs for a yield prediction model of cucumbers.

There are also more sophisticated techniques used as sensors in agriculture. *Taurino et al.* (2002) used a semiconductor thin film based sensor for discrimination of different olive oils. They used it to discriminate commercial oil from the local products. *Cosio et al.* (2006) used an electronic nose and tongue to identify geographical origin of olive oils. Electronic nose was also used by *Martin et al.*, (2001) to characterize different vegetable oils.

Schmilovich et al. (1999) used Near Infrared (NIR) spectrometer to develop a system for maturity determination of dates. *Saranwong et al.* (2004) used NIR sensors to predict the ripening stage of mangos.

The digital camera is a common sensor for many agriculture applications and has been widely applied for quality sorting of tomatoes (Laykin et al., 2002), classify ripening bananas (Mendoza & Aguilera, 2004) and detection of defects in citrus (Blasco et al., 2007).

The development of the new sensing techniques had triggered the development of novel prediction methods such as artificial neural networks (Kominakis et al., 2002; Salehi et al., 1998; Grzesiak et al., 2006), fuzzy logic (Salehi et al., 2002; Carvajal et al., 1997) and Mahalanobis distance (Diaz et al., 2004).

2.2.3 Features for classification and sorting – One of the common usages of sensors in agriculture is for collecting physical information about the agriculture product. The collected information is analyzed and quantitative features are extracted. The features are then used to establish a mathematical model to predict or estimate the quality of the product. Table 2 shows examples of features extracted by imaging sensors for several sorting and classification applications.

Table 2 - Examples of features extracted by imaging and NIR sensors

Purpose	Extracted features	Sensor	Reference
Ripened bananas sorting	L, a, b, brown area percentage, number of brown spots per cm ² , homogeneity, correlation, entropy	Digital camera	Mendoza & Aguilera, 2004
Orange sorting	Height width ratio, roughness, R, G, Feret's diameter, texture	Digital camera	Kondo et al., 2000
Tomatoes classification	Color, color homogeneity, defects, shape	Digital camera	Laykin et al., 2002
Watermelons quality determination	Weight, Height, Internal defects, Sugar content, soluble solid contents	NIR spectrometer	Lee et al., 2008
Pickling cucumbers	Intensity reflectance of	NIR	Ariana et al.,

classification	wavelength in range of 950-1650 nm	spectrometer	2006
Olive classification	Size , Shape, Texture, Color, Defects	Digital camera	Laykin et al., 2008
Potato classification	Intensity reflectance of wavelength in range of 450-870 nm	Digital camera and multispectral sensor	Noordam et al., 2005
Cherry classification	Intensity reflectance of wavelength in range of 680-1280 nm	NIR spectrometer	Guyer & Yang, 2000

2.3 Artificial Neural Networks

"Artificial Neural Networks (ANNs) are a set of technologies often encompassed with artificial intelligence that attempt to simulate the function of the human brain." (Haung et al., 2007). The rapid development of rapid algorithms and computer technologies was the driving force of wide applications of ANNs in research and routine life (Haung et al., 2007). The common uses of ANNs are in process control, medical diagnosis, forensic analysis, weather forecasting, financial applications and investments analysis (Haung et al., 2007). The application of ANNs in the field of food science is still in early development stages (Haung et al., 2007).

The ANN technique is a powerful empirical modeling approach (Kaul et al., 2005). The ANNs may able to efficiently solve some difficult data analysis that conventional methods cannot accomplish (Haung et al., 2007). It is specially suited for nonlinear problems. The main advantage of this method is its ability to analyze complex problems without understanding the underline characteristics (Haung et al., 2007).

Biological systems are known to be complex due to inherent variability and unknown external condition (Kominakis et al., 2002). There are usually several influencing factors with mutual effects (Kominakis et al., 2002; Carvajal & Nebot, 1998). This combined with changing external conditions (Kominakis et al., 2002) makes it hard to implement prediction techniques used in other known industries. These facts make the ANN method suitable technique for such tasks.

Neural networks are simple models of the way the nervous system operates. The basic units are neurons, which are typically organized into layers, as shown in Figure 5.

Each neuron in ANN receives a set of input information (x_i) connected to a weight factor (w_i). All the values connected to neuron are summed and passes to a transfer function to generate an output. The output information is then sent to another neuron as input or used directly as the ANN result. The weights are referred as the connection strength between the neurons and can imply on the importance of each input. The weights are adjusted during the training of the network according to the training target, which is mostly minimizing the Mean Standard Error (MSE, Haung et al., 2007).

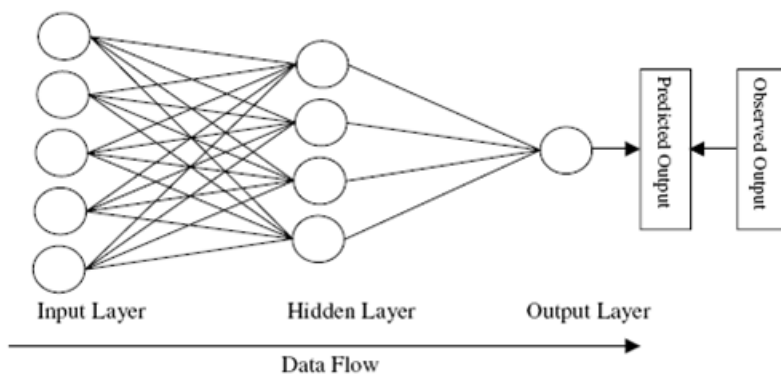


Figure 5– Structure of a neural network (Kaul et al., 2005)

Neurons in one layer send output information to the next layer and may sometimes receive information back from the next layer. ANNs which have neurons that send information back are called feedback networks in contrary to feed-forward networks which only send information forward. One of the most commonly used networks is a three layer feed-forward network (Haung et al., 2007) as seen in Figure 5. The input layer receives input information from an input file and passes the information to the next layer (the input layer usually does not process the information), and then the information is processed by the transfer function and sent as output. The hidden layer is in between the input layer and the output layer. Generally one hidden layer is sufficient for a network, although more than one hidden layer may be used for complicated applications. Knight (1990) found out that that increasing the hidden layer neurons increases greatly the possibility of over fitting which leads to poor generalization of the network.

The learning process can be either supervised or unsupervised. Supervised learning requires output set as targets and it is the common learning process (Haung et al.,

2007). The back-propagation algorithm is the most common supervised learning process and usually used to train feed-forward networks (Haung et al., 2007). In back-propagation training information from the input layer is fed forward through the hidden layers to the output layer, and output error is back propagating through the hidden layers to the input layer (Haung et al., 2007). The weights are adjusted to minimize the error function such as MSE (Haung et al., 2007).

The sum weighted input is passed to a transfer function to generate the output information which can be linear or non linear (Haung et al., 2007). The most commonly used transfer function is the log sigmoid which perform:

$\frac{1}{(1+\exp(-(\sum w_i))}$ (Vogl et al., 1988). Also used frequently as transfer function is the

tangents sigmoid which perform $\frac{2}{(1+\exp(-2(\sum w_i))} - 1$ (Vogl et al., 1988). Linear transfer function is usually a pure line which performs: $b + a\sum w_i$.

The weight adjustment is normally conducted in a way that always decreases the output error $\varepsilon = \frac{1}{n} \sum_{i=1}^n (O_f - \tilde{O}_f)^2$ (Haung et al., 2007). Where O_f is the target output and \tilde{O}_f is the output prediction. The weight adjustment is expressed as

$\Delta W_{ab} = k \frac{\partial \varepsilon}{\partial W_{ab}} = \eta \delta_b x_a$ where η is the learning rate, $\delta_i = (\tilde{O}_i - O_i)[O_i(1-O_i)]$ (for output neurons) and $\delta_j = O_j(1-O_j) \sum_{i=1}^m (\delta_i W_{ji})$ for all other neurons (Haung et al., 2007).

The settings of the learning rates are important for computational speed (Haung et al., 2007). The use of smaller learning rates usually yields acceptable results but needs longer training time because of the larger amount of updating steps (Haung et al., 2007).

Initially, all weights are assigned a random value. The network learns through training. Examples for which the output is known are repeatedly presented to the network, and the answers it gives are compared to the known outcomes. Information from this comparison is back propagating through the network, gradually changing the weights. As training progresses, the network becomes increasingly accurate in replicating the known outcomes. In order to prevent over fitting, the network's performance is tested on a validation set after each iteration. The validation set is

randomly drawn from the data set and is not used in the training process. If the accuracy of the prediction has improved, additional iterations are conducted, and if there is no improvement training is stopped (Bishop, 1995). Eventually, the network is tested on a testing set which was randomly drawn from the data set before the training process and is used to predict the accuracy of the prediction in future cases.

"Machine perception is one of the most promising application areas of ANNs in the field of food science with the most significant being machine vision and electronic nose, which have been embraced by some as revolution in sensory analysis" (Haung et al., 2007). The applications of ANNs in the food science are shown in the following table:

Table 3- Examples of food science ANN applications

Field	Prediction purpose	Methods	Results	Reference
Quality control	Nuts classification	Decision tree and ANN	94.8%, 87.1%	Ghazanfari et al., 1997
Quality control	Orange and Eggplants classification	ANN	74%-94%	Kanali et al., 1998
Quality control	Detect cherry defects	Genetic ANN	73%	Guyer & Yang, 2000
Component prediction	Sugar and acid content in Oranges	ANN	90%, 91%	Komdo et al., 2000
Quality control	Olive oil classifications	ANN	96%	Angerosa et al., 1996
Physical properties	Wheat milling criteria	ANN	98%	Fang et al., 1998
Quality control	Eggplants classification	ANN and Minimum distance classifier	71.9% - 91.5%	Saito et al., 2003
Yield prediction	Corn and soybean yield	MLR and ANN	87.7%-90%	Kaul et al., 2005

2.4 Dimension reduction

Dimension reduction is the process of reducing the number of random variables (features) under consideration. This process is sometimes referred as features extraction which means extracting the multidimensional space into a space of fewer dimensions. The main idea of this process is to choose a subset of input variables by eliminating features with little or no predictive information (Kim et al., 2003).

The main linear technique for dimensionality reduction is principal components analysis (PCA), which performs a linear mapping of the data to a lower dimensional space in such a way, that the variance of the data in the low-dimensional representation is maximized. In practice, the correlation matrix of the data is constructed and the eigenvectors on this matrix are computed. The eigenvectors that correspond to the largest eigenvalues (the principal components) can now be used to reconstruct a large fraction of the variance of the original data.

Multi-collinearity is a statistical phenomenon in which two or more predictor variables in a multiple regression model are highly correlated. In this situation the coefficient estimates may change erratically in response to small changes in the model or the data.

One of the solutions for such phenomenon is PCA which ensure orthogonal and uncorrelated set of components (Guo et al., 2002).

The produced components are a linear combination of the original features, and the connection between them is not obvious. Factor analysis can be performed in order to extract knowledge from the new component by rotating the axes. There are varies methods for rotations such as (Harman, 1976): VariMax, Quartimax, ProMax, Equamax and direct oblimin. Some of the methods leave the axes orthogonal such as VariMax, Quartimax and Equamax (Harman, 1976).

The VariMax rotation maximizes the squared factor loadings in each factor and simplifies the interpretation of the features composing the components. The Quartimax rotation maximizes the variance of the squared factor loadings in each variable and simplifies the interpretation of the components composing the features. The Equamax rotation maximizes the weighted sum of the VariMax and Quartimax criteria which simplifies the interpretation of the components and the factors.

Factor Analysis (FA) was applied by *Uylaser et al.*, (2008) to classify *Gemlik* olives by their origin district. They measured eight physical and chemical features such as

width, height, flesh/stone ratio and fatty acid composition, and later perform PCA on the data of each class of olives. Next they used VariMax rotation on the first principal component of each analysis to identify the main feature. By the results they were able to identify most significant feature for each class which explained over 99% of the variance.

Rezzai et al. (2005) used NMR to classify olive oils. The output of the NMR was comprised 12,000 variables which were reduced to 50 by PCA. The 50 components captured 99% of the information.

Sato (1994) used the reflectance of NIR to classify vegetable oils. He projected wavelengths ranges between 1600 nm to 2300 nm and measured the level of reflectance and the first and second derivatives of reflectance. He found out that the 2nd PC of the raw reflectance and first two PC of the first and second derivatives could successfully classify between the different oils.

Another common technique for dimension reduction is the stepwise method. In this method F tests are used to determine which feature should enter the MLR model and which feature should be excluded (Darper & Smith, 1981).

Uylaser et al., (2008) used the stepwise regression method to investigate the correlation between features of olives grown in different regions. They revealed similarities between olives with different characteristics and from different regions.

Yang et al. (2004) used airborne hyper spectral images of cotton fields to map crop yield variability. The raw hyper spectral images contained 128 bands between 457 and 922 nm. Stepwise regression performed on the yield and hyper spectral data identified significant bands and band combinations, which were able to explain 69% and 61% of the variability in yield in two fields.

2.5 Machine Vision

Many applications using machine vision technology have been developed in agricultural sectors, such as land-based and aerial-based remote sensing for natural resources assessments, precision farming, post harvest product quality and safety detection, classification and sorting, and process automation (Chen et al., 2002). Advantages of using imaging technology for sensing are that it can be fairly accurate, nondestructive, and yields consistent results (Chen et al., 2002). It holds great potential and benefits for the agricultural industry because of its simplicity, low cost, rapid inspection rate, and broad range of other applications (Chen et al., 2002).

"The big advantage of computer vision is its ability to be objective and consistent over long period while human's ability of perception is known to be limited to 400–700 runs and dynamic range of human's ability of perception is limited to less than 100 gray levels" (Saito et al., 2003).

Image processing includes three steps (Chen et al., 2002): (1) image enhancement, (2) image feature extraction, and (3) image feature classification. With a well-chosen lighting system, the incident light will present the objects or scenes in the optimal way to be recognized or analyzed, thereby eliminating many tedious image processing procedures that otherwise would be needed (Chen et al., 2002). The extraction of the image features is done usually by statistical procedures like mean and variance analysis (Chen et al., 2002). The next step after extracting the image features is classification which can be achieved using different numerical techniques (Chen et al., 2002). Neural networks and fuzzy inference systems can be successfully applied and are advantageous for the unstructured and highly variable agriculture domain (Chen et al., 2002).

Machine vision is a technique that has been widely used in agricultural to define many characteristics of fruits, vegetables, meat and fishes (Zheng et al., 2006). The information that can be drawn by image processing can be categorized into four features (Zheng et al., 2006): color, size, shape and texture.

Color is one of the most important features, mostly because it contains the basic information correlating to human eyes (Zheng et al., 2006). "Human visual inspection is a highly subjective, tedious, time-consuming, and labor intensive process, by contrast, instrumental techniques (such as colorimeters) allow accurate and reproducible measurements of the colors not influenced by the observer or surroundings" (Mendoza and Aguilera, 2004). Only a single value is necessary to represent each pixel of grey level pictures while 3 values (0-255) are necessary for that in color images (Zheng et al., 2006). There are several ways to represent color pictures. RGB (red, green, blue) that originally comes from color digital cameras is the most common one. It appears to be inadequate across the variant applications (Zheng et al., 2006). YIQ (Illuminance, in-phase, quadarture) is another color space representation which originated form broadcast contemplation and is hardware oriented (Zheng et al., 2006). HSI (hue, saturation, intensity), HSL (hue, saturation, lightness), and HSV (hue, saturation, value) are color spaces that describe color

information similar to ways that are used in a human vision system, thus they are known as human-orientated color spaces. (Zheng et al., 2006). CIE and L*a*b*, are the measurements usually adopted in instruments such as colorimeter, accordingly, they are referred to as instrumental color spaces. (Zheng et al., 2006).

Size is usually measured in 3 dimensions, but because the information of the third dimension is dropped in the imaging process the size of objects is represented only in 2 dimensions (Zheng et al., 2006). Since digital images are composed of pixels, the two primary size features are area and perimeter which can be acquired by counting the number of pixels in images and by summing the distance between every two neighboring pixels on the boundary, respectively (Zheng et al., 2006). Length and width are more difficult to measure because of the irregularity of the shape of the food products, which caused the development of other measurements (Zheng et al., 2006).

Feret's diameter, which is determined by the distance of two pixels with the smallest and the largest coordinates at different orientations; **Major axis**, which is the longest line that can be drawn across food products and can be calculated by measuring the distance between every combination of two boundary pixels and by taking the longest and **Minor axis**, which is the longest line that can be drawn through the object perpendicular to the major axis (Zheng et al., 2006).

Shape is the geometric structure of an object. The way to determine the shape of a digital image is to combine different size parameters into dimensionless expression which defines the shape (Zheng et al., 2006). The common expressions to determine shape are: **compactness**, which is the ratio of area over the square perimeter; **elongation**, which is the ratio of major axis over the minor axis; **convexity**, which is the ratio of convex perimeter over the perimeter; and **roughness**, which is the ratio of area over the square major axis (Zheng et al., 2006).

Texture tries to discriminate different patterns of images by extracting the dependency of intensity between pixels and their neighboring pixels or by obtaining the variance of intensity across pixels (Zheng et al., 2006). There are 4 methods to determine texture: statistical texture; structural method; model-based texture and transform-based texture (Zheng et al., 2006).

Thygesen (2001) used image processing techniques to predict the chemical compounds of potatoes. *Laykin* (2002) used machine vision to classify tomatoes by their color, defects and color homogeneity.

Mendoza and Aguilera (2004) developed a machine vision based technique to classify bananas into 7 ripening stages, procedure that is usually made by human workers. They picked the most 5 significant features out of the nine collected on each fruit, and used discriminate analysis, simple regression and analysis of variance to classify the images to the correct ripening stage. They obtained 98% accuracy.

Diaz et al. (2000) showed significant advantage of machine vision over human eye to classify table olives. He claims that olive experts made huge errors in the separation of the best qualities because, in the case of doubt, they prefer to assign an olive to the worst category. The results of the machine were a little better when separating the first and fourth classes, but were much worse in the case of the intermediate categories due to the great number of olives per image.

2.6 Low Resolution Nuclear Magnetic Resonance (LR-NMR)

NMR spectrometry is a widely used analytical technique for structural elucidation and identification of chemical species in the analysis of many different materials including organic chemicals, inorganic complexes and large biological molecules (Nordon, 2001).

NMR spectrometry is very useful as it is nondestructive and does not require the measurement probe to be inserted into the process liquors, which avoids fouling (Nordon, 2001).

In the past decade, small, dedicated low-field (< 60 MHz) NMR systems, based on permanent magnet technology, have been developed, which in turn has led to more reports of at-line and on-line process applications (Nordon, 2001). Most low-field NMR applications involve the measurement of spin–spin (T₂) and/or spin–lattice (T₁) relaxation times, which are then related to a specific physical property such as viscosity, surface area and moisture content (Nordon, 2001).

Low-field, low-resolution NMR spectrometry has been used extensively in several industries including those involving the manufacture of food, pharmaceuticals and petrochemicals (Nordon, 2001). Example applications include the determination of moisture content, fat content, hydrogen content and fluorine content (Nordon, 2001).

One of the most common areas of application of low-field, low-resolution NMR spectrometry is to determine the quantity of moisture in materials such as corn, zeolites and soil (Nordon, 2001).

The analysis of materials defer mostly in the frequency of the measurement. A 4.1 MHz NMR spectrometer was used to determine the moisture content of samples of rice, which were contained within 40 mm NMR tubes (Nordon, 2001). It has been shown that low-resolution NMR (20 MHz) can be used for the determination of ethanol in alcoholic beverages (Nordon, 2001). Low-field, high-resolution ^1H NMR spectrometry at 60 MHz has been used to monitor alcohols in fuels (Nordon, 2001). A variety of dairy products, e.g., whipping cream, whole milk and skimmed milk, has been analyzed using ^1H NMR spectrometry at 42 MHz (Nordon, 2001).

NMR spectrometry is also being used for on-line process measurements. The moisture content of coal, which was fed through the sample coil from a hopper under gravity at a rate of 100 g per hour, has been determined. The ^1H NMR signal intensity was used to determine the hydrogen content of the coal (Nordon, 2001). A small on-line process NMR spectrometer has been used to monitor the moisture content and surface area of reduction grade aluminum oxide as it leaves a rotary kiln (Nordon, 2001). As early as 1956, a process analyzer was designed to monitor the ratio of two organic liquids flowing through the probe of a 30 MHz continuous wave spectrometer (Nordon, 2001).

NMR is an extremely powerful tool for the structural characterization of organic molecules, such as components of humic substances and contaminant transformation products (Cardoza et al., 2004). Despite its lower sensitivity compared with other environmental analytical techniques, NMR has nonetheless proved its utility in investigating environmental interactions between natural organic matter and contaminants, and has given investigators new approaches to exploring issues related to the environmental transport and fate of these substances (Cardoza et al., 2004).

Various application of NMR in food agriculture can be found in Table 4.

Table 4 – Examples of application of NMR in food and agriculture

Product	Features	Reference
Avocado and cherry	Oil water ratio	Kim et al. (1999)
Blended coffee	Chemical composition	Charlton et al. (2002)
Optimize quality of cooked meat	changes in characteristic of the water in 7 temperature levels of cooked meat	Bertram el al. (2006)
'Bella Della Daunia' olives	changes in sugar water and	Brescia et al. (2007)

	oil content during ripening	
Geographical origin of olive oils	Resonance spectrum of olive oil	Rezzy et al. (2005)
Detecting adulteration of olive oils	Resonance spectrum of olive oil in combination with chemometric methods	Ogrinc et al., 2003

3. Methodology

3.1 Data collection

Four hundred *Souri* and four hundred *Picual* olives were manually harvested from Re'em plantation in the Negev which surrounds in a typical dry land area. The olives were harvested every week along the ripening season, from the same ten trees which were randomly selected. First, olives were randomly picked from all around the trees and put in a bucket, and later four hundred of them were randomly drawn from the bucket. *Souri* olives were harvested along 9 weeks during Oct-Nov 2007 and *Picual* olives were harvested along 8 weeks during Nov. 2007-Jan 2008.

The harvested olives were inspected by a single human and manually classified into three groups of colours – green, purple or black. Each olive was weighed and sampled by a Canon F5 digital camera with 3 CCD colour sensors and a resolution of 4368X2912 pixels. All images were taken in a fixed illumination photo cell specially designed for this purpose (Figure 6), which ensured equal light distribution and consistent lighting conditions.

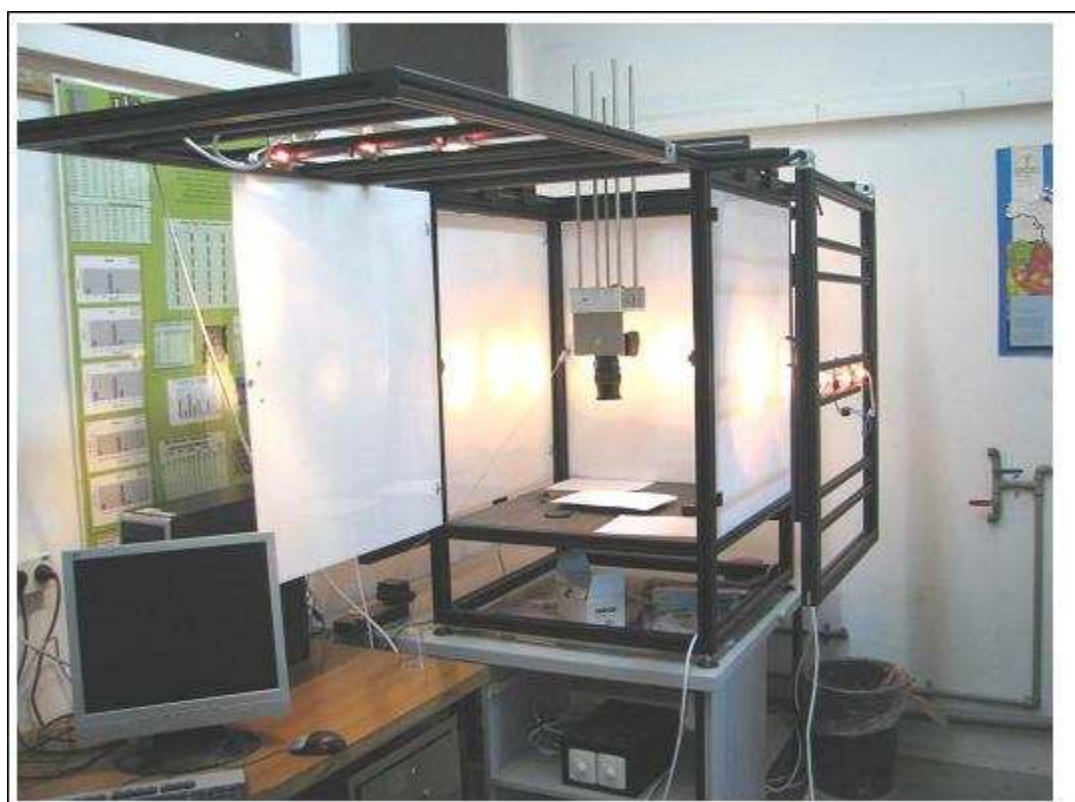


Figure 6– Fixed illumination photo cell

The olives were placed on a white plate and were sampled in groups of 10 olives per image (Figure 7). The camera was set at a height of 30 cm above the plate surface, resulting in an average resolution of 412 pixels per cm. To sample both sides of the olives, the olives were manually turned between consecutive images and each olive was sampled twice.

The olives were then placed in an oven at temperature of 70° C for 3 days in order to vaporize all their water content. Each olive was weighed again for its dry weight after they were taken out of the oven. The oil content of each dried olive was measured by Low Resolution Nuclear Magnetic Resonance (LR-NMR) which has been known to be accurate and useful for oil content determination (Nordon et al., 2001). The oil percent received from the NMR was calculated according to a calibration curve determined using the ISO 565 protocol, multiplied by the dry weight and divided by the fresh weight.

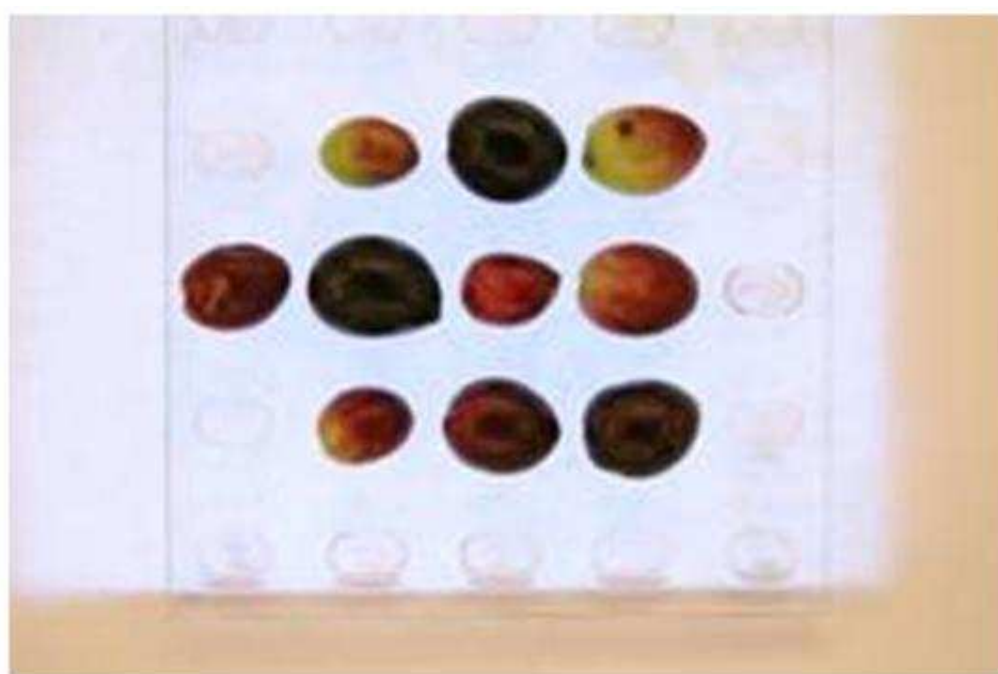


Figure 7– Picture of one sample - a group of 10 olives

Image processing procedures developed in MATLAB by *Laykin et al.*, (2008) for extracting features from the olives' images were used to analyze each picture, and 29 features were extracted for each side of each olive (Table 5).

In addition, for fallout (olives that dropped from the tree to the ground) analysis, ten *Souri* trees were chosen and marked and every week during 8 weeks all the fallout from the trees were collected and weighed.

3.2 Data analysis

3.2.1 Descriptive statistics – The average oil weight, average oil percentage and color distribution in a single fruit of each sample of each variety was calculated. Graphical analysis was used to study the trends and correlations between the different features along the sampling period of both oil accumulation and fallout analysis.

Table 5–Features derived by the image processing algorithms

Feature	Implementation	Description
Area	Black White (BW) matrix	Number of relevant pixels
Length		Length of olive bounding box
Width		Width of olive bounding box
Eccentricity		L1/L2: Ellipse (same second moment as the region) centers distance (L1) by Long Axis (L2) (~1 – Circle; ~0 - Area Line).
Equivalent Diameter		Diameter of same area circle
Compactness		Shape - Perimeter/Area^2
Maximum Distance		maximum distance from center to edge
Length vector		The distance vector length
FD1 (1 st FFT coefficient)		Average Radius
FD2 (2nd FFT coefficient)		Bendingness
FD3		Elongation
FD4		
FD5		
Ratio Elongation		(FD(1)-2*(FD(3)))/(FD(1)+2*(FD(3)))
Average Green/Hue	Red Green Blue (RGB)/Hue Saturation Intensity (HSI) matrix	Color
Variance Green/Hue		Color Variance
Defect area	Gray matrix	Ratio between defect area and non defect area
Mean		Texture - Average intensity (GrayImage).
Standard deviation		Texture - Standard deviation – measure of average contrast
Smoothness	Gray/HSI matrix	Texture - $R = 1 - 1/(1 + \sigma^2)$
3 rd moment		Texture - Measure of the skewness of the histogram
Uniformity		Texture - $U = \sum_{i=0}^{L-1} p^2(z_i)$
Entropy		Measure of randomness

3.2.2 Both sides features analysis – The values obtained from images of different sides of the fruit were compared by the statistical paired T test for each feature.

3.2.3 Varieties separation analysis –To evaluate the need to develop a model for each specific variety or a general model applicable to all varieties the following analyses were conducted:

(a) **Variance analysis** –The difference in the oil amount between varieties was calculated by ANOVA using the following hypotheses:

H_0 : The average oil content of single olive in both varieties is equal.

H_1 : The average oil content of single olive in both varieties is not equal.

95% confidence intervals of the average values of the oil amount in each variety were calculated and graphically presented.

(b) **Multiple linear regression (MLR)** was used to calculate the correlation between the features obtained by the image processing routines to the oil amount values. MLR was applied first on the data of both varieties together and then on each variety alone.

3.3.4 Preprocessing – To detect problems in the datasets such as unreasonable data and multi-collinearity between features several statistics measures are calculated for all features of both varieties. The statistics include minimum value, maximum value, mean value, standard deviation, skewness and linear correlation with the oil content. Next, the correlation between features is calculated for multi-collinearity detection.

3.2.5 Dimension reduction (Factor Analysis) - The MLR model coefficients and their variances were calculated and found extremely high which implied on high effect of multi-collinearity.

New sets of uncorrelated features were extracted for each variety by PCA and rotated in EquaMax method (Harman, 1976). The new factors were ranked by their eigenvalues from highest to lowest and only factors with eigenvalues above the threshold of 1 were selected.

3.3 Prediction Models

Prediction models were developed separately for each olive variety.

3.3.1 Methods – Two prediction models were developed:

(a) Multiple Linear Regression. (b) Artificial Neural Network.

For both models three different inputs were considered: (a) Original dataset of all 29 features obtained by the image processing routines. (b) Set of factors obtained by the

FA. (c) Set of features selected by applying stepwise over the original set of features. The enter criteria was p value ≤ 0.05 and removal criteria was p value > 0.1 .

Each model was obtained using a randomly drawn training set which was composed from 80% of the mentioned datasets, and tested with the remaining data.

3.3.2 Output – A prediction of the oil amount in the olive.

3.3.3 Performance measures – Five models were obtained and tested using different sets of training and testing. The sets were randomly drawn from the original database each time. To ensure consistency of the performances of the model, the average values of the following performance measures of the five models were considered.

The following values were used as performance measures:

(a) Average R^2 of the five tested models (sum of squared error of the model divided by the sum squared difference from the average without the model).

(b) Average standard error of the five tested models (MSE – mean squared error).

3.3.4 Multiple linear regressions

The training set was used for extracting the coefficients of the models and the testing set was used for testing the models with unknown data.

3.3.5 Artificial neural networks

3.3.5.1 Networks properties - The training set was randomly divided into training and validating sets in proportion of 75:25, the topology of all networks was: two layers (29:1), and log sigmoid was used as transfer function in all neurons.

3.3.5.2 Training parameters – Back-propagation by Levenberg-Marquardet algorithm (Kelly 1999), stopping criteria: 100 epochs, 5 consecutive epochs of gradient smaller than 1e-10 or MSE equal to 0.

3.4 Sensitivity analyses

The sensitivity of the models to changes in the following properties was tested for two models of each variety: the model based on the original data set and the model based on a reduced number of variables resulting from the factor analysis. The considered properties were as follows:

3.4.1 Training/Testing proportions – Several proportions between training set and testing set are considered: 67:33, 70:30, 80:20, and 90:10. In the ANN model the validation set was drawn from the training set and was equal to the testing set, which created the following proportions: 34:33:33, 40:30:30, 60:20:20, 80:10:10 (training set, validating set, testing set).

3.4.2 Topology – For the ANN models several topologies were considered (number of neurons in the first layer: second layer: output layer): 29:29:1, 29:20:1, 29:15:1, 29:10:1, 29:5:1, 29:3:1, 29:2:1 and 29:1.

3.4.3 Transfer function – Three transfer functions were considered in each layer in the ANN: Log sigmoid, Tangents sigmoid and pure line.

4. Results

4.1 Data analysis

4.1.1 Descriptive statistics - Figure 8 and Figure 10 depict the average oil content and the average oil percent of single olive in each sample in the *Picual* and *Souri* varieties respectively along the sampling period. It can be seen that while the oil percent increases along the sampling period the oil amount reaches a peak level and stays around it from then on. Figure 9 and Figure 11 depict the average weight of a single olive during the sampling period of *Picual* and *Souri* olives respectively. The olive weight increases until a certain level and then starts to decline in both cases. This phenomenon is caused by the rotting process which causes the olive to shrivel due to loss of moisture which can explain the stagnation in the oil amount while the oil percent increases.

Figure 12 depicts the weight of the collected fallout along the sampling period vs. the average oil amount in the olives. It can be seen that the fallout remains more or less constant at the beginning and from a certain point rapidly increases. This point occurs before the olives reached their maximum oil amount. The fallen olives cannot be used for oil extraction due to the poor oil they contain and they are counted as a loss of oil potential and subtracted from the total yield of the grove.

Figure 13 depicts the distribution of black, purple and green olives compared to the fallout weight along the sampling period. The color distribution seems to be more or less constant at the beginning and from a certain point the proportion of black olives increases on behalf of the purple and green olives. It can be noticed that the fallout and the proportion of black olives behave with very similar trends.

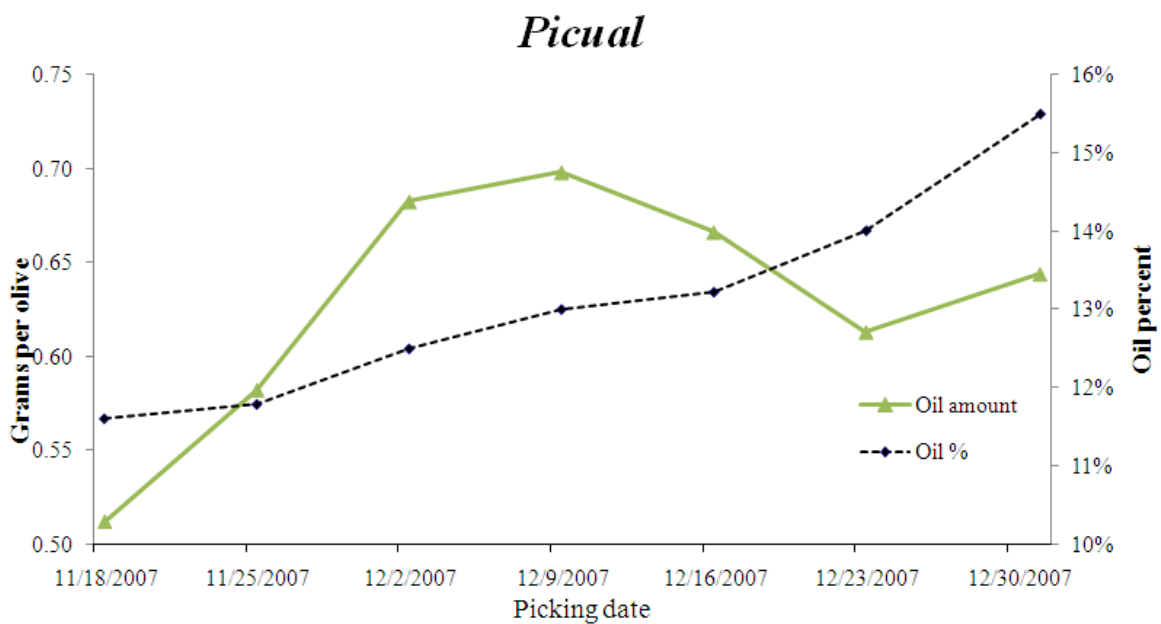


Figure 8– Average oil content and average Oil percent vs. sampling time – *Picual*

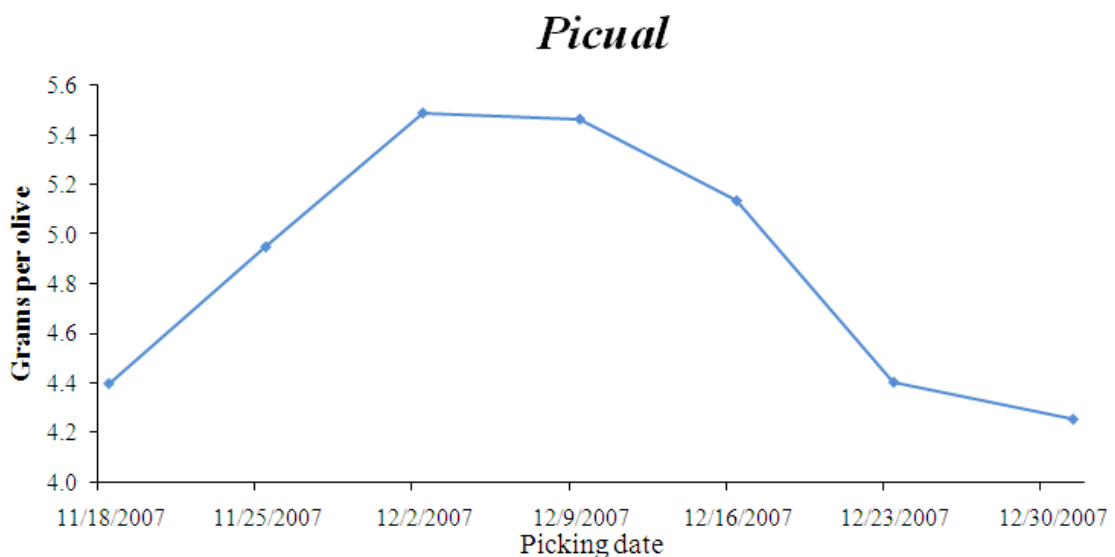


Figure 9– Average weight vs. sampling time - *Picual*

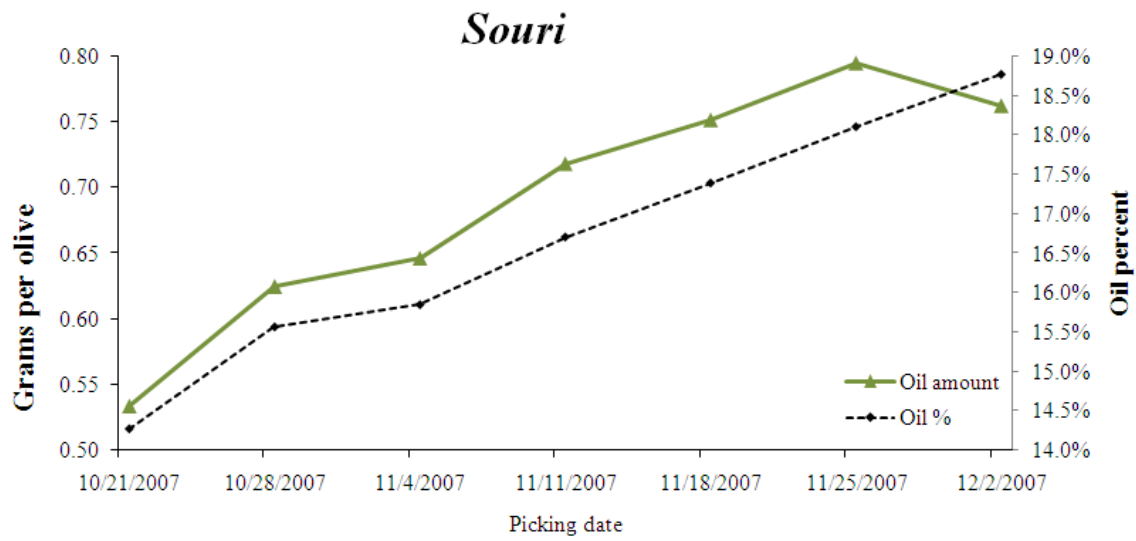


Figure 10– Average oil content and avearge oil percent vs. sampling time – *Souri*

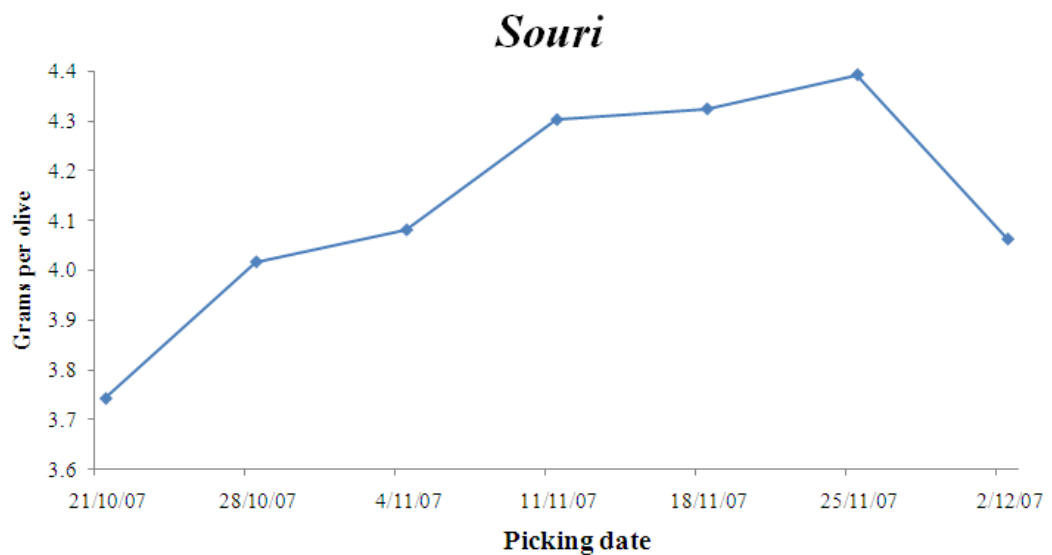


Figure 11 - Average weight vs. sampling time – *Souri*

Fallout vs. Oil Quantity

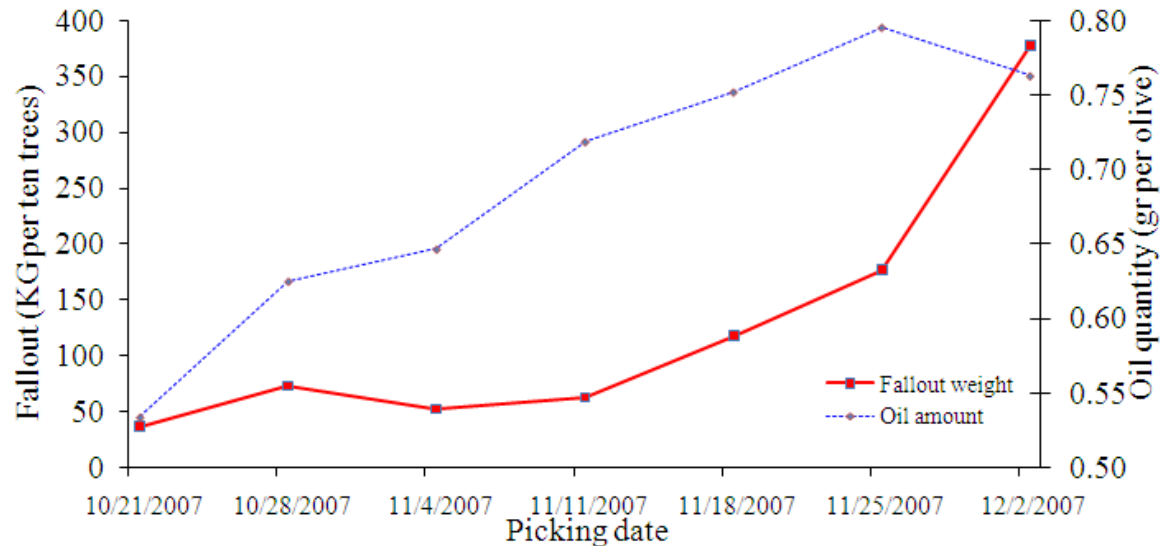


Figure 12– Fallout and oil content vs. sampling time – *Souri*

Fallout vs. Color Distribution

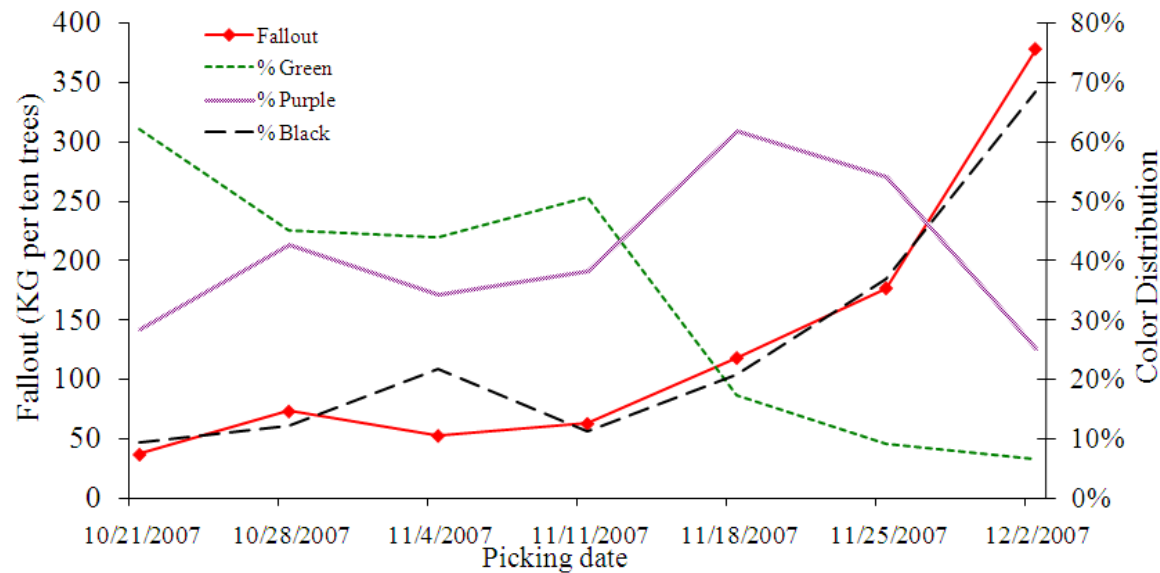


Figure 13 - Fallout vs. color distribution – *Souri*

4.1.2 Both sides features analysis –Table 6 and Table 7 show the results of a paired T test between features of different sides. Table 6 shows the results of the T test of *Picual* features and Table 7 shows the results of the T test of *Souri* features. It can be seen that most of the features in both varieties were found statistically different between sides. The meaning of the results is that the values of features extracted from the image of one side of the olives are consistently lower or higher than the values of the same feature extracted from the image of the other side. These differences require the consideration of values of both sides in order to define a single value which will represent the feature's value. These differences lead to the decision to use the maximum value of both sides of size related features such as length and width, and to use the average value of both sides of all other features.

The notion standing behind this division is that features extracted from size related attributes should not have different values between sides, and the differences are caused due to measurements' errors, such as different positions of the fruit in plate or small changes in the position of the plate. These changes can only decrease the values of the features and the maximum value is probably closer to the real value. On the other hand, the differences in values of other features can be caused by many reasons, some embedded in the nature of the fruits, (such as difference in color between sides or defects in one side only) and others caused by measurements' errors.

Table 6 - Results of paired T test of the difference between Picual image features of opposite sides

Paired Samples Test										
		Paired Differences				t	df	Sig. (2-tailed)		
		Mean	Std. Deviation	Std. Error Mean	95% Confidence Interval of the Difference					
					Lower	Upper				
Pair 1	Area_side_A - Area_side_B	-381.449	6338.03318	141.29947	-658.558	-104.341	-2.700	2011	.007	
Pair 2	length_side_A - length_side_B	-1.00671	13.88635	.30958	-1.61384	-.39958	-3.252	2011	.001	
Pair 3	width_side_A - width_side_B	.04175	14.08524	.31401	-.57408	.65758	.133	2011	.894	
Pair 4	Eccentricity_side_A - Eccentricity_side_B	-.00256	.02923	.00065	-.00384	-.00128	-3.930	2011	.000	
Pair 5	EquiveD_side_A - EquiveD_side_B	-.41319	7.21769	.16091	-.72876	-.09763	-2.568	2011	.010	
Pair 6	Compctness_side_A - Compctness_side_B	-.01838	.55064	.01228	-.04245	.00570	-1.497	2011	.135	
Pair 7	MaxDist_side_A - MaxDist_side_B	-1.00976	7.71009	.17189	-1.34685	-.67266	-5.875	2011	.000	
Pair 8	LengthVec_side_A - LengthVec_side_B	-3.06213	41.70635	.92980	-4.88559	-1.23866	-3.293	2011	.001	
Pair 9	FD1_side_A - FD1_side_B	.80257	5.45510	.12162	.56406	1.04107	6.599	2011	.000	
Pair 10	FD2_side_A - FD2_side_B	-.20957	2.38488	.05317	-.31384	-.10530	-3.942	2011	.000	
Pair 11	FD3_side_A - FD3_side_B	-.75446	4.43495	.09887	-.94837	-.56056	-7.631	2011	.000	
Pair 12	FD4_side_A - FD4_side_B	.46606	1.85071	.04126	.38514	.54697	11.296	2011	.000	
Pair 13	FD5_side_A - FD5_side_B	.29468	1.38177	.03081	.23426	.35509	9.566	2011	.000	
Pair 14	RatioElong_side_A - RatioElong_side_B	.01034	.05908	.00132	.00776	.01292	7.850	2011	.000	
Pair 15	Av#G_side_A - Av#G_side_B	-.17720	9.86893	.22002	-.60869	.25428	-.805	2011	.421	
Pair 16	DefectArea_side_A - DefectArea_side_B	.51540	15.80442	.35234	-.17560	1.20639	1.463	2011	.144	
Pair 17	Mean_Gr_side_A - Mean_Gr_side_B	-.04728	8.81347	.19649	-.43262	.33806	-.241	2011	.810	
Pair 18	SD_Gr_side_A - SD_Gr_side_B	-.23994	3.66740	.08176	-.40029	-.07960	-2.935	2011	.003	
Pair 19	Smooth_Gr_side_A - Smooth_Gr_side_B	-.00022	.00347	.00008	-.00037	-.00007	-2.876	2011	.004	
Pair 20	@3rd_Moment_Gr_side_A - @3rd_Moment_Gr_side_B	-.00301	.24151	.00538	-.01357	.00755	-.558	2011	.577	
Pair 21	Uniformity_Gr_side_A - Uniformity_Gr_side_B	.00010	.00363	.00008	-.00005	.00026	1.289	2011	.198	
Pair 22	Entropy_Gr_side_A - Entropy_Gr_side_B	-.00685	.23388	.00521	-.01708	.00337	-1.315	2011	.189	
Pair 23	Mean_Hue_side_A - Mean_Hue_side_B	.20189	7.90240	.17618	-.14361	.54740	1.146	2011	.252	
Pair 24	SD_Hue_side_A - SD_Hue_side_B	.34334	8.99308	.20049	-.04985	.73653	1.712	2011	.087	
Pair 25	Smooth_Hue_side_A - Smooth_Hue_side_B	.00059	.01620	.00036	-.00012	.00129	1.623	2011	.105	
Pair 26	@3rd_Moment_Hue_side_A - @3rd_Moment_Hue_side_B	.01341	2.24007	.04994	-.08453	.11135	.268	2011	.788	
Pair 27	Uniformity_Hue_side_A - Uniformity_Hue_side_B	-.00026	.00975	.00022	-.00068	.00017	-1.174	2011	.241	
Pair 28	Entropy_Hue_side_A - Entropy_Hue_side_B	.00929	.26586	.00593	-.00233	.02092	1.568	2011	.117	

Table 7 - Results of paired T test of the difference between Souri image features of opposite sides

Paired Samples Test											
	Paired Differences					t	df	Sig. (2-tailed)			
	Mean	Std. Deviation	Std. Error Mean	95% Confidence Interval of the Difference							
				Lower	Upper						
Pair 1	Area_side_A - Area_side_B	-881.152	6605.83323	110.86984	-1098.53	-663.777	-7.948	3549 .000			
Pair 2	length_side_A - length_side_B	-1.86141	15.12061	.25378	-2.35898	-1.36384	-7.335	3549 .000			
Pair 3	width_side_A - width_side_B	-.74789	11.58690	.19447	-1.12917	-.36660	-3.846	3549 .000			
Pair 4	Eccentricity_side_A - Eccentricity_side_B	-.00069	.01869	.00031	-.00130	-.00007	-2.189	3549 .029			
Pair 5	EquiveD_side_A - EquiveD_side_B	-1.01084	7.38272	.12391	-1.25378	-.76790	-8.158	3549 .000			
Pair 6	Compctness_side_A - Compctness_side_B	.04581	.69926	.01174	.02280	.06882	3.903	3549 .000			
Pair 7	MaxDist_side_A - MaxDist_side_B	-.71493	7.83502	.13150	-.97275	-.45711	-5.437	3549 .000			
Pair 8	LengthVec_side_A - LengthVec_side_B	-.52169	46.04116	.77274	-2.03674	.99336	-.675	3549 .500			
Pair 9	FD1_side_A - FD1_side_B	.66436	4.94330	.08297	.50169	.82702	8.008	3549 .000			
Pair 10	FD2_side_A - FD2_side_B	-1.21078	2.54517	.04272	-1.29454	-1.12703	-28.344	3549 .000			
Pair 11	FD3_side_A - FD3_side_B	-2.33927	4.59062	.07705	-2.49033	-2.18821	-30.362	3549 .000			
Pair 12	FD4_side_A - FD4_side_B	1.66951	1.64717	.02765	1.61531	1.72371	60.390	3549 .000			
Pair 13	FD5_side_A - FD5_side_B	.94414	1.32625	.02226	.90050	.98778	42.415	3549 .000			
Pair 14	RatioElong_side_A - RatioElong_side_B	.03079	.06049	.00102	.02880	.03278	30.323	3549 .000			
Pair 15	Av#G_side_A - Av#G_side_B	.35868	12.42050	.20846	-.05003	.76740	1.721	3549 .085			
Pair 16	DefectArea_side_A - DefectArea_side_B	.21328	3.08370	.05176	.11180	.31475	4.121	3549 .000			
Pair 17	Mean_Gr_side_A - Mean_Gr_side_B	.28787	10.67774	.17921	-.06350	.63924	1.606	3549 .108			
Pair 18	SD_Gr_side_A - SD_Gr_side_B	.36093	4.31318	.07239	.21900	.50286	4.986	3549 .000			
Pair 19	Smooth_Gr_side_A - Smooth_Gr_side_B	.00024	.00328	.00005	.00013	.00035	4.371	3549 .000			
Pair 20	@3rd_Moment_Gr_side_A - @3rd_Moment_Gr_side_B	.00168	.21016	.00353	-.00524	.00859	.476	3549 .634			
Pair 21	Uniformity_Gr_side_A - Uniformity_Gr_side_B	-.00069	.00441	.00007	-.00083	-.00054	-9.297	3549 .000			
Pair 22	Entropy_Gr_side_A - Entropy_Gr_side_B	.03911	.28226	.00474	.02982	.04840	8.256	3549 .000			
Pair 23	Mean_Hue_side_A - Mean_Hue_side_B	1.06531	4.83346	.08112	.90626	1.22436	13.132	3549 .000			
Pair 24	SD_Hue_side_A - SD_Hue_side_B	.98783	5.97719	.10032	.79114	1.18452	9.847	3549 .000			
Pair 25	Smooth_Hue_side_A - Smooth_Hue_side_B	.00161	.01061	.00018	.00126	.00196	9.044	3549 .000			
Pair 26	@3rd_Moment_Hue_side_A - @3rd_Moment_Hue_side_B	.09927	1.44218	.02421	.05181	.14672	4.101	3549 .000			
Pair 27	Uniformity_Hue_side_A - Uniformity_Hue_side_B	-.00080	.02034	.00034	-.00147	-.00013	-2.350	3549 .019			
Pair 28	Entropy_Hue_side_A - Entropy_Hue_side_B	.03136	.31550	.00530	.02097	.04174	5.922	3549 .000			

The features that their values are taken as maximum between both sides are: area, length, width, eccentricity, Equivalent Diameter, compactness, Maximum Distance

and Length vector. Features that their values are taken as average between both sides are: FD1, FD2, FD3, FD4, FD5, Ratio Elongation, Average Green, Variance Green, Defect Area, Mean Gray/Hue, Standard Deviation Gray/Hue, Smoothness Gray/Hue, 3rd Moment Gray/Hue, Uniformity Gray/Hue and Entropy Gray/Hue.

Table 8 depicts the R values received from a regression between features of side A, Side B and both sides adjusted features. It can be seen that the R values of both sides' models are higher in both varieties and the combination of both sides contributes to the accuracy of the models.

Table 8 – R values of regression models

	Side A	Side B	Both sides
Souri	0.863	0.861	0.866
Picual	0.763	0.754	0.764

4.1.3 Varieties' models separation analysis

Variance analysis - The result of the variance analysis supports the rejection of the null hypothesis which claims that the oil content in both varieties is equal (Table 10). The first row presents the difference between average oil content of olives of different varieties, and second row present the difference between oil content of olive of the same variety. The P value is smaller than 0.001, which suggests that the probability that the oil amount in both varieties is in the same range, is less than 0.1%. Therefore, the statistical analyses should be conducted for each variety separately.

In Table 9 it can be seen that the average *Souri* olive contains 0.668 gr. of oil with a standard deviation of 0.16 gr., while the average *Picual* olive contains only 0.621 gr. with a standard deviation of 0.2 gr.

Table 9 – Descriptive statistic of oil amount

	N	Mean	Std. Deviation	Std. Error	95% Confidence Interval for Mean		Minimum	Maximum
					Lower Bound	Upper Bound		
Picual	2012	.6214	.20895	.00466	.6123	.6306	.15	1.30
Souri	3550	.6680	.16025	.00269	.6628	.6733	.20	1.21
Total	5562	.6512	.18073	.00242	.6464	.6559	.15	1.30

Table 10 – ANOVA variance analysis of oil amount table

	Sum of Squares	df	Mean Square	F	Sig.
Between Groups	2.787	1	2.787	86.643	.000
Within Groups	178.848	5560	.032		
Total	181.635	5561			

4.1.4 Multiple Linear Regression - MLRs were applied on three databases that contain the features and oil amount of: (a) both varieties. (b) *Souri* variety and (c) *Picual* variety. The results of the R and MSE of the MLRs are presented in Table 11.

Table 11 - MLR results of models for each variety separately & together

	<i>Picual</i>	<i>Souri</i>	Both varieties
R	0.764	0.866	0.782
MSE	0.1356	0.0804	0.1129

It can be seen that the model based on both varieties was worse than the model based on the *Souri* data alone and slightly better than a model based on the *Picual* alone. However, the average result of a separate model for each variety is 0.815 which is better than the results of the unified model. These results support the use of different models for each olive variety.

4.1.5 Preprocessing – Table 12 and Table 13 present an overview of the statistics of the new features received after the combination of both sides. The features are sorted from high to low by the correlation with the oil content. The description of the fields presented in tables can be found in Table 5.

The first two columns present the minimum and the maximum value of each feature and third column presents the average value. The fourth and the eighth columns present the correlation and covariance of each feature with the oil content, the fifth column is the t value representing the correlation and seventh column is the p value derived from the t value. The ninth column presents the standard deviation of each feature and tenth column present the skewness (measure of the asymmetry) of the histogram of each feature.

In both varieties the features, Area, length and width have the best correlation with oil amount. This phenomenon is expected because naturally large olives contain more oil. In both varieties the correlation of these three features is above 60%. However, as seen by the correlations presented in Table 16 and Table 17 all three features have high correlation with each other and the marginal contribution of each one is very low. This issue will be addressed later on.

Table 16 shows several features in *Picual* olives with correlations above 0.5, and Table 17 shows several features in *Souri* olives with correlations above 0.87. These

tables present only the couples with the highest correlation due to the large size of the tables. These high correlations indicate multi-collinearity of the models' variables.

Table 14 and Table 15 show the coefficients of each feature in the MLR models. It can be seen that some coefficients have high variances which result in wide confidence intervals. The most right column shows the probability of zero value of the coefficient. In can be seen that probability of zero value is high for many coefficients and thus do not affect the oil amount in the olive.

Table 12- Descriptive statistics of image features -Picual

Field	Min	Max	Mean	Correlation	Correlation T	Correlation T sig.	Covariance	Std. Dev	Skewness
<i>Oil amount</i>	0.147	1.295	0.621	--	--	--	--	0.209	0.391
<i>Area</i>	86255	430908	235382.1	0.691	42.886	0	9355.052	64801.21	0.345
<i>length</i>	395	872	622.602	0.656	38.948	0	12.202	89.087	0.058
<i>width</i>	283	698	482.061	0.693	43.117	0	10.032	69.295	0.073
<i>EquiveD</i>	259.554	740.709	541.508	0.674	40.924	0	10.803	76.726	-0.024
<i>AVG_Var.Hue</i>	0.001	0.21	0.084	-0.28	-13.062	0	-0.002	0.041	0.363
<i>AVG_MaxDist</i>	147.125	442.615	315.196	0.643	37.646	0	6.181	46.025	-0.012
<i>AVG_LengthVec</i>	790	2376	1657.42	0.662	39.643	0	32.864	237.548	-0.016
<i>AVG_Av.G</i>	32.91	192.61	62.568	-0.376	-18.181	0	-2.057	26.213	2.049
<i>AVG_DefectArea</i>	0.008	88.405	9.451	0.389	18.945	0	1.377	16.94	3.347
<i>AVG_Mean_Gr</i>	34.495	187.198	69.954	-0.455	-22.921	0	-2.568	27.008	1.49
<i>AVG_SD_Gr</i>	9.51	49.641	32.547	0.226	10.388	0	0.23	4.873	-1.022
<i>AVG_Smooth_Gr</i>	0.001	0.037	0.016	0.207	9.495	0	0	0.004	-0.406
<i>AVG_3rd Moment</i>	-0.696	1.962	0.9	0.427	21.155	0	0.047	0.532	-0.438
<i>AVG_Uniformity_Gr</i>	0.007	0.039	0.017	0.325	15.396	0	0	0.005	0.363
<i>AVG_Entropy_Gr</i>	5.011	7.299	6.456	-0.266	-12.388	0	-0.017	0.308	-0.131
<i>AVG_SD_Hue</i>	8.798	116.906	71.03	-0.221	-10.181	0	-0.895	19.359	-0.256
<i>AVG_Smooth_Hue</i>	0.001	0.174	0.076	-0.27	-12.561	0	-0.002	0.035	0.226
<i>AVG_3rd Moment_Hue</i>	-1.77	19.11	9.253	-0.307	-14.474	0	-0.315	4.909	0.203
<i>AVG_Uniformity_Hue</i>	0.017	0.141	0.034	-0.293	-13.757	0	-0.001	0.012	2.341
<i>AVG_Entropy_Hue</i>	3.342	6.45	5.613	0.301	14.161	0	0.025	0.39	-1.017
<i>AVG_FD2</i>	0.027	10.227	3.026	-0.059	-2.63	0.009	-0.021	1.728	0.565
<i>AVG_FD3</i>	0.311	27.316	12.677	0.047	2.121	0.034	0.04	4.067	-0.035
<i>AVG_RatioElong</i>	0.62	0.995	0.824	-0.046	-2.043	0.041	-0.001	0.055	0.048
<i>Eccentricity</i>	0.295	0.795	0.648	-0.044	-1.958	0.05	0	0.05	-0.567
<i>AVG_FD4</i>	0.051	5.406	1.863	0.038	1.687	0.092	0.007	0.907	0.622
<i>AVG_Compctness</i>	10.15	15.462	10.935	-0.028	-1.27	0.204	-0.003	0.439	2.702
<i>AVG_Mean_Hue</i>	27.324	127.749	55.309	0.026	1.147	0.252	0.066	12.322	0.478
<i>AVG_Av.Hue</i>	0.107	0.501	0.217	0.025	1.124	0.261	0	0.048	0.478
<i>AVG_FD1</i>	225.238	282.364	260.336	0.023	1.012	0.312	0.033	6.95	-0.405
<i>AVG_Var.G</i>	109.041	2664.534	1273.136	-0.021	-0.948	0.343	-1.522	344.78	-0.148
<i>AVG_FD5</i>	0.04	3.753	1.23	0.013	0.584	0.559	0.002	0.62	0.642

Table 13 – Descriptive statistics of image features - Souris

Field	Min	Max	Mean	Correlation	Correlation T	Correlation T sig.	Covariance	Std. Dev	Skewness
<i>Oil amount</i>	0.201	1.211	0.668	--	--	--	--	0.16	0.143
<i>Area</i>	125346	407444	252011.2	0.706	59.406	0	3619.845	31989.15	0.174
<i>length</i>	488	883	674.853	0.585	42.998	0	4.534	48.341	-0.025
<i>width</i>	334	627	488.536	0.662	52.654	0	3.646	34.353	0.076
<i>Eccentricity</i>	0.506	0.824	0.694	-0.092	-5.501	0	-0.001	0.045	-0.503
<i>EquiiveD</i>	399.494	720.26	565.306	0.712	60.458	0	4.116	36.062	-0.074
<i>AVG_Av.Hue</i>	0.039	0.311	0.17	0.255	15.701	0	0.002	0.046	-0.497
<i>AVG_Var.Hue</i>	0	0.175	0.045	0.479	32.513	0	0.004	0.05	0.489
<i>AVG_Compctness</i>	10.133	27.051	11.039	-0.186	-11.259	0	-0.014	0.485	11.86
<i>AVG_MaxDist</i>	243.281	439.648	341.096	0.591	43.67	0	2.314	24.428	-0.024
<i>AVG_LengthVec</i>	1276.5	2220	1740.799	0.644	50.099	0	11.813	114.529	0.129
<i>AVG_FD1</i>	225.325	274.805	252.556	0.095	5.665	0	0.113	7.423	-0.08
<i>AVG_Av.G</i>	39.866	197.405	107.168	-0.556	-39.86	0	-4.505	50.556	0.091
<i>AVG_Var.G</i>	44.868	2445.368	750.154	0.471	31.763	0	33.633	446.054	-0.093
<i>AVG_DefectArea</i>	0.001	22.367	3.181	0.371	23.777	0	0.187	3.149	1.408
<i>AVG_Mean_Gr</i>	45.555	185.842	108.288	-0.563	-40.549	0	-3.825	42.416	-0.021
<i>AVG_SD_Gr</i>	7.208	44.822	24.313	0.512	35.478	0	0.688	8.39	-0.199
<i>AVG_Smooth_Gr</i>	0.001	0.03	0.01	0.511	35.41	0	0	0.006	0.084
<i>AVG_3rd Moment</i>	-0.998	1.606	0.379	0.518	36.038	0	0.04	0.48	0.576
<i>AVG_Uniformity_Gr</i>	0.008	0.043	0.018	-0.38	-24.47	0	0	0.006	0.644
<i>AVG_Entropy_Gr</i>	4.835	7.178	6.249	0.42	27.561	0	0.031	0.457	-0.502
<i>AVG_Mean_Hue</i>	9.921	79.258	43.469	0.255	15.679	0	0.475	11.639	-0.499
<i>AVG_SD_Hue</i>	1.51	106.655	40.765	0.522	36.426	0	2.975	35.586	0.203
<i>AVG_Smooth_Hue</i>	0	0.149	0.041	0.487	33.19	0	0.003	0.044	0.443
<i>AVG_3rd Moment_Hue</i>	-0.008	18.631	5.755	0.485	33.042	0	0.477	6.135	0.382
<i>AVG_Uniformity_Hue</i>	0.021	0.2	0.071	-0.468	-31.569	0	-0.003	0.043	0.917
<i>AVG_Entropy_Hue</i>	2.602	6.017	4.586	0.518	36.045	0	0.077	0.93	-0.392
<i>AVG_FD2</i>	0.038	11.411	3.411	-0.057	-3.406	0.001	-0.017	1.869	0.349
<i>AVG_FD4</i>	0.01	6.507	2.099	-0.035	-2.107	0.035	-0.005	0.895	0.415
<i>AVG_FD5</i>	0.025	4.125	1.294	-0.026	-1.573	0.116	-0.003	0.604	0.283
<i>AVG_FD3</i>	2.651	30.351	15.446	0.01	0.621	0.535	0.007	4.069	0.065
<i>AVG_RatioElong</i>	0.582	0.961	0.783	-0.001	-0.061	0.951	0	0.055	-0.049

Table 14 – Coefficients table of MLR model of *Picual* variety

Model		Unstandardized Coefficients		Standardized Coefficients	t	Sig.
		B	Std. Error			
1	(Constant)	2.680	2.001		1.339	.181
	Area	1.80E-006	.000	.557	3.631	.000
	length	.000	.000	-.110	-.938	.348
	width	.001	.000	.326	3.572	.000
	Eccentricity	.255	.158	.061	1.621	.105
	EquiveD	-.002	.001	-.834	-2.766	.006
	Compctness	-.023	.011	-.069	-2.134	.033
	MaxDist	.001	.001	.148	.655	.513
	LengthVec	.000	.000	.464	2.278	.023
	AVG_FD1	.002	.002	.073	1.175	.240
	AVG_FD2	.003	.002	.026	1.369	.171
	AVG_FD3	-.010	.028	-.201	-.370	.711
	AVG_FD4	-.001	.004	-.005	-.297	.767
	AVG_FD5	-.003	.005	-.010	-.624	.533
	AVG_RatioElong	-.739	2.127	-.194	-.348	.728
	AVG_Av#G	.000	.002	-.058	-.264	.792
	AVG_Var#G	-8.8E-005	.000	-.146	-1.882	.060
	AVG_DefectArea	.001	.000	.044	2.131	.033
	AVG_Mean_Gr	-.002	.002	-.206	-.868	.385
	AVG_SD_Gr	.022	.009	.508	2.423	.015
	AVG_Smooth_Gr	-5.049	8.876	-.106	-.569	.570
	AVG_3rd_Moment	-.085	.026	-.218	-3.227	.001
	AVG_Uniformity_Gr	-18.336	4.887	-.437	-3.752	.000
	AVG_Entropy_Gr	-.363	.105	-.536	-3.470	.001
	AVG_Mean_Hue	.009	.001	.537	7.732	.000
	AVG_SD_Hue	.001	.003	.053	.225	.822
	AVG_Smooth_Hue	-6.710	1.345	-1.122	-4.990	.000
	AVG_3rd_Moment_Hue	.032	.004	.753	8.482	.000
	AVG_Uniformity_Hue	-.680	1.045	-.040	-.651	.515
	AVG_Entropy_Hue	-.027	.041	-.051	-.659	.510

Table 15 – Coefficients table of MLR model Souri variety

Model	Unstandardized Coefficients		Beta	t	Sig.
	B	Std. Error			
1 (Constant)	-3.769	.902		-4.176	.000
Area	4.20E-007	.000	.084	.483	.629
length	.000	.000	.121	2.279	.023
width	1.60E-006	.000	.000	.008	.993
Eccentricity	-.384	.098	-.108	-3.930	.000
EquiveD	.003	.001	.633	3.252	.001
Compctness	.003	.004	.013	.687	.492
MaxDist	.000	.001	-.037	-.485	.627
LengthVec	.000	.000	-.125	-2.278	.023
AVG_FD1	-.003	.001	-.116	-2.666	.008
AVG_FD2	-.002	.001	-.018	-1.461	.144
AVG_FD3	.034	.012	.854	2.729	.006
AVG_FD4	.002	.002	.011	1.241	.215
AVG_FD5	-.003	.003	-.013	-1.302	.193
AVG_RatioElong	2.705	.948	.934	2.854	.004
AVG_Av#G	-.002	.001	-.549	-1.293	.196
AVG_Var#G	.000	.000	-.661	-6.986	.000
AVG_DefectArea	.002	.001	.042	3.430	.001
AVG_Mean_Gr	.003	.001	.781	2.138	.033
AVG_SD_Gr	.022	.003	1.162	6.824	.000
AVG_Smooth_Gr	-5.797	3.976	-.217	-1.458	.145
AVG_3rd_Moment	.065	.016	.195	4.005	.000
AVG_Uniformity_Gr	8.096	2.110	.309	3.837	.000
AVG_Entropy_Gr	.087	.044	.247	1.948	.052
AVG_Mean_Hue	.002	.001	.114	1.272	.203
AVG_SD_Hue	.003	.001	.695	5.043	.000
AVG_Smooth_Hue	-2.202	.821	-.611	-2.683	.007
AVG_3rd_Moment_Hue	-.002	.003	-.086	-.719	.472
AVG_Uniformity_Hue	-1.006	.260	-.269	-3.867	.000
AVG_Entropy_Hue	-.020	.018	-.113	-1.096	.273

Table 16 – Correlation table - Picual

Feature [*]	Feature [*]	Correlation
<i>Area</i>	<i>Length</i>	0.974
<i>Area</i>	<i>Width</i>	0.971
<i>Area</i>	<i>EquiveD</i>	0.988
<i>Area</i>	<i>AVG_MaxDist</i>	0.966
<i>Area</i>	<i>AVG_LengthVec</i>	0.981
<i>length</i>	<i>EquiveD</i>	0.967
<i>length</i>	<i>AVG_MaxDist</i>	0.982
<i>length</i>	<i>AVG_LengthVec</i>	0.971
<i>width</i>	<i>EquiveD</i>	0.962
<i>width</i>	<i>AVG_MaxDist</i>	0.913
<i>width</i>	<i>AVG_LengthVec</i>	0.949
<i>Eccentricity</i>	<i>AVG_FDI</i>	-0.837
<i>Eccentricity</i>	<i>AVG_FD3</i>	0.605
<i>Eccentricity</i>	<i>AVG_RatioElong</i>	-0.633
<i>EquiveD</i>	<i>AVG_MaxDist</i>	0.978
<i>EquiveD</i>	<i>AVG_LengthVec</i>	0.993
<i>AVG_Av.Hue</i>	<i>AVG_Var.Hue</i>	0.632
<i>AVG_Av.Hue</i>	<i>AVG_3rd</i>	0.524
<i>AVG_Av.Hue</i>	<i>AVG_SD_Hue</i>	0.626
<i>AVG_Av.Hue</i>	<i>AVG_Smooth_Hue</i>	0.629
<i>AVG_Var.Hue</i>	<i>AVG_Smooth_Hue</i>	0.999
<i>AVG_MaxDist</i>	<i>AVG_LengthVec</i>	0.983
<i>AVG_FD3</i>	<i>AVG_RatioElong</i>	-0.998
<i>AVG_Var.G</i>	<i>AVG_SD_Gr</i>	0.861
<i>AVG_Var.G</i>	<i>AVG_Smooth_Gr</i>	0.869
<i>AVG_Var.G</i>	<i>AVG_Uniformity_Gr</i>	-0.549
<i>AVG_Var.G</i>	<i>AVG_Entropy_Gr</i>	0.708
<i>AVG_Mean_Gr</i>	<i>AVG_3rd Moment</i>	-0.803
<i>AVG_SD_Gr</i>	<i>AVG_Uniformity_Hue</i>	-0.565
<i>AVG_SD_Gr</i>	<i>AVG_Entropy_Hue</i>	0.642
<i>AVG_Smooth_Gr</i>	<i>AVG_Uniformity_Hue</i>	-0.538
<i>AVG_Smooth_Gr</i>	<i>AVG_Entropy_Hue</i>	0.621
<i>AVG_3rd Moment</i>	<i>AVG_Mean_Hue</i>	0.524
<i>AVG_3rd Moment</i>	<i>AVG_Entropy_Hue</i>	0.547
<i>AVG_Uniformity_Gr</i>	<i>AVG_Entropy_Gr</i>	-0.968
<i>AVG_Uniformity_Gr</i>	<i>AVG_3rd Moment_Hue</i>	-0.576
<i>AVG_Entropy_Gr</i>	<i>AVG_3rd</i>	0.551
<i>AVG_Mean_Hue</i>	<i>AVG_SD_Hue</i>	0.625
<i>AVG_Mean_Hue</i>	<i>AVG_Smooth_Hue</i>	0.628
<i>AVG_Uniformity_Hue</i>	<i>AVG_Entropy_Hue</i>	-0.944

Table 17 – Correlation table - Souri

Feature*	Feature*	Correlation
<i>AVG_RatioElong</i>	<i>AVG_FD3</i>	-0.997
<i>AVG_Entropy_Gr</i>	<i>AVG_Uniformity_Gr</i>	-0.984
<i>AVG_Entropy_Hue</i>	<i>AVG_Uniformity_Hue</i>	-0.962
<i>AVG_SD_Gr</i>	<i>AVG_Av.G</i>	-0.938
<i>AVG_SD_Gr</i>	<i>AVG_Mean_Gr</i>	-0.928
<i>AVG_Smooth_Gr</i>	<i>AVG_Av.G</i>	-0.925
<i>AVG_Mean_Gr</i>	<i>AVG_3rd Moment</i>	-0.921
<i>AVG_Smooth_Gr</i>	<i>AVG_Mean_Gr</i>	-0.92
<i>AVG_3rd Moment</i>	<i>AVG_Av.G</i>	-0.893
<i>AVG_Var.G</i>	<i>AVG_Av.G</i>	-0.891
<i>AVG_FDI</i>	<i>Eccentricity</i>	-0.882
<i>AVG_Uniformity_Hue</i>	<i>AVG_Entropy_Gr</i>	-0.871
<i>AVG_Entropy_Hue</i>	<i>AVG_Var.G</i>	0.869
<i>AVG_MaxDist</i>	<i>Area</i>	0.879
<i>AVG_MaxDist</i>	<i>EquiveD</i>	0.881
<i>AVG_SD_Hue</i>	<i>AVG_Entropy_Hue</i>	0.881
<i>AVG_Entropy_Hue</i>	<i>AVG_SD_Hue</i>	0.881
<i>length</i>	<i>Area</i>	0.882
<i>EquiveD</i>	<i>length</i>	0.883
<i>width</i>	<i>Area</i>	0.896
<i>EquiveD</i>	<i>width</i>	0.896
<i>AVG_LengthVec</i>	<i>length</i>	0.904
<i>AVG_Entropy_Gr</i>	<i>AVG_SD_Gr</i>	0.905
<i>AVG_LengthVec</i>	<i>AVG_MaxDist</i>	0.91
<i>AVG_Entropy_Gr</i>	<i>AVG_Var.G</i>	0.915
<i>EquiveD</i>	<i>AVG_LengthVec</i>	0.962
<i>AVG_LengthVec</i>	<i>EquiveD</i>	0.962
<i>AVG_Smooth_Gr</i>	<i>AVG_Var.G</i>	0.98
<i>AVG_SD_Hue</i>	<i>AVG_3rd Moment_Hue</i>	0.982
<i>length</i>	<i>AVG_MaxDist</i>	0.982
<i>AVG_SD_Hue</i>	<i>AVG_Var.Hue</i>	0.982
<i>AVG_3rd Moment_Hue</i>	<i>AVG_Var.Hue</i>	0.983
<i>AVG_Var.G</i>	<i>AVG_SD_Gr</i>	0.984
<i>AVG_Smooth_Hue</i>	<i>AVG_3rd Moment_Hue</i>	0.985
<i>AVG_SD_Hue</i>	<i>AVG_Smooth_Hue</i>	0.986
<i>AVG_SD_Gr</i>	<i>AVG_Smooth_Gr</i>	0.992
<i>AVG_Av.G</i>	<i>AVG_Mean_Gr</i>	0.994
<i>Area</i>	<i>EquiveD</i>	0.999
<i>AVG_RatioElong</i>	<i>AVG_FD3</i>	-0.997

* Defined in appendix F

Dimension reduction (Factor Analysis) –Table 18 and Table 19 show the results of the factor analysis. The results of the *Picual* analysis indicate that there are six factors with eigenvalues above 1. It can also be seen that the new six factors capture 81.23% of the variance of all features. The results of the *Souri* analysis indicate that there are five factors with eigenvalues above 1, and they capture 83.98% of the variance of all features. Figure 14 and Figure 15 show the values of the eigenvalues of the extracted components, the steep decrease in the eigenvalues of the 7th factor (*Picual*) and the 6th (*Souri*) is obvious and indicates on the small marginal contribution of the rest of the factors.

Table 20 and Table 21 show the weight of each feature in each factor. The most significant features composing each factor are highlighted. It can be seen in Table 20 that the first component in the *Picual* variety analysis is comprised mostly of features related to the size of the fruit (i.e., Area, length, Equivalent Diameter), which support the reasonable assumption that larger olives contain more olive oil. The significant features in the 2nd and the 3rd factors are related to the dispersing of the colours on the skin of the fruit (i.e., uniformity hue and gray, smoothness hue and gray, entropy hue) which are influenced mostly by the texture of the skin. The most significant features in the 4th factor are related to the average and the variance of the colour of the olives (i.e., mean hue mean green shade, variance hue). The significant features in the 5th and the 6th factors are strongly connected to the shape of the fruits (i.e., ratio elongation, compactness).

Table 21 shows the components of each factor of the *Souri* factor analysis. The most significant features composing the 1st factor are related to the green shade of the olive (i.e., variance, entropy and smoothness of green matrix). The most significant features composing the 2nd factor are strongly connected to the general hue of the olive (i.e., mean hue, Standard deviation of hue, smoothness hue). The most significant features composing the 3rd factor are mostly related to the size of the fruit (i.e., area, length, Equivalent diameter). The most significant features composing the 4th and the 5th factors are related to the shape of the fruit (i.e., eccentricity, ratio elongation).

Table 18 – Variance explained by extracted component – Picual

Total Variance Explained^a

Component	Initial Eigenvalues			Extraction Sums of Squared Loadings			Rotation Sums of Squared Loadings		
	Total	% of Variance	Cumulative %	Total	% of Variance	Cumulative %	Total	% of Variance	Cumulative %
1	8.140	27.132	27.132	8.140	27.132	27.132	5.864	19.546	19.546
2	5.708	19.026	46.158	5.708	19.026	46.158	4.522	15.074	34.621
3	3.815	12.715	58.873	3.815	12.715	58.873	4.029	13.430	48.051
4	2.663	8.877	67.750	2.663	8.877	67.750	4.022	13.408	61.459
5	2.218	7.394	75.144	2.218	7.394	75.144	3.926	13.087	74.546
6	1.828	6.094	81.238	1.828	6.094	81.238	2.008	6.692	81.238
7	.985	3.282	84.520						
8	.814	2.713	87.234						
9	.766	2.554	89.787						
10	.738	2.460	92.247						
11	.678	2.262	94.508						
12	.583	1.943	96.451						
13	.429	1.431	97.882						
14	.199	.664	98.546						
15	.148	.494	99.041						
16	.088	.295	99.335						
17	.050	.167	99.502						
18	.038	.125	99.627						
19	.030	.100	99.728						
20	.025	.084	99.811						
21	.019	.062	99.873						
22	.011	.037	99.910						
23	.007	.025	99.935						
24	.006	.020	99.954						
25	.004	.014	99.969						
26	.004	.013	99.982						
27	.002	.006	99.988						
28	.002	.006	99.994						
29	.002	.005	99.999						
30	.000	.001	100.000						

Extraction Method: Principal Component Analysis.

a. Only cases for which Variety_Code = Picual are used in the analysis phase.

Table 19 – Variance explained by extracted component – Souri

Total Variance Explained^a

Component	Initial Eigenvalues			Extraction Sums of Squared Loadings			Rotation Sums of Squared Loadings		
	Total	% of Variance	Cumulative %	Total	% of Variance	Cumulative %	Total	% of Variance	Cumulative %
1	11.625	38.748	38.748	11.625	38.748	38.748	7.413	24.709	24.709
2	5.775	19.249	57.997	5.775	19.249	57.997	5.830	19.434	44.144
3	3.944	13.148	71.146	3.944	13.148	71.146	5.384	17.946	62.090
4	2.109	7.028	78.174	2.109	7.028	78.174	4.469	14.896	76.986
5	1.744	5.812	83.986	1.744	5.812	83.986	2.100	6.999	83.986
6	.972	3.239	87.225						
7	.835	2.783	90.008						
8	.696	2.320	92.328						
9	.569	1.898	94.226						
10	.475	1.585	95.811						
11	.416	1.387	97.198						
12	.243	.811	98.009						
13	.194	.646	98.654						
14	.112	.374	99.028						
15	.091	.302	99.330						
16	.049	.164	99.494						
17	.038	.126	99.620						
18	.035	.116	99.736						
19	.020	.066	99.802						
20	.016	.052	99.854						
21	.015	.050	99.904						
22	.009	.029	99.933						
23	.008	.027	99.960						
24	.004	.013	99.973						
25	.003	.011	99.984						
26	.002	.006	99.990						
27	.002	.005	99.995						
28	.001	.004	99.998						
29	.000	.001	99.999						
30	.000	.001	100.000						

Extraction Method: Principal Component Analysis.

a. Only cases for which Variety_Code = Souri are used in the analysis phase.

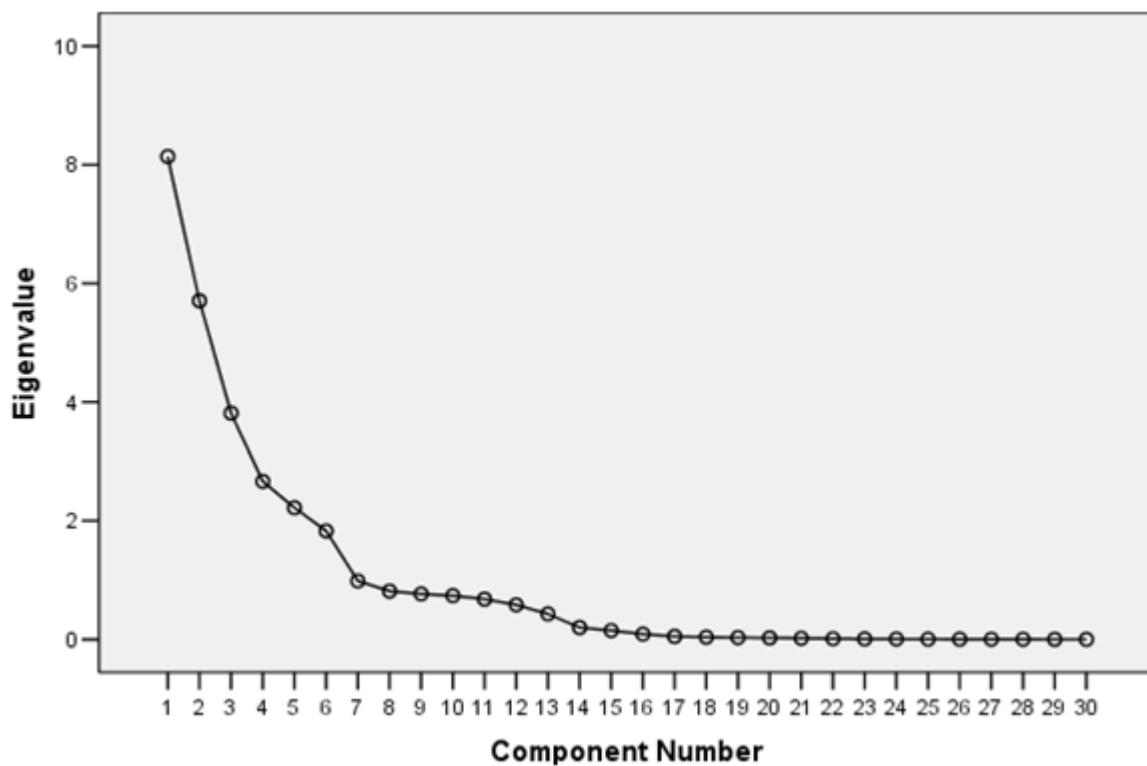


Figure 14– Eigenvalues of extracted components - *Picual*

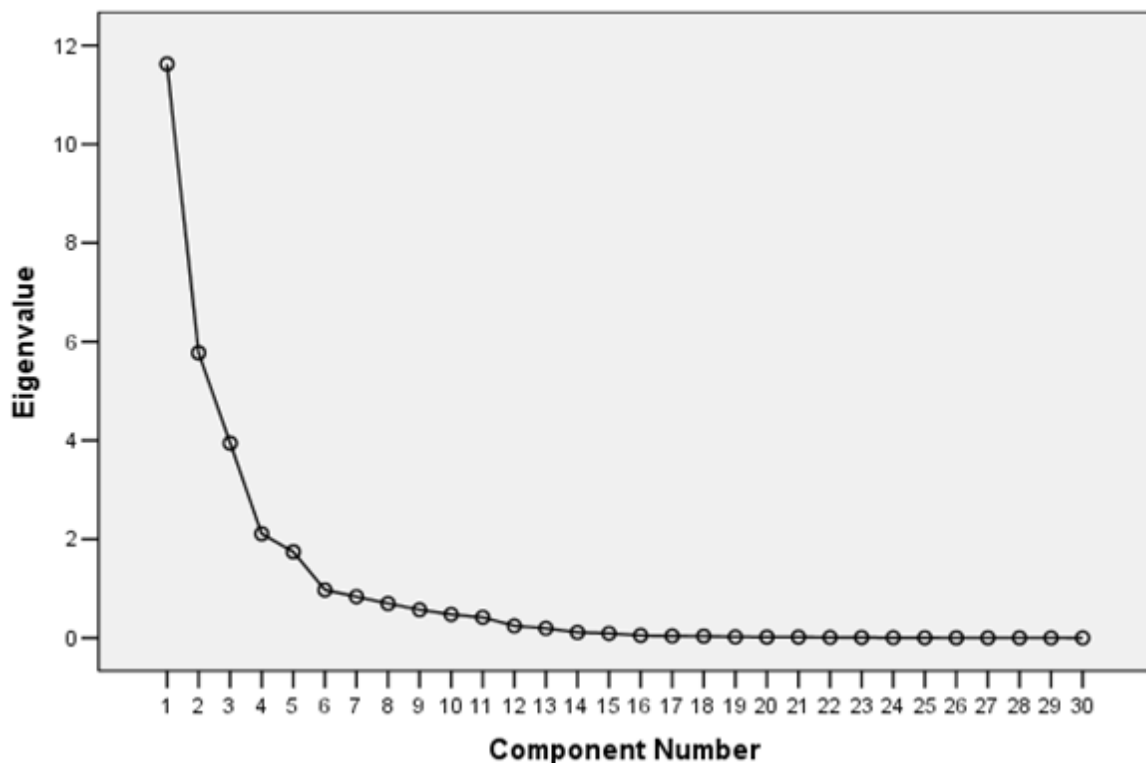


Figure 15– Eigenvalues of extracted components - *Souri*

Table 20 – Significance of extracted factors – Picual

Feature*	Component					
	1	2	3	4	5	6
Area	0.952	0.084	-0.213	0.160	0.056	-0.019
length	0.934	0.069	-0.198	0.127	0.212	0.048
width	0.933	0.097	-0.224	0.176	-0.096	-0.063
Eccentricity	0.022	-0.109	0.027	-0.080	0.827	0.342
EquiveD	0.959	0.074	-0.197	0.147	0.062	-0.013
Compctness	-0.028	0.204	-0.171	-0.037	0.355	0.305
MaxDist	0.934	0.058	-0.193	0.127	0.221	0.071
LengthVec	0.940	0.098	-0.217	0.136	0.111	0.033
AVG_FD1	-0.041	0.067	0.041	0.061	-0.810	-0.327
AVG_FD2	-0.049	-0.068	0.075	-0.095	-0.021	0.786
AVG_FD3	0.134	-0.020	-0.021	-0.003	0.909	-0.217
AVG_FD4	0.029	0.035	-0.078	0.068	0.101	0.596
AVG_FD5	0.034	-0.006	-0.011	0.037	-0.003	0.691
AVG_RatioElong	-0.135	0.023	0.022	0.008	-0.926	0.181
AVG_Av#G	-0.186	-0.108	-0.225	-0.863	0.044	-0.002
AVG_Var#G	-0.003	0.883	0.329	-0.117	-0.039	-0.014
AVG_DefectArea	0.199	0.190	-0.387	0.299	-0.022	0.004
AVG_Mean_Gr	-0.231	-0.118	0.013	-0.895	0.025	-0.015
AVG_SD_Gr	0.134	0.878	0.217	0.300	-0.058	-0.019
AVG_Smooth_Gr	0.125	0.881	0.178	0.266	-0.058	-0.014
AVG_3rd_Moment	0.230	0.418	-0.149	0.789	-0.052	0.006
AVG_Uniformity_Gr	0.165	-0.397	-0.568	0.624	-0.008	0.019
AVG_Entropy_Gr	-0.133	0.558	0.567	-0.538	-0.005	-0.026
AVG_Mean_Hue	-0.177	0.350	0.297	0.624	-0.117	-0.019
AVG_SD_Hue	-0.238	0.178	0.880	0.287	-0.088	-0.048
AVG_Smooth_Hue	-0.272	0.097	0.884	0.266	-0.086	-0.043
AVG_3rd_Moment_Hue	-0.204	-0.081	0.920	-0.096	-0.042	-0.052
AVG_Uniformity_Hue	-0.137	-0.770	0.322	-0.128	0.004	-0.027
AVG_Entropy_Hue	0.095	0.787	-0.289	0.301	0.007	0.049

Table 21 – Significance of extracted factors – *Souri*

Feature*	Component				
	1	2	3	4	5
Area	0.033	0.060	0.989	-0.009	-0.071
length	0.021	0.037	0.898	0.391	0.082
width	0.014	0.061	0.887	-0.374	-0.173
Eccentricity	-0.061	-0.026	0.060	0.896	0.287
EquiveD	0.044	0.066	0.989	-0.010	-0.064
Compctness	-0.297	-0.068	0.045	0.215	0.244
MaxDist	0.016	0.034	0.903	0.384	0.093
LengthVec	-0.068	0.028	0.963	0.081	0.024
AVG_FD1	0.062	0.050	-0.063	-0.894	-0.227
AVG_FD2	0.045	0.058	-0.058	0.040	0.807
AVG_FD3	0.011	0.011	0.071	0.880	-0.342
AVG_FD4	0.007	-0.013	-0.016	0.024	0.561
AVG_FD5	0.022	0.008	0.008	-0.121	0.748
AVG_RatioElong	-0.005	-0.006	-0.073	-0.907	0.299
AVG_Av#G	-0.730	-0.609	-0.109	0.086	0.012
AVG_Var#G	0.859	0.436	0.015	-0.110	-0.003
AVG_DefectArea	0.587	0.413	-0.002	-0.056	0.007
AVG_Mean_Gr	-0.694	-0.633	-0.120	0.075	0.008
AVG_SD_Gr	0.841	0.498	0.035	-0.093	0.001
AVG_Smooth_Gr	0.800	0.524	0.046	-0.110	-0.003
AVG_3rd_Moment	0.479	0.705	0.123	-0.106	-0.014
AVG_Uniformity_Gr	-0.926	-0.159	0.004	0.035	-0.001
AVG_Entropy_Gr	0.938	0.239	-0.002	-0.049	0.003
AVG_Mean_Hue	-0.194	0.921	0.011	0.054	0.030
AVG_SD_Hue	0.473	0.856	0.074	-0.029	0.002
AVG_Smooth_Hue	0.390	0.901	0.065	-0.043	0.000
AVG_3rd_Moment_Hue	0.413	0.856	0.082	-0.025	0.000
AVG_Uniformity_Hue	-0.830	-0.391	0.017	0.036	-0.005
AVG_Entropy_Hue	0.740	0.579	0.019	-0.027	0.007

* Defined in appendix F

4.2 Prediction models

Multiple Linear Regressions

Picual

Original data set –

Table 22 shows the results of five MLR models based on the original data set comprised of the 29 features. Each model was established based on an 80% randomly drawn data set and tested on the remains 20%. The average linear correlation was 0.757 with an average standard error of 0.138 grams.

Table 22- Original data set MLR results - Picual

	Run #1	Run #2	Run #3	Run #4	Run #5	Average
R	0.751	0.783	0.752	0.744	0.755	0.757
Standard error	0.139	0.133	0.14	0.137	0.142	0.138

Stepwise selected features –Table 23 shows the results of five MLR models obtained by the stepwise method. The average linear correlation was 0.753 with an average standard error of 0.138 grams, which is slightly worse (not statistically significant) than the original data set based model (0.757 & 0.138). The best out of the five models was comprised of only 9 features (

Table 24) as compared to 29 in the original data set.

Table 23- Stepwise MLR results - Picual

	Run #1	Run #2	Run #3	Run #4	Run #5	Average
R	0.734	0.733	0.784	0.76	0.755	0.753
Standard error	0.147	0.138	0.136	0.133	0.138	0.138

Table 24 shows the selected features by the best stepwise model of *Picual*. The best model is comprised of 9 features which are related to size color and texture of the olives. Area and width are related to the size of the olive; Mean Hue and Mean green are related to color of the skin, Defect area, Uniformity Gr, 3rd moment hue and 3rd moment are related to the texture of the skin.

Table 24– Selected model by stepwise -Picual

Features	Coefficient	stdv	Sig.
(Constant)	-0.112	0.074	0.131
width	9.56E-04	0	0
AVG_Mean_Gr	-2.47E-03	0	0
AVG_DefectArea	5.60E-04	0	0.038
Area	7.85E-07	0	0.001
AVG_3rd_Moment	-2.82E-02	0.014	0.049
AVG_Smooth_Hue	-6.61	0.667	0
AVG_3rd_Moment_Hue	3.25E-02	0.004	0
AVG_Mean_Hue	9.53E-03	0.001	0
AVG_Uniformity_Gr	-2.728	0.985	0.006

Factor analysis set – Table 25 shows the results of five ANN models obtained by the new set of factors which was produced by the FA. The average linear correlation was 0.732 with an average standard error of 0.142, which is statistically worse (P value = 0.01) than the original data set based model (0.757 & 0.138). The models were comprised of only 6 variables compared to 29 the original data set.

Table 25 - FA set MLR results -Picual

	Run #1	Run #2	Run #3	Run #4	Run #5	Average
R	0.73	0.722	0.724	0.734	0.75	0.732
Standard error	0.144	0.144	0.148	0.137	0.137	0.142

Table 26 shows the coefficients of the best model. It can be seen that not all coefficients are statistically significant and 6th factor can be excluded from the model (P value > 0.1).

Table 26– Best FA MLR model – Picual

Features	Coefficient	stdv	Sig.
(Constant)	0.622	0.004	0
FAC1_2	0.130	0.004	0
FAC5_2	6.12E-02	0.004	0
FAC3_2	-3.90E-02	0.004	0
FAC2_2	2.16E-02	0.004	0
FAC4_2	6.95E-03	0.004	0.058
FAC6_2	-1.82E-03	0.004	0.621

Souri

Original data set – Table 27 shows the results of five MLR models based on the original data set comprised of the 29 features. Each model was established based on 80% randomly drawn data set and tested on the other 20%. The average linear correlation was 0.865 with an average standard error of 0.082 grams.

Table 27 - Original data set MLR results -Souri

	Run #1	Run #2	Run #3	Run #4	Run #5	Average
R	0.847	0.881	0.864	0.86	0.876	0.865
Standard error	0.085	0.079	0.083	0.085	0.078	0.082

Stepwise selected features –Table 28 shows the results of five MLR models received by the stepwise method. The average linear correlation was 0.861 and the average standard error was 0.0861, which is slightly worse (not statistically significant) than the original data set based model (0.865 & 0.082). The best out of the five models was comprised of only 11 features (

Table 29) compared to 29 in the original data set.

Table 28- Stepwise MLR results -Souri

	Run #1	Run #2	Run #3	Run #4	Run #5	Average
R	0.855	0.873	0.843	0.856	0.881	0.861
Standard error	0.082	0.081	0.087	0.083	0.076	0.081

Table 29 shows the selected features by the best stepwise model of *Souri*. The best model is comprised of 11 features which are related to all categories of features. The EquivD is related to size of the olive, Eccentricity is related to the shape of the olive, Av_mean Gr is related to the color of the olive and 3rd moment, Defect area, SD hue, Uniformity hue, Smooth hue, SD Gr, Var G and Entropy Gr are derived from the texture of the skin. The color of the skin has only limited effect on the oil amount by this model, which expressed by average green shade of the skin. However, the derivatives of the color such as standard deviation and uniformity have a wide effect on the oil amount.

Table 29– Selected model by stepwise – Souri

Features*	Coefficient	stdv	Sig.
(Constant)	-0.851	0.094	0
EquiveD	2.94E-03	0	0
AVG_3rd_Moment	3.47E-02	0.013	0.006
Eccentricity	-0.268	0.035	0
AVG_DefectArea	2.54E-03	0.001	0
AVG_Smooth_Hue	-1.654	0.252	0
AVG_SD_Hue	2.63E-03	0	0
AVG_Uniformity_Hue	-0.844	0.094	0
AVG_SD_Gr	2.12E-02	0.002	0
AVG_Var#G	-2.55E-04	0	0
AVG_Entropy_Gr	-6.22E-02	0.014	0
AVG_Mean_Gr	1.00E-03	0	0

Factor analysis set – Table 30 shows the results of five ANN models obtained by the new set of factors which was produced by the FA. The average linear correlation was 0.847 with an average standard error was 0.085, which is slightly worse (not statistically significant) than the original data set based model (0.865 & 0.082). The models were composed of only 5 variables compared to 29 the original data set.

Table 30- FA set MLR results -Souri

	Run #1	Run #2	Run #3	Run #4	Run #5	Average
R	0.871	0.84	0.843	0.836	0.849	0.847
Standard error	0.079	0.088	0.089	0.088	0.084	0.085

* - defined in appendix F

Table 31 shows the coefficients of the best model. All coefficients are statistically significant.

Table 31– Best FA MLR model – *Souri*

Features	Coefficient	stdv	Sig.
constant	0.669	0.002	0
FAC3_1	1.07E-01	0.002	0
FAC1_1	6.03E-02	0.002	0
FAC2_1	0.055	0.002	0
FAC5_1	-1.31E-02	0.002	0
FAC4_1	0.0117	0.002	0

Artificial Neural Networks

Picual

Original data set – Table 32 shows the results of five ANN models based the original data set which comprised of the 29 features. The average linear correlation was 0.722 with an average standard error of 0.143 grams. The performances are statistically worse than the original data set MLR model (0.757 & 0.138). The P value is equal to 0.03 and 0.04 for the R T test and standard error T test respectively.

Table 32- Original data set ANN results - *Picual*

	Run #1	Run #2	Run #3	Run #4	Run #5	Average
R	0.694	0.735	0.7287	0.6993	0.7532	0.722
Standard error	0.141	0.14	0.143	0.1484	0.1439	0.143

Stepwise selected features –Table 33 shows the results of five ANN models obtained by the 9 features selected by the stepwise method. The average linear correlation was 0.734 with an average standard error of 0.139 grams, which is worse (not statistically significant) than the original data set based MLR model (0.757 & 0.138).

Table 33- Results of ANN model based on stepwise selected features - *Picual*

	Run #1	Run #2	Run #3	Run #4	Run #5	Average
R	0.7689	0.6833	0.7668	0.7517	0.7009	0.734
Standard error	0.1332	0.1466	0.1329	0.1311	0.1527	0.139

Factor analysis set – Table 34 shows the results of five ANN models obtained by the new set of factors which was produced by the FA. The average linear correlation was 0.758 with an average standard error of 0.1366, which is slightly better (not statistically significant) than the original data set based MLR model (0.757 & 0.138). The models were composed of only 6 variables compared to 29 the original data set.

Table 34- FA set ANN results -Picual

	Run #1	Run #2	Run #3	Run #4	Run #5	Average
R	0.764	0.7565	0.7537	0.752	0.768	0.758
Standard error	0.1341	0.1334	0.1341	0.1401	0.1413	0.1366

Souri

Original data set – Table 35 shows the results of five ANN models based the original data set which comprised of the 29 features. The average linear correlation was 0.855 with an average standard error of 0.0828 grams. These results are slightly worse (not statistically significant) than the original data set based MLR model (0.865 & 0.082).

Table 35 - Original data set ANN results -Souri

	Run #1	Run #2	Run #3	Run #4	Run #5	Average
R	0.8617	0.8565	0.8591	0.836	0.8619	0.855
Standard error	0.0835	0.0838	0.0821	0.0873	0.0775	0.0828

Stepwise selected features –Table 36 shows the results of five ANN models based on the features obtained by the stepwise method. The average linear correlation was 0.857 with an average standard error of 0.0832, which is slightly worse (not statistically significant) than the original data set based MLR model (0.865 & 0.082).

Table 36- Results of ANN model based on stepwise selected features -Souri

	Run #1	Run #2	Run #3	Run #4	Run #5	Average
R	0.8681	0.873	0.8245	0.8465	0.8758	0.857
Standard error	0.0785	0.0819	0.0897	0.0884	0.0777	0.0832

Factor analysis set – Table 37 shows the results of five ANN models obtained by the new set of factors which were produced by the FA. The average linear correlation was 0.861 with an average standard error of 0.080, which is slightly better (not statistically significant) than the original data set based model (0.865 & 0.082). The models were composed of only 5 variables compared to 29 the original data set.

Table 37- FA set ANN results -*Souri*

	Run #1	Run #2	Run #3	Run #4	Run #5	Average
R	0.8614	0.8476	0.8802	0.8579	0.8599	0.861
Standard error	0.0807	0.082	0.0766	0.0822	0.0808	0.080

Results' summary - Table 38 shows a summary of the results. It can be seen that in both varieties the ANN model based on the FA factors showed the best performance.

Table 38 - Average standard errors

	Original data set		Stepwise set		FA set	
	MLR	ANN	MLR	ANN	MLR	ANN
Picual	0.138	0.143	0.138	0.139	0.142	0.1366
Souri	0.082	0.0828	0.081	0.0832	0.085	0.080

4.3 Sensitivity analysis

MLR

Picual

Training/Testing proportions – Figure 16 shows the results of MLR models based on different proportions between training and testing sets of the *Picual* variety. The results are the average standard error of ten models which were obtained using different randomly drawn data sets. It can be seen from the results that the MLR based on the original data set which comprised from the 29 features is better than the FA based MLR models. Its supremacy is expressed only on the 67:33, 70:30 and 80:20 proportions, and it is statistically significant (P value = 1.8e-4). The best results were obtained by the original data set based model with a proportion of 80:20 between training and testing. The model showed a standard error of 0.1362 grams which was not statistically better than the other models.

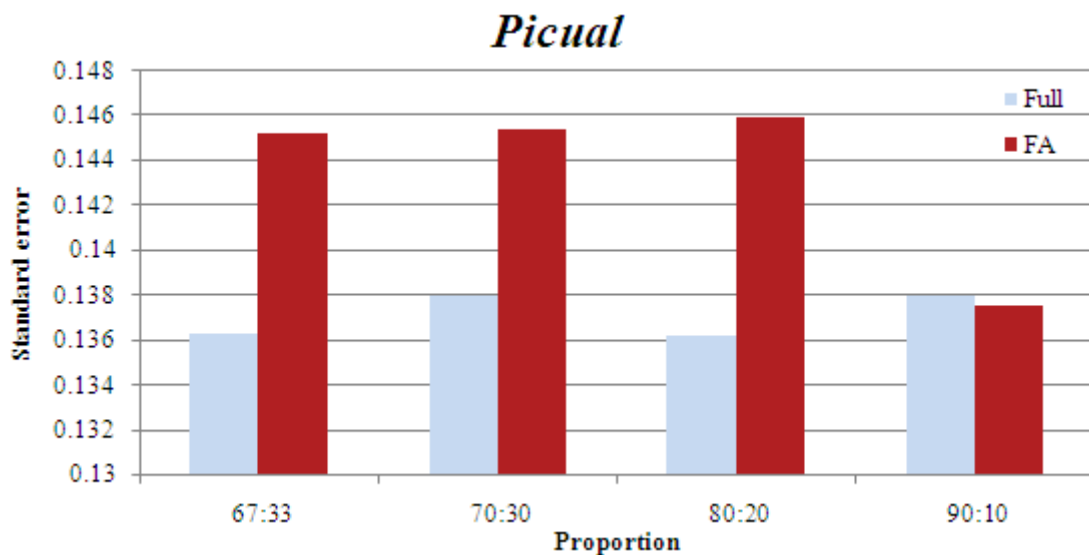


Figure 16 - Results of MLR with different proportions between training and testing - *Picual*

Figure 17 shows the results of MLR models based on different proportions between training and testing sets of the *Souri* variety. It can be seen that the original data set based model were consistently better than FA based models. Their supremacy is statistically significant (P value = 0.004). The best results were obtained by the original data set based model with a proportion of 90:10 between training and testing. The model showed a standard error of 0.0812 grams which was not statistically better than the other models.

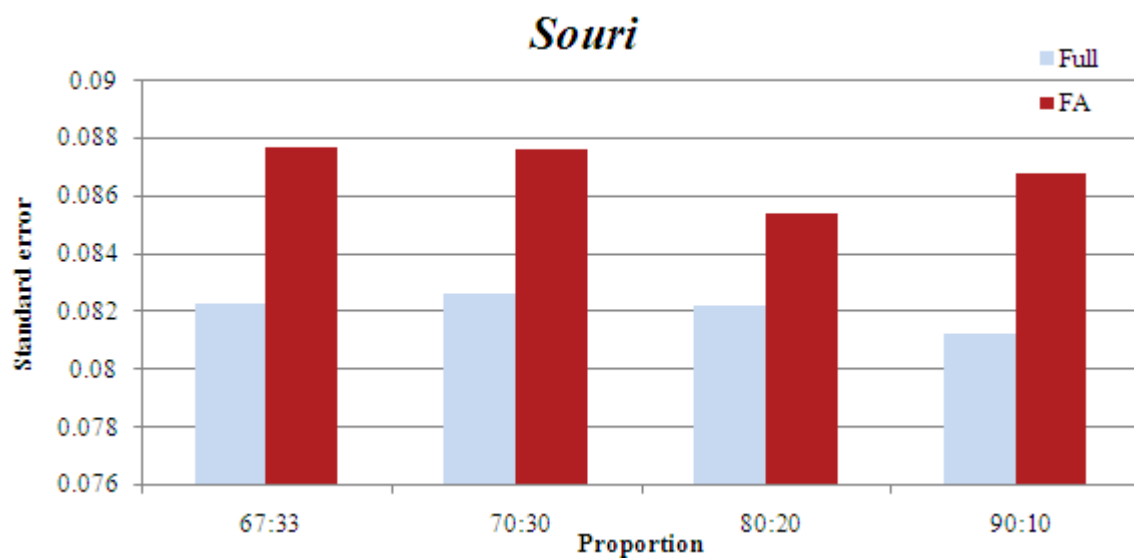


Figure 17- Results of MLR with different proportions between training and testing - *Souri*

ANN

Training/ Validating / Testing

Picual

Figure 18 shows the results obtained from ANN models trained with different proportion of data sets. 4 ratios were considered: 34:33:33, 40:30:30, 60:20:20 and 80:10:10. The results are the average standard error of ten networks that were trained each with ten different sets. It can be seen that lower proportions produce more accurate predictions, and the full model which is more complex improves more than the simple FA model. The FA model is more accurate than the full model and the best model was obtained with the proportion of 80:10:10 which obtained a standard error of 0.137 grams.

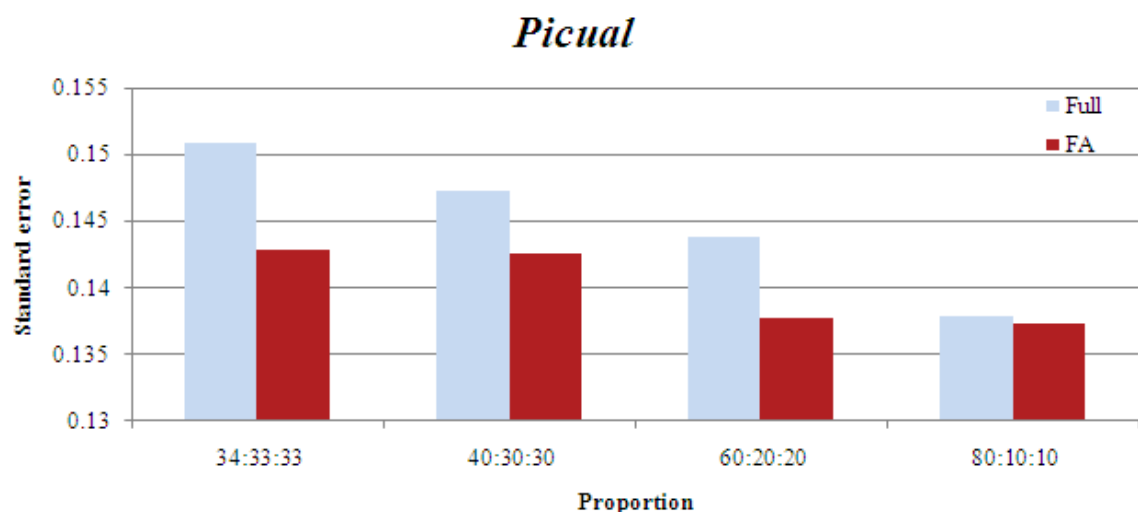


Figure 18 – Results of ANNs with different proportion between training validation and testing –

Picual

Souri

Figure 19 shows the results obtained from ANN models trained with different proportion of data sets. 4 ratios were considered: 34:33:33, 40:30:30, 60:20:20 and 80:10:10. The results are the average standard error of ten networks that were trained each with ten different sets. It can be seen that lower proportions produce more accurate predictions, and the full model which is more complex improves more than the simple FA model. The FA model was more accurate than the full model when the proportions were 34:33:33, 40:30:30 and 60:20:20 (P value < 0.01). The best model was obtained with the proportion of 80:10:10 which obtained a standard error of 0.0823 grams.

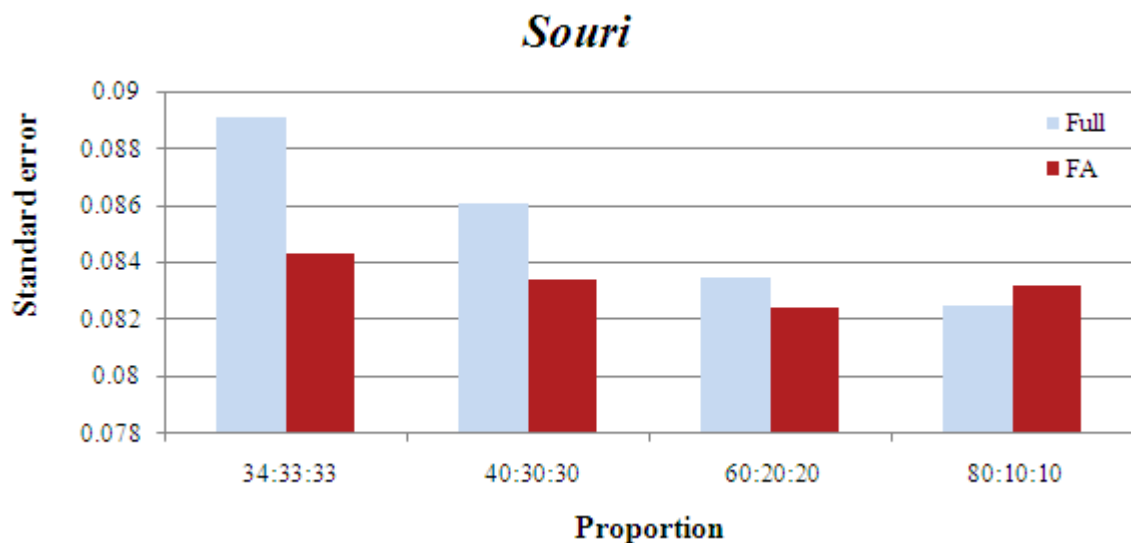


Figure 19 – Results of ANNs with different proportion between trainning validation and testing –
Souri

Topology

Picual

ANNs with different topologies were considered: 29:29:1, 29:20:2, 29:15:1, 29:10:1, 29:5:1, 29:3:1, 29:2:1 and 29:1. Figure 20 shows the results of ANN models with the mentioned topologies. The results are the average standard error of ten networks that were trained each with ten different sets. It can be seen that models based on FA are consistently better than the original data set based models (P value <0.01). The best model was the model with topology of 29:29:1 which obtained a standard error of 0.1386 grams which was not statistically significant.

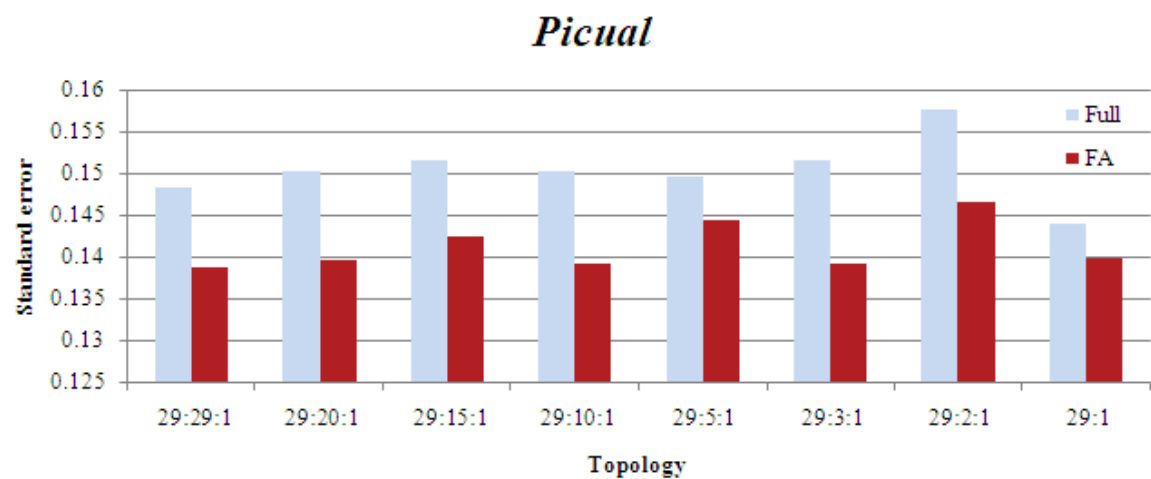


Figure 20 - Results of ANNs in different topologies (Input, Hidden and Output) - Picual

Souri

Figure 21 shows the results of ANN models with the mentioned topologies. The results are the average standard error of ten networks that were trained each with ten different sets. It can be seen that models based on FA are consistently better than the original data set based models (P value <0.01). The best model was the model with topology of 29:15:1 which obtained a standard error of 0.0813 grams which was not statistically significant.

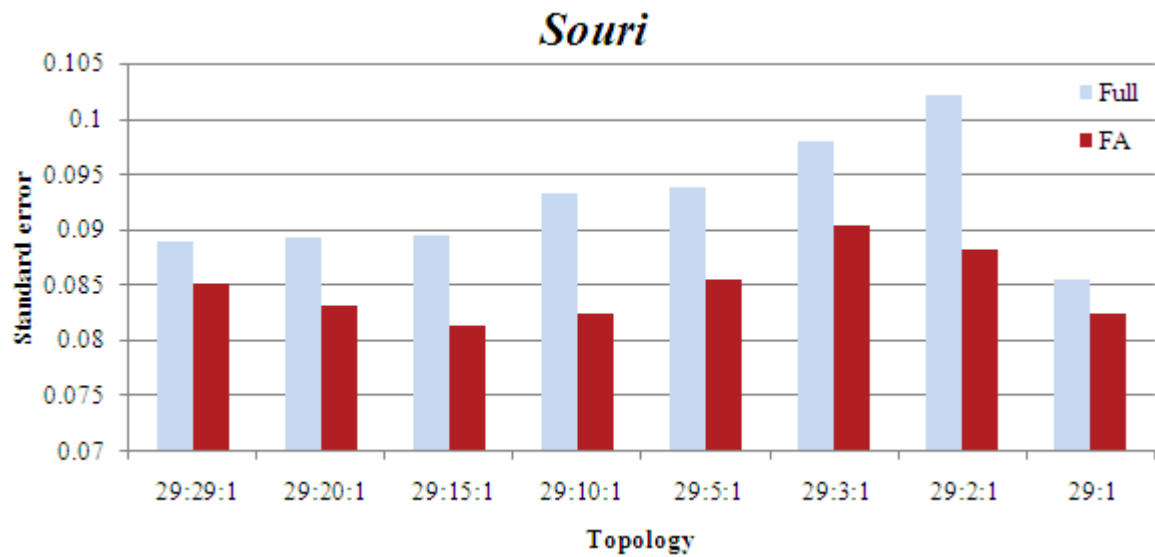


Figure 21 - Results of ANNs in different topologies (Input, Hidden and Output) - Souri

Transfer function

Picual

ANN models with three transfer functions were considered in each layer: Tangents sigmoid, Log sigmoid and pure line. Figure 22 shows the results of the results ANN models with the mentioned transfer functions. The results are the average standard error of ten networks that were trained each with ten different sets. It can be seen that the transfer functions that obtained the best prediction accuracy for FA based models are the log sigmoid in the first layer and the pure line in the second layer and a pure line transfer function in both layers for original data set based models. The FA based model with the structure of log sigmoid, log sigmoid showed the best performance with a standard error of 0.1377 grams. The results were not statistically significant. The supremacy FA based models was not consistent through all structures and in some structures the full features based model showed better performance. The structure of pure line as the transfer function of the first layer and log sigmoid as transfer function of the second layer showed extremely poor performance in both varieties.

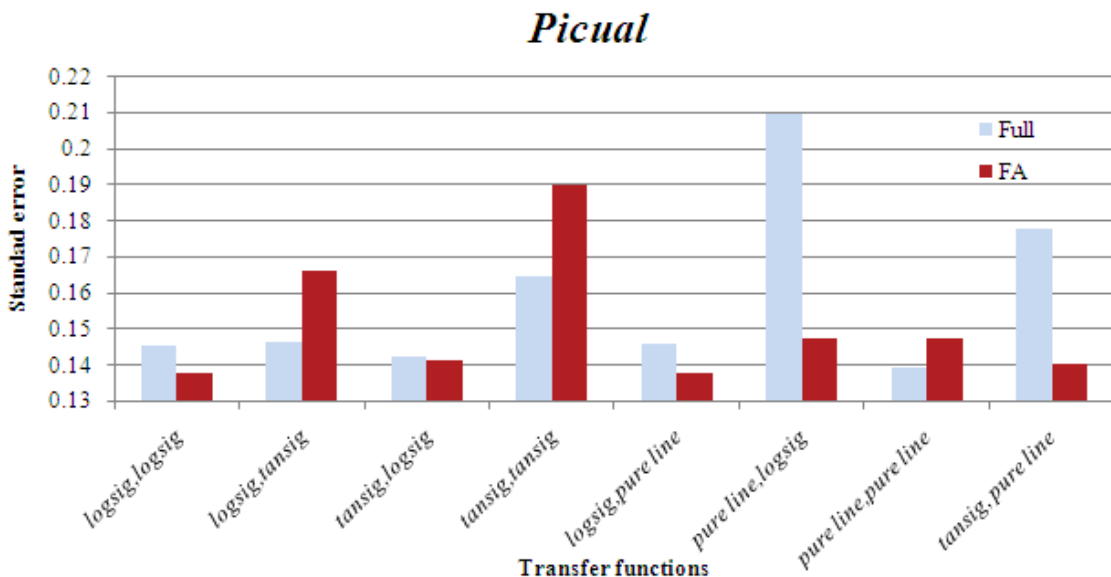


Figure 22 – Results of different transfer functions – *Picual*

Souri

Figure 23 shows the results of the results ANN models with the motioned transfer functions. The results are the average standard error of ten networks that were trained each with ten different sets. It can be seen that the structure of log sigmoid as the transfer function of the first layer and pure line as the transfer function of the second layer has the best prediction accuracy for FA based models, and transfer function of log sigmoid in both layers for original data set based models. The FA based model with the structure of log sigmoid, pure line showed the best performance with a standard error of 0.0779 grams. The results were statistically significant (P value < 0.01). The structure of pure line as the transfer function of the first layer and log sigmoid as transfer function of the second layer showed extremely poor performance in both varieties.

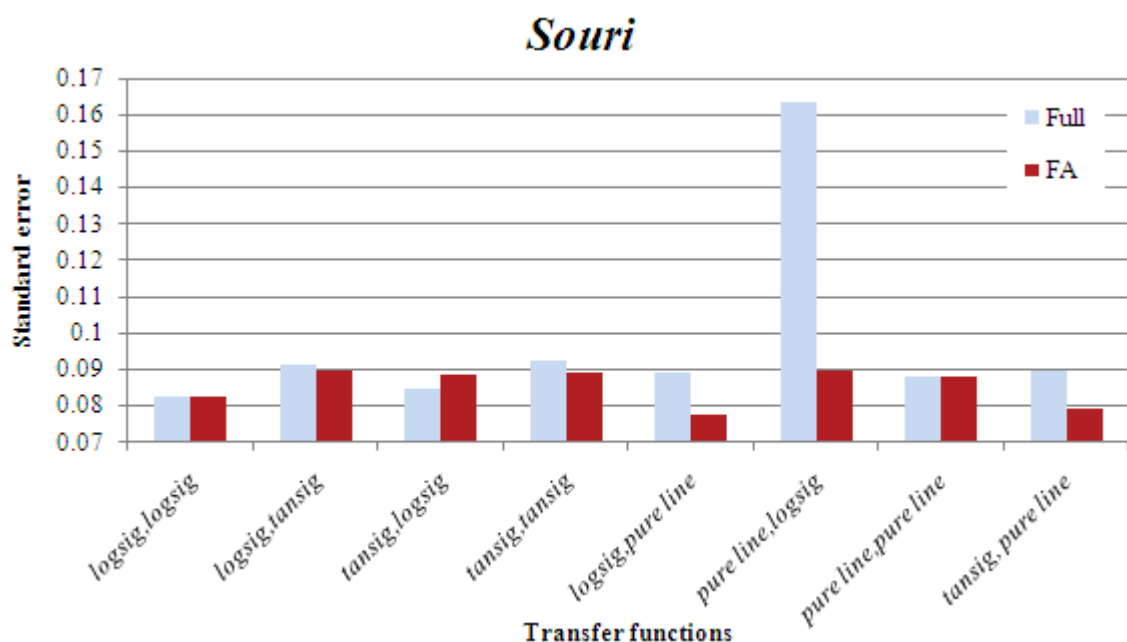


Figure 23 – Results of different transfer functions – *Souri*

4.4 Best prediction model

T tests were performed in order to determine the best proportion, topology and structure of the prediction model for each variety. The best prediction model for each variety is proposed based on the results. For each variety the network structure that had best performance was chosen and trained 100 times, in each of the training sessions with different initial weights. Based on the assumption that new inputs will have the same attributes as the current input, each of the final networks was simulated

on 100 random sets drawn from the inputs and the network with the lowest average standard error was selected.

Picual Model

The best prediction model for *Picual* olives was composed of a network with a topology of 29:1 with a log sigmoid transfer function in both layers and proportion of 80/10/10 between training validating and testing (Figure 24).

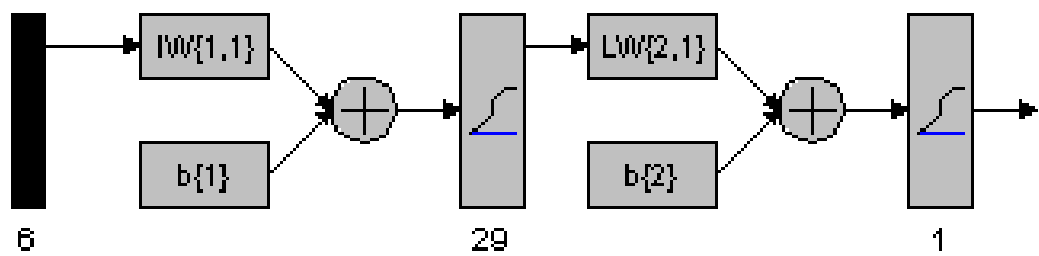


Figure 24 – Structure of best model - *Picual*

The selected network showed an average standard error of 0.1201 gr. with a standard deviation of 4.36e-04. This performance reflects a linear correlation of 0.817 between the predicted value and the actual value of the oil amount (Figure 26) which is a decrease of 11.4% from the standard error of the full MLR model. The weights and biases of network can be found in appendix G.

Souri Model

The best prediction model for *Souri* olives was composed of a network with a topology of 29:1 with a log sigmoid transfer function in the first layer and a pure line transfer function in the second. The proportion between training validating and testing was 60/20/20 (Figure 25).

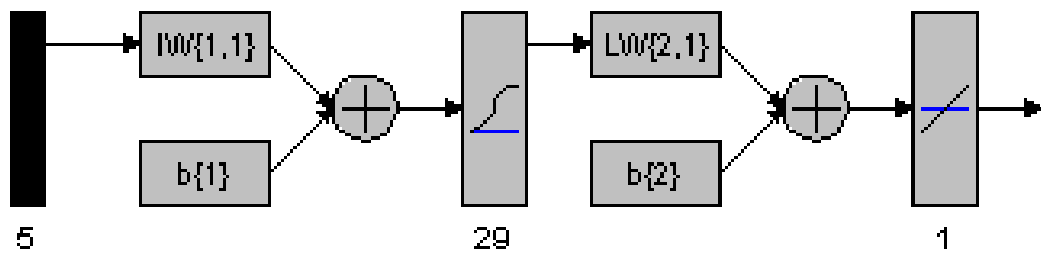


Figure 25 – Structure of best model - Souri

The selected network showed an average standard error of 0.0764 gr. with standard deviation of 3.14e-04. This performance reflects a linear correlation of 0.876 between the predicted value and the actual value of the oil amount (Figure 27) which is a decrease of 9.7% from the standard error of the full MLR model. The weights and biases of network can be found in appendix G.

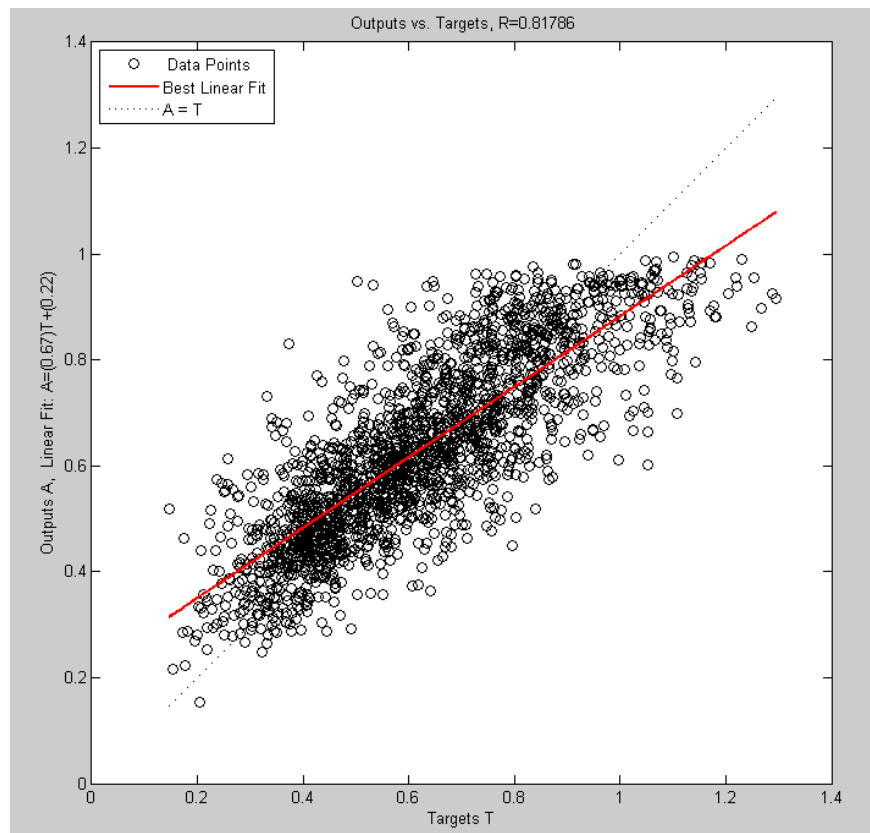


Figure 26 – Regression between best model prediction and actual values - Picual

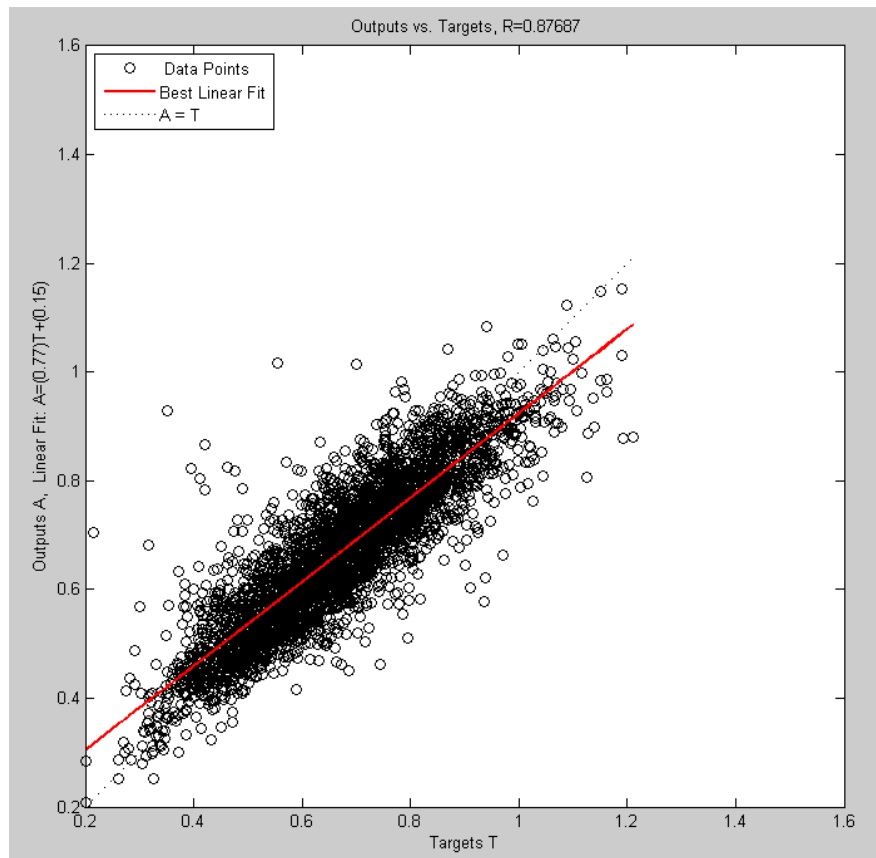


Figure 27 – Regression between best model prediction and actual values - Souris

5. Discussion

The experimental results obtained in the present study clearly show that the olive oil percent increases constantly throughout the olives growing season until the oil accumulation stops at a certain point. As claimed by *Vossen* (2004) and *Mailer* (2005) the reason for this is the decline in the olives' weight due to loss of moisture in the rotting process. The conclusion from these findings is that seeking the maximum oil percent will not necessarily lead to full exploitation of the oil potential in the olives' grove.

The olives fallout rate is rarely considered when looking for the optimal harvest time. Many studies intending to find the optimal harvesting time did not consider this issue as a factor (Mailer et al., 2005; Romero & Diaz, 2002; Salvador et al., 2001). *Beltran et al* (2004) addressed this issue and suggested that olive groves should be harvested earlier because of the increasing fallout. In the current experiment the fallout was found constant at the beginning of the season, but rapidly increased before the oil fully accumulated in the olives. Hence, in order to determine the point when the oil potential is at its maximum level, it is necessary to determine the point where the rate of potential oil loss caused by olives fallout is equal to the rate of potential oil gained by the natural process of oil accumulation in the fruits. To calculate this equilibrium it is necessary to know the fruits' weight on the tree.

Fallout rate and the proportion of black olives to green olives were found very similar in their behavior. The small numbers of observations prevent a valid statistical analysis, however based on the similar behavior it was concluded that there is a good chance to establish a prediction model for the fallout rate based on this proportion, and such data may provide the main information necessary to determine the optimal harvesting time.

The features extracted from the images of both sides of the olives were found statistically different. The meaning of this phenomenon is that although the pictures of both sides were taken consecutively one after the other, and the only action taken in between is manual reversal of the olives on the plate, there is a consistent change between the extracted features. A possible cause for this phenomenon could be inaccuracies in the measurements caused by the act of reversing the olives. This could have been caused by the changed photographing angle resulting from slight

movements in the position of the plate relative to the camera. Even though these differences were minor and probably did not significantly affect the results, it is important that they are eliminated in future experiments so the plate should have a fixed position. To the best of our knowledge no reports of such phenomenon were yet reported.

In the MLR test it was found that there is an advantage to combine values of features received from the analysis of both sides of the olive images. This advantage raises the need to further investigate if a larger number of images of each olive and more sophisticated combination of data will increase the accuracy of the model.

Many of the features were found extremely highly correlated between themselves. This high correlation is derived from natural relations that exist between some features. An example for such a relation is the relation between the area, length and width. This relation is not perfect because the shape of the olive is undefined and there is not a specific formula that describes this relation, but it is probable to find that increase in one will be followed by increase in the other and vice versa. In color related features there is also high correlation derived from the natural ripening process of olives. When the olive changes its color from yellow to purple it also becomes darker, which implies that its average hue increases together with its average brightness (which is represented by the average gray feature). When the olive changes its color from green to yellow it becomes brighter which implies its average green decreases when its average gray increases. This phenomenon affects the standard deviations of the coefficients in the MLR model and in fact reduces the level of certainty of its accuracy. The implication of such a situation can cause the model to over fit the data set and a probable reduction in its accuracy on different sets with different multi-collinearity (Yu, 2008), which must be considered in future research.

The problem of high multi-collinearity was treated by Principal Component Analysis (PCA) in order to extract a new uncorrelated set of features (factors). Each factor is a linear combination of the original features. The next step was rotation of the axes in a way that highlights the most important features in each factor, and enables simple interpretation of each factor. The Factor Analysis (FA) process created a set of factors which are rated by their effect on the oil amount in the olive and are comprised from a group of features related to characteristics of the olive.

Based on the FA the order of importance of the characteristics affecting the oil amount in *Picual* olives is: size, texture, color and shape and in *Souri* olives is: color, texture, size and shape. In both varieties shape was found the least significant feature and texture was rated second. The difference of the importance of the color feature in both varieties could be caused from different reasons which could be natural or experiment dependent such as late sampling period which prevented it from covering the whole range of color changes. The changes of olives along the ripening period were studied by *Beltran et al.* (2004) and *Mailer et al.* (2005). They documented the average weight and the average MI of several varieties. They found out that the changes in the mentioned attributes occurs at different times and depend on the variety and the water abundance. These findings are in line with the claim of late sampling.

The aim of this research was to examine the ability to predict the oil amount in a certain olive based on the features extracted from its image. The models that were examined in this work were Artificial Neural Network (ANN) and Multiple Linear Regression (MLR). Several network structures were tested with two input sets (original data set and factors extracted by FA).

The chosen ANN best model of both varieties had 10% smaller standard error when compared to actual oil amount (determined from NMR) and was consistent over different data sets (differences between performances on different data sets were close to zero). One concern that should be considered before using these prediction models on new data sets is changes in the characteristics of the data due to natural differences between groves or seasons (*Rial & Flaque*, 2003). These differences if exist should be considered in future research.

Significant difference between the varieties was found consistently. The oil amount was found different by the ANOVA test, when different factors were extracted for each variety and eventually a different network structure was found as the best model for each variety. These findings indicate on profound differences in the qualities and appearances of different olive varieties. These findings are supported by the findings of *Laykin et al.* (2008) which developed classification models for 21 varieties of table olives. In Laykin's model maximum accuracy was obtained only when each variety had a different model.

6. Summary and Future Work

6.1 Summary

In this work, a prediction model of the oil content in an intact olive was established based on the features extracted by processing its images. Samples *Souri* and *Picual* olives varieties were taken weekly during a 9 weeks ripening season. The sampled olives were photographed from both sides by a color digital camera and their oil content was measured later (after 72 hours) by LR-NMR.

Twenty nine features derived from the size, shape, texture and color were received from the image processing program for each image of the olive. Since there was a significant difference between the same features of different sides a combination of the different sides' features was included in the prediction model. This included the maximum value of size related features and the average value of other features. The combined features presented better fitting in a regression when the model was compared to all single side features regression models.

The oil content in both varieties were analyzed by ANOVA and found statistically different, which indicated two separate populations. High correlations between features were found due to natural embedded effects exists between features which were treated by factor analysis. The 29 features of each variety were analyzed by factor analysis which included PCA and axes rotation (which was made by Equamax). This analysis produced new sets of five and six uncorrelated factors composed from the original 29 of the *Souri* and the *Picual*, respectively. Each factor was comprised mostly from features derived from one characteristic of the olive where the texture was found highly affecting the oil amount and the shape was found the least affecting the oil amount.

The ANN prediction models of the oil amount based on the new factors and the original features was found better than a multiple linear regression (MLR) model for all input sets.

The network's structure which showed the best performance for each variety was selected. The final *Picual* model had a standard error of 0.1201 grams with a linear correlation 0.81 and the *Souri* model had a standard error of 0.0764 grams with a linear correlation of 0.87. The chosen models were 10% better than the MLR models.

6.2 Future Work

In order to validate the repeatability of the models in different seasons, it is necessary to perform an additional experiment. The experiment should include samples of *Souri* and *Picual* olives from the same groves which will be photographed in the same conditions. The images will be processed and the extracted features will be used to calculate the estimated oil amount by the proposed model. The results of the model will be compared to the real value which will be measured by any other accurate technique such as NMR.

The benefit of higher resolutions images of each olive can be examined in an experiment. The experiment can be conducted in a similar methodology, but instead taking higher resolution pictures of each olive. The benefit of improving resolution can be measured by establishing models based on data from the new pictures and compare them to the current models. Eventually the optimal resolution of pictures can be found. In the same way, different methods for combining the data from pictures of different sides can be compared and the best method can be found.

In this research we found a correlation between the olives' fallout and the proportion of black olives. An additional experiment should be conducted to establish a model which will be able estimate the fall out rate and together with the current model estimate the total loss of potential oil. The experiment should include collecting the fallout of certain amount of trees every week for several weeks and in parallel taking samples of olives from the same trees. The proportion of black olives in each sample will be calculated and the correlation to the fallout will be found. The amount of selected trees should be large enough to enable valid statistical analysis, and the time range should be long enough to capture all the changes in colors and in the fallout rate. The difference between varieties should be considered. The current image processing can be used for color classification of the olives in the sample in order to save on labor in the future.

In order to estimate to the total amount of oil potential in the grove it is necessary to design a sampling plan which will cover enough olives and enough trees in the grove. The plan should consider the variance between trees and the variance within trees. These variances can be analyzed by two way ANOVA test. Based on the variances it will be possible to establish a confidence interval of the average oil amount in the olives in the grove. Although the knowledge of the average oil amount is sufficient in

order to make a decision on the best harvest time the estimation of the total oil potential can provide extra information which can be useful for income estimation. This can be obtained by estimating the amount of olives on the trees and multiplies it by the average oil amount. This requirement is not straightforward and will probably be the most difficult.

The current results showed an obvious difference in the obtained models of each variety. This issue can be a problem for growers who grow several varieties in their grove which is a common practice. This issue can be solved by designing a single general model for all olive varieties. One option for such a model is to combine the proposed model with an olive variety classification model which will be applied as a preliminary stage before estimating the oil amount. The general process should include image acquisition, image processing, feature extraction, variety classification and oil content estimation by the appropriate model. The significant differences that were found between varieties will enable to easily develop such a model.

7 .References

1. Abdullah M. Z., Guan L. C. 2002. Color vision system for ripeness inspection of oil palm '*Elais Guineensis*'. Journal of Food Processing Preservation 26: 213-235.
2. Angerosa F., Giacinto A. D., Vito R., Cumitini S. 1996. Sensory evaluation of virgin olive oils by artificial neural network processing of dynamic headspace gas chromatographic data. Journal of the Science of Food and Agricultural 72:323-328.
3. Ariana D., Lu R., Guyer D., 2006. Near-infrared hyper spectral reflectance imaging for detection of bruises on pickling cucumbers. Computer and Electronics in Agriculture 53:60-70.
4. Beltran G., del Rio C., Sanchez S., Martinez L. 2004. Seasonal changes in olive fruit characteristics and oil accumulation during ripening process. Journal of the Science of Food and Agriculture 84:1783:1790.
5. Bertram H. C., Wu Z., Van den Berg F., Andersen H. J. 2006. NMR relaxometry and differential scanning colorimetric during meat cooking. Meat Science 74: 684-689.
6. Bishop C. M., 1995. Neural networks for pattern recognition. Oxford University Press. Oxford, UK.
7. Blasco J., Aleixos N., Molto E. 2007. Computer vision detection of peel defects in citrus by means of a region oriented segmentation algorithm. Journal of Food Engineering 81: 535–543.
8. Brescia M. A., Pugliese T., Hardy E., Sacco A. 2007. Compositional and structural investigations of ripening of table olives, Bella della Daunia, by means of traditional and magnetic resonance imaging analyses. Food Chemistry 105: 400–404.
9. Cardoza L.A., Korir A.K., Otto W.H., Wurrey C.J., Larive C.K. 2004. Applications of NMR spectroscopy in environmental science. Elsevier. 49: 209-238
10. Carvajal R., A. Nebot 1998. Growth model for white shrimp in semi-intensive farming using inductive reasoning methodology. Computers and Electronics in Agriculture 19: 187-210.
11. Charlton A. J., Farrington W., Brereton P. 2002. Application of ^1H NMR and Multivariate Statistics for Screening Complex Mixtures: Quality Control and

Authenticity of Instant Coffee. *Journal of Agriculture and Food Chemistry* 50: 3098-3103

12. Chen Y. R., Chao K., Kim S. M. 2002. Machine vision technology for agricultural applications. *Computers and Electronics in Agriculture* 36: 173-191.
13. Cosio S., Ballabio D., Benedetti S., Gigliotti C. 2006. Geographical origin and authentication of extra virgin olive oils by an electronic nose in combination with artificial neural networks. *Analytica Chimica Acta* 567 :202–210
14. Darper N., Smith H. 1981. *Applied Regression Analysis*, 2nd edition, John Wiley and Sons pp. 307-312. NY, USA.
15. Diaz R., Faus G., Blasco M., Molto E. 2000. The application of a fast algorithm for the classification of olives by machine vision. *Journal of Food Engineering Food Research International* 33: 305-309.
16. Diaz R., Gil L., Serrano C., Blasco M., Molto E., Blasco J. 2004. Comparison of three algorithms in the classification of table olives by means of computer vision. *Journal of Food Engineering* 61: 101–107.
17. Fang Q., Biby G., Haque E., Hanna M. A., Spillman C. K. 1998 Neural network modeling of physical properties of ground wheat. *Cereal Chemistry* 75(2):251:253.
18. Ghazanfari A., Irudayaraj J., Kusalik A., Romanuk K. 1997. Machine vision grading of pistachio nuts using Fourier descriptions. *Journal of Agricultural Engineering Research* 68:247-252.
19. Grzesiak W., Błaszczyk P., Lacroix R. 2006. Methods of predicting milk yield in dairy cows—Predictive capabilities of Wood's lactation curve and artificial neural networks (ANNs). *Computers and Electronics in Agriculture* 54: 69–83
20. Guyer D., Yang W. 2000. Use of genetic artificial neural networks and spectral imaging for defect detection on cherries. *Computers and Electronics in Agriculture* 29:179-194.
21. Guo Q., Wu W., Massat D. L., Boucon C., de Jong S. 2002. Feature Selection in Principal Component Analysis of Analytical Data. *Chemometrics and Intelligent Laboratory Systems* 61:123-132
22. Harman, H. H., 1976. *Modern Factor Analysis*. 3rd edition, University of Chicago Press. Chicago, USA.

23. Haung Y., Kangas L., Rasco A. B. 2007. Applications of artificial Neural Networks (ANNs) in Food Science. *Critical Reviews in Food Science and Nutrition* 47:113-126.
24. Ho Yu C. 2008. Multi-collinearity Variance Inflation and Orthogonalization in Regression. <http://www.creative-wisdom.com/computer/sas/collinear.html>
25. Hueso J. J., Perez M., Alonso F., Cuevas J. 2007. Harvest prediction in 'Algerie' loquat. *International Journal of Biometeorol* 51:449-455.
26. Kanali C., Murase H., Honami N. 1998. Three dimensional shape recognition using a charge simulation method to process primary image features. *Journal of Agricultural Engineering Research* 70:195-208.
27. Kaul M., Hill L. R., Walthall C. 2005. Artificial neural networks for corn and soybean yield prediction. *Agricultural Systems* 85:1-18.
28. Kelly C. T. 1999. Iterative Methods for Optimization. Society for Industrial and Applied Mathematics. Raleigh, North Carolina.
29. Kin S. M., Chen P., McCarthy M. J., Zion B., 1999. Fruit Internal Quality Evaluation using On-line Nuclear Magnetic Resonance Sensors. *Journal of Agricultural Engineering Research* 74:293-301.
30. Kim Y., Street N. W., Merezer F. 2003. Feature Selection in Data Mining. Idea Group Inc. 5:80-106
31. Knight K. 1990. Connectionist, ideas and algorithms. *Communication ACM* 33(11):59-73.
32. Kominakis A. P., Abas Z., Maltaris I., Rogdakis E. 2002. A preliminary study of the application of artificial neural networks to prediction of milk yield in dairy sheep. *Computers and Electronics in Agriculture* 35:35-48.
33. Kondo N., Ahmad U., Monta M., Murase H. 2000. Machine vision based quality evaluation of lyokan orange fruit using neural networks. *Computers and electronics in agriculture* 29:135-147.
34. Laykin S., Alchanatis V., Edan Y. 2002. Image processing algorithms for tomato classifications. *Transactions of ASAE* 45(3): 851–858.
35. Laykin S., Alchanatis V., Edan Y., Weisman Z. 2008. Image processing algorithms for table olives classification. *International Conference on Agricultural Engineering* 2008: OP-2090

36. Lee K., Choi W., Noh S., Kang S., Son J., Kim G. 2008. Nondestructive determination of soluble solid contents for watermelon using optical characters. International Conference on Agricultural Engineering 2008:OP-950.
37. Lotze E., Bergh. 2004. Early prediction of harvest fruit size distribution of an apple and pear cultivar. *Scientia Horticularae* 101:281:290
38. Luchetti F. 2002. Importance and future of olive oil in the world market – an introduction to olive oil. *European Journal of Lipid Science and Technology*. 104: 559-563.
39. Machado R. M. A., Bussieres P., Koutsos T., Prieto M. H., Ho L. C. 2004. Prediction of optimal harvest date for processing tomato based on accumulation of daily heat units over the fruit ripening period. *Journal of horticultural science and biotechnology* 79:452-457.
40. Mailer R., Conlan D., Ayton J. 2005. Harvest timing for optimal olive oil quality. Rural Industries Research and Development Corporation 05/013.
41. Marcelis L. F. M., Gijzen H. 1998. Evaluation under commercial conditions of a model of prediction of the yield and quality of cucumber fruits. *Scientia Horticularae* 76: 171-181.
42. Martin G. Y., Oliveros C. C., Pavon J. L. P., Pinto C. G., Cordero B. M. 2001. Electronic nose based on metal oxide semiconductor sensors and pattern recognition techniques: characterization of vegetable oils. *Analytica Chimica Acta* 449: 69-80
43. Mendoza L., Aguilera J.M. 2004. Application of image analysis for classification of ripening bananas. *Journal of Food Science* 69: 471-477.
44. Mili S. 2004. Prospects for Olive Oil Marketing in Non-traditional Markets. International Conference of Sustainable Development and Globalization of Agri-Food Markets :Session 10
45. Morello J. R., Romero M. P., Motilva M. J. 2006. Influence of Seasonal Conditions on the Composition and Quality Parameters of Monovarietal Virgin Olive Oils. *Journal of the American Oil Chemists' Society* 83: 683-690.
46. Noordam J., van de Broek W., Buydens L., 2005. Detection and classification of latent defects and diseases on raw French fries with multispectral imaging. *Journal of the Science of Food and Agriculture* 85:2249-2259.
47. Nordon A., McGill C. A., Littlejohn D. 2001. Process NMR spectrometry. *Analyst*. 126: 260-272.

48. Ogrinc N., Kosir I. J., Spamgenberg J. E. Kidric J. 2003. The application of NMR and MS methods for detection of adulteration of wine, fruit juices and olive oil. *Analytical Bioanalytical Chemistry* 376: 424-430.
49. Rezzi S., Axelson D. E., Héberger K., Reniero F., Mariani C., Guillou C. 2005. Classification of olive oils using high throughput flow ^1H NMR fingerprinting with principal component analysis, linear discriminant analysis and probabilistic neural networks. *Analytica Chimica Acta*. 552:13–24.
50. Rial D. J., Falque E. 2003. Characteristics of olive fruits and extra-virgin olive oils obtained from olive trees growing in Appellation of Controlled Origin ‘Sierra Maǵina’. *Journal of the Science of Food and Agriculture* 83:912:919.
51. Romero A., Díaz I., Tous, J. 2002. Optimal harvesting period for "Arbequina" olive cultivar in Catalonia (spain). IV International Symposium on Olive Growing 586:393-396.
52. Saito Y., Hatanaka T., Katsuji U., Hidekazu S. 2003. Neural Network Application to Eggplant Classification. *Lecture Notes in Computer Science* 2774:933-940.
53. Salehi F., Lacroix R., Waid K. M. 1998. Improving dairy yield predictions through combined record classifiers and specialized artificial neural networks. *Computers and Electronics in Agriculture* 20:199-213.
54. Salehi F., Lacroix R., Waid K. M. 2002. Development of neuro-fuzzifiers for qualitative analyses of milk yield. *Computers and Electronics in Agriculture* 28:171-86.
55. Salvador M.D, Aranda F., Fregapane G. 2001. Influence of fruit ripening on 'cornicabra' virgin olive oil quality. A study of four successive crop seasons. *Food Chemistry* 73: 45-53.
56. Saranwong S., Sornsrivichai J., Kawano S. 2004. Prediction of ripe-stage eating quality of mango fruit from its harvest quality measured nondestructively by near infrared spectroscopy. *Postharvest Biology and Technology* 31:137–145.
57. Sato T. 1994. Application of principal component analysis on Near Infrared spectroscopic data of vegetable oils for their classification. *Japan Canada Oil Sands Limited* 71:1-6.
58. Schmilovich Z., Hoffman A., Egozi H., Ben-Zvi R., Bernstein Z., Alchanatis V. 1999. Maturity determination of fresh dates by near infra red spectrometry. *Journal of Science of Food and Agriculture* 79:86-90.

59. Taurino A., Capone S., Epifani M., Rella R., Siciliano P. 2002. Recognition of olive oils by means of an integrated sol-gel SnO₂ Electronic Nose. *Thin Solid Films* 418:59-65.
60. Thygesen L.G., Thybo A.K., Engelsen S.B. 2001. Prediction of Sensory Texture Quality of Boiled Potatoes From Low-field¹H NMR of Raw Potatoes. The Role of Chemical Constituents. *Lebensmittel-Wissenschaft und-Technologie* 34: 469-477.
61. Uylaser V., Tamer C., Inceday B., Vural H., Copur O., 2008. The quantitative analysis of some qulity criteria of Gemlik quality olives 6:26-30.
62. Vogl, T.P., Mangis J.K., Rigler A.K., Zink W.T., Alkon D.L. 1988. Accelerating the convergence of the backpropagation method, *Biological Cybernetics* 59: 257-263.
63. Vossen P. 2004. Variety and maturity the two largest influences on olive oil quality. University of California Cooperative Extension.
64. Vossen P. 2007. Current Opportunities in the California Olive Oil Industry. Plant and Soil Conference of the California Chapter of the American Society of Agronomy pp. 157-167.
65. Yang C., Everitt J., Bradford J., 2004. Airborne Hyperspectral Imagery and Yield Monitor Data for Mapping Cotton Yield Variability 5:445-461.
66. Zheng C., Sun D. W., Zheng L. 2006. Recent developments and applications of image features for food quality evaluation and inspection e a review. *Trends in Food Science & Technology* 17: 642-655.

8. Appendices

Appendix A. MLR results

Picual

FA	Run 1	Run 2	Run 3	Run 4	Run 5	Run 6	Run 7	Run 8	Run 9	Run 10
67:33	0.147	0.146	0.147	0.144	0.143	0.148	0.143	0.143	0.143	0.148
70:30	0.144	0.152	0.149	0.141	0.145	0.143	0.14	0.143	0.147	0.15
80:20	0.146	0.141	0.147	0.15	0.141	0.141	0.144	0.149	0.149	0.151
90:10	0.135	0.139	0.134	0.14	0.139	0.128	0.138	0.133	0.145	0.144

Full	Run 1	Run 2	Run 3	Run 4	Run 5	Run 6	Run 7	Run 8	Run 9	Run 10
67:33	0.137	0.133	0.144	0.134	0.136	0.135	0.136	0.138	0.138	0.132
70:30	0.132	0.141	0.141	0.147	0.131	0.14	0.132	0.142	0.133	0.141
80:20	0.129	0.141	0.133	0.143	0.136	0.133	0.134	0.139	0.13	0.144
90:10	0.139	0.143	0.14	0.138	0.129	0.14	0.127	0.153	0.141	0.13

Souri

FA	Run 1	Run 2	Run 3	Run 4	Run 5	Run 6	Run 7	Run 8	Run 9	Run 10
67:33	0.086	0.088	0.085	0.09	0.09	0.088	0.086	0.089	0.084	0.091
70:30	0.086	0.087	0.086	0.092	0.092	0.088	0.086	0.084	0.088	0.087
80:20	0.086	0.087	0.084	0.089	0.081	0.084	0.085	0.088	0.085	0.085
90:10	0.088	0.089	0.089	0.091	0.088	0.09	0.083	0.085	0.082	0.083

Full	Run 1	Run 2	Run 3	Run 4	Run 5	Run 6	Run 7	Run 8	Run 9	Run 10
67:33	0.083	0.082	0.083	0.085	0.083	0.08	0.081	0.082	0.083	0.081
70:30	0.083	0.081	0.083	0.083	0.087	0.082	0.082	0.086	0.081	0.078
80:20	0.079	0.085	0.085	0.079	0.086	0.076	0.083	0.081	0.081	0.087
90:10	0.087	0.085	0.082	0.083	0.081	0.074	0.076	0.077	0.082	0.085

Appendix B. ANN results

Original data set

Picual	0.1425	0.1553	0.149	0.1511	0.1579	0.1471	0.1462	0.1475	0.15	0.152
29:1	0.1536	0.15	0.1434	0.1518	0.1462	0.1435	0.151	0.1586	0.1519	0.1635
logsig,logsig	0.1653	0.1526	0.1443	0.1477	0.1452	0.1403	0.1548	0.1453	0.142	0.1407
34:33:33	0.1429	0.1576	0.1442	0.1435	0.1507	0.1447	0.1382	0.1441	0.1857	0.15
0.150874	0.1519	0.1499	0.1497	0.1503	0.1502	0.1435	0.147	0.1496	0.1506	0.1558
0.013805	0.1461	0.1527	0.1462	0.1503	0.1533	0.1543	0.1517	0.1526	0.1511	0.1494
	0.1504	0.1471	0.1433	0.1424	0.1543	0.1544	0.1473	0.1487	0.153	0.1461
	0.1426	0.1592	0.1459	0.1471	0.1529	0.1493	0.1586	0.1494	0.1448	0.1586
	0.1522	0.1419	0.1507	0.1504	0.1551	0.1505	0.1612	0.1925	0.1398	0.1504

	0.1388	0.1403	0.1448	0.1494	0.1451	0.1327	0.1474	0.2624	0.1474	0.1409
--	--------	--------	--------	--------	--------	--------	--------	--------	--------	--------

Picual	0.1498	0.1413	0.1376	0.1559	0.147	0.1374	0.1446	0.1388	0.1461	0.1416
29:1	0.1434	0.1448	0.1454	0.1452	0.139	0.1512	0.1504	0.1504	0.1852	0.1456
logsig,logsig	0.1452	0.1501	0.1451	0.1456	0.1433	0.1537	0.1497	0.1456	0.1481	0.1721
40:30:30	0.1422	0.1471	0.1554	0.1556	0.1378	0.2145	0.1362	0.1423	0.1395	0.1485
0.147244	0.1565	0.1513	0.1398	0.143	0.1438	0.1408	0.1377	0.1452	0.1429	0.14
0.010865	0.1493	0.1516	0.1369	0.1408	0.1524	0.1454	0.1381	0.146	0.141	0.1441
	0.1409	0.1544	0.1433	0.1434	0.1397	0.1455	0.1336	0.1381	0.1388	0.1391
	0.1522	0.1377	0.1432	0.1537	0.1461	0.156	0.1413	0.1473	0.1435	0.1488
	0.139	0.1405	0.1421	0.1448	0.1487	0.1468	0.1466	0.1372	0.1607	0.1515
	0.1858	0.1442	0.1557	0.164	0.147	0.1479	0.1471	0.1409	0.1485	0.1539

Picual	0.1486	0.1666	0.1743	0.1414	0.1562	0.1548	0.1481	0.1477	0.1567	0.1409
29:1	0.1473	0.1359	0.1412	0.1436	0.1429	0.1358	0.1334	0.1348	0.1486	0.1431
logsig,logsig	0.1433	0.1434	0.1479	0.1418	0.1435	0.146	0.139	0.1432	0.138	0.1364
60:20:20	0.1383	0.1412	0.1466	0.1463	0.1372	0.1365	0.1372	0.1433	0.1322	0.1478
0.143866	0.1282	0.1417	0.1314	0.1361	0.1291	0.1395	0.1428	0.1374	0.1455	0.1268
0.012038	0.1422	0.132	0.1432	0.1478	0.1997	0.1412	0.143	0.1429	0.1447	0.1366
	0.143	0.1419	0.1319	0.146	0.1467	0.1503	0.1477	0.1466	0.1441	0.1454
	0.1527	0.1422	0.1429	0.1453	0.1488	0.1405	0.1853	0.1453	0.1427	0.1407
	0.1351	0.1396	0.1356	0.136	0.1337	0.1391	0.14	0.1347	0.135	0.1409
	0.1362	0.1403	0.1439	0.1405	0.1398	0.1451	0.1399	0.138	0.1505	0.2099

Picual	0.1333	0.1373	0.1347	0.1261	0.1433	0.1393	0.1293	0.1366	0.1432	0.132
29:1	0.1314	0.1341	0.1342	0.1412	0.1503	0.1276	0.1244	0.1254	0.1374	0.2116
logsig,logsig	0.1373	0.1383	0.151	0.1499	0.1387	0.1488	0.146	0.1398	0.224	0.1422
80:10:10	0.1341	0.1237	0.1316	0.1494	0.1273	0.1256	0.1351	0.1296	0.1248	0.1337
0.137896	0.139	0.1479	0.1553	0.1473	0.1384	0.1425	0.1538	0.142	0.1443	0.1374
0.014535	0.131	0.1287	0.1233	0.13	0.1184	0.1259	0.1262	0.1247	0.1223	0.1181
	0.1428	0.1352	0.1237	0.1309	0.1267	0.1324	0.1322	0.1303	0.1304	0.1321
	0.1426	0.1343	0.1371	0.1387	0.1232	0.1351	0.1305	0.13	0.1356	0.1656
	0.1324	0.1396	0.1367	0.1334	0.1319	0.1363	0.1349	0.1297	0.132	0.1339
	0.1456	0.1467	0.1512	0.1496	0.1523	0.1406	0.1384	0.1515	0.1373	0.1461

Picual	0.1562	0.1392	0.1514	0.1378	0.1446	0.1429	0.1567	0.1424	0.1431	0.1485
29:1	0.1469	0.1415	0.1424	0.1373	0.1453	0.1457	0.1479	0.1436	0.1489	0.1439
logsig,logsig	0.1331	0.1661	0.1395	0.1369	0.1367	0.1418	0.1348	0.1304	0.1482	0.138
80:10:10	0.1375	0.1362	0.1459	0.135	0.134	0.1277	0.141	0.1319	0.1388	0.1375
0.145199	0.1464	0.1509	0.149	0.1345	0.1456	0.1555	0.1388	0.1519	0.1494	0.1522
0.014336	0.1387	0.1334	0.1359	0.132	0.1422	0.138	0.1415	0.1369	0.1309	0.1442
	0.1558	0.1498	0.1523	0.1558	0.144	0.1446	0.1465	0.1482	0.1476	0.1458
	0.1408	0.1437	0.1378	0.149	0.1436	0.2017	0.1428	0.138	0.1429	0.1434
	0.2428	0.1469	0.1552	0.1353	0.1425	0.1393	0.1574	0.1826	0.143	0.1483
	0.1429	0.1389	0.135	0.1375	0.1364	0.1352	0.1755	0.147	0.132	0.147

Picual	0.1752	0.1361	0.1312	0.1363	0.1394	0.3182	0.1396	0.1458	0.1548	0.1358
29:1	0.1338	0.1445	0.1476	0.1454	0.141	0.1378	0.1507	0.1391	0.1411	0.148
logsig,tansig	0.1282	0.1262	0.1422	0.2259	0.1322	0.1319	0.1296	0.139	0.1353	0.1377
60:20:20	0.1276	0.1326	0.1329	0.1259	0.1262	0.1544	0.1383	0.1407	0.1423	0.131
0.146242	0.1392	0.1472	0.179	0.1437	0.139	0.2225	0.1562	0.1499	0.1562	0.2674
0.026684	0.1341	0.1382	0.1325	0.1366	0.1352	0.1383	0.1343	0.1326	0.1271	0.1458
	0.1456	0.1439	0.1404	0.1604	0.1451	0.1542	0.1388	0.1539	0.1363	0.1509
	0.1431	0.1476	0.1432	0.1358	0.1359	0.1329	0.132	0.1376	0.1402	0.1546
	0.1424	0.2021	0.142	0.13	0.1421	0.1351	0.1408	0.1529	0.1459	0.1377
	0.1389	0.1366	0.1362	0.1503	0.1484	0.1371	0.1306	0.1506	0.1395	0.1361

Picual	0.1448	0.1515	0.1349	0.1468	0.1431	0.1467	0.1395	0.151	0.1365	0.1508
29:1	0.1419	0.1337	0.1338	0.1416	0.146	0.1313	0.1383	0.1412	0.137	0.1332
tansig,logsig	0.1415	0.1436	0.1385	0.1514	0.1394	0.1441	0.1361	0.1352	0.1391	0.1544
60:20:20	0.1373	0.1408	0.1398	0.14	0.1388	0.136	0.1664	0.1363	0.138	0.1374
0.142165	0.1385	0.1438	0.1396	0.1355	0.1466	0.1378	0.1454	0.1491	0.1463	0.1404
0.006648	0.1523	0.1426	0.1413	0.14	0.1457	0.143	0.1496	0.1361	0.1415	0.154
	0.1424	0.1456	0.137	0.1447	0.144	0.144	0.1462	0.1453	0.1439	0.1466
	0.1423	0.1401	0.1511	0.1395	0.1438	0.1349	0.1429	0.1345	0.156	0.1381
	0.1419	0.1451	0.1425	0.1375	0.1427	0.1505	0.1441	0.1403	0.1378	0.1412
	0.1361	0.1371	0.1376	0.1729	0.144	0.1373	0.1375	0.1362	0.1333	0.1312

Picual	0.1626	0.1416	0.1405	0.1511	0.1506	0.1533	0.1532	0.1483	0.1448	0.1666
29:1	0.1381	0.1387	0.1485	0.1436	0.1433	0.139	0.1481	0.1378	0.137	0.139
tansig,tansig	0.1338	0.3256	0.1548	0.1347	0.1786	0.3436	0.1408	0.138	0.1415	0.1456
60:20:20	0.1431	0.3378	0.1419	0.2516	0.1387	0.1418	0.1465	0.1427	0.1417	0.1883
0.164724	0.4904	0.1355	0.1348	0.1407	0.1497	0.1476	0.1347	0.1416	0.1363	0.2886
0.059058	0.1404	0.1398	0.1484	0.1462	0.1446	0.2034	0.146	0.1406	0.154	0.1404
	0.1453	0.3098	0.1514	0.1482	0.1492	0.1472	0.1583	0.1492	0.1473	0.157
	0.1305	0.261	0.3666	0.1435	0.1351	0.1304	0.2744	0.1416	0.1583	0.1419
	0.1484	0.1962	0.1512	0.144	0.1407	0.1416	0.1411	0.1374	0.1428	0.147
	0.1483	0.1452	0.2093	0.1387	0.1441	0.1365	0.1369	0.1509	0.1365	0.1489

Picual	0.1459	0.1428	0.1426	0.1444	0.1468	0.151	0.1448	0.1397	0.1691	0.1455
29:1	0.1457	0.1473	0.1539	0.1447	0.1436	0.1473	0.1462	0.1445	0.1455	0.1559
logsig,pure line	0.1535	0.1456	0.1494	0.1464	0.1512	0.1455	0.1442	0.1414	0.1482	0.1386
60:20:20	0.1459	0.1433	0.1444	0.1481	0.1399	0.1389	0.1369	0.1377	0.1481	0.1414
0.14582	0.1433	0.1302	0.1414	0.1525	0.1442	0.1322	0.1426	0.1411	0.1391	0.1487
0.007366	0.1487	0.1496	0.1474	0.1604	0.1504	0.1487	0.1512	0.1559	0.1401	0.1571
	0.1479	0.1668	0.1395	0.1467	0.1463	0.1579	0.1588	0.1437	0.1485	0.1563
	0.1412	0.1532	0.1408	0.1703	0.156	0.1405	0.1471	0.1473	0.1385	0.1448
	0.1442	0.1349	0.1519	0.1386	0.1415	0.1357	0.1575	0.1398	0.1312	0.1484
	0.141	0.1415	0.1415	0.1405	0.1361	0.1362	0.1462	0.1395	0.1478	0.1353

Picual	0.208	0.208	0.208	0.208	0.208	0.208	0.208	0.208	0.208	0.208
29:1	0.2089	0.2089	0.2089	0.2089	0.2089	0.2089	0.2089	0.2089	0.2089	0.2089
pure line,logsig	0.213	0.213	0.213	0.213	0.213	0.213	0.213	0.213	0.213	0.213
60:20:20	0.2025	0.2025	0.2025	0.2025	0.2025	0.2025	0.2025	0.2025	0.2025	0.2025
0.21007	0.2172	0.2172	0.2172	0.2172	0.2172	0.2172	0.2172	0.2172	0.2172	0.2172
0.005902	0.204	0.204	0.204	0.204	0.204	0.204	0.204	0.204	0.204	0.204
	0.2114	0.2114	0.2114	0.2114	0.2114	0.2114	0.2114	0.2114	0.2114	0.2114
	0.2087	0.2087	0.2087	0.2087	0.2087	0.2087	0.2087	0.2087	0.2087	0.2087
	0.2046	0.2046	0.2046	0.2046	0.2046	0.2046	0.2046	0.2046	0.2046	0.2046
	0.2224	0.2224	0.2224	0.2224	0.2224	0.2224	0.2224	0.2224	0.2224	0.2224

Picual	0.136	0.1368	0.1375	0.1357	0.137	0.1372	0.1369	0.1354	0.1361	0.1367
29:1	0.1351	0.2639	0.1363	0.1339	0.1347	0.1355	0.1343	0.1363	0.1355	0.1364
pure line,pure line	0.1415	0.1409	0.1413	0.1407	0.1408	0.1417	0.1413	0.1406	0.1412	0.1412
60:20:20	0.1373	0.1379	0.1377	0.1376	0.1369	0.1372	0.1374	0.1369	0.1363	0.1378
0.260095	0.1293	0.1295	0.1298	12.2568	0.1301	0.13	0.13	0.1295	0.1298	0.1302
1.211861	0.1453	0.1459	0.1497	0.1462	0.1453	0.1458	0.1464	0.1468	0.146	0.1466
	0.1396	0.1399	0.1404	0.1401	0.1406	0.1402	0.1401	0.1398	0.1404	0.1395
	0.1365	0.1367	0.1373	0.1367	0.1368	0.1366	0.1369	0.1365	0.1368	0.1366
	0.1364	0.1365	0.1362	0.1361	0.1365	0.1361	0.1364	0.1364	0.136	0.1364
	0.1358	0.1362	0.1356	0.1355	0.1358	0.1363	0.1358	0.1358	0.1358	0.1355

Picual	0.1694	0.1819	0.167	0.186	0.1644	0.1706	0.1765	0.16	0.1598	0.1691
29:1	0.1784	0.2036	0.3069	0.164	0.1533	0.1602	0.1742	0.1731	0.1604	0.1717
tansig, pure line	0.1646	0.2021	0.1553	0.1633	0.4577	0.1892	0.1658	0.1652	0.1605	0.1925
60:20:20	0.1543	0.1606	0.1605	0.1718	0.1846	0.1521	0.1767	0.1722	0.1739	0.1909
0.177705	0.1636	0.1687	0.1582	0.1575	0.1952	0.1643	0.1946	0.1561	0.1645	0.1799
0.04171	0.1887	0.1897	0.1795	0.1696	0.1876	0.1595	0.1842	0.1853	0.1829	0.1793
	0.1526	0.1654	0.2031	0.1751	0.1705	0.1722	0.1817	0.165	0.1879	0.1673
	0.1576	0.163	0.1596	0.1465	0.1425	0.1532	0.1685	0.1417	0.1807	0.1706
	0.178	0.1644	0.1647	0.1891	0.174	0.179	0.1622	0.1662	0.1707	0.4149
	0.1675	0.1805	0.1806	0.1768	0.1614	0.1684	0.1709	0.1854	0.1722	0.1457

Picual	0.1583	0.1404	0.2151	0.1581	0.1462	0.1543	0.1463	0.1556	0.1454	0.1485
29:29:1	0.1417	0.1452	0.1488	0.1591	0.1403	0.1421	0.1461	0.1545	0.1437	0.1432
logsig,logsig	0.1398	0.1347	0.1412	0.1459	0.146	0.138	0.1444	0.1503	0.1474	0.207
60:20:20	0.1784	0.1528	0.143	0.1448	0.1451	0.1402	0.1485	0.1346	0.1413	0.1364
0.148368	0.1423	0.1531	0.1502	0.1416	0.1284	0.1918	0.151	0.1499	0.1363	0.1429
0.016384	0.1357	0.1517	0.1524	0.1471	0.1498	0.1445	0.1385	0.1477	0.1484	0.1504
	0.1424	0.1295	0.1321	0.1331	0.1373	0.1484	0.2019	0.1341	0.1385	0.141
	0.1478	0.1462	0.1478	0.1424	0.1502	0.1534	0.1429	0.1447	0.1359	0.1413
	0.1485	0.1479	0.1478	0.1447	0.2185	0.1473	0.1468	0.1515	0.143	0.1543
	0.1421	0.1424	0.1391	0.1365	0.1411	0.1316	0.1472	0.1387	0.1994	0.1311

Picual	0.1458	0.215	0.1458	0.1424	0.1439	0.1439	0.1489	0.1469	0.1486	0.1408
29:20:1	0.1423	0.1464	0.1498	0.1533	0.1459	0.1486	0.1543	0.1502	0.1529	0.1514
logsid,logsig	0.1321	0.137	0.1322	0.1503	0.1365	0.1327	0.1324	0.1468	0.1377	0.2062
60:20:20	0.1428	0.1358	0.1519	0.1491	0.1493	0.1498	0.1534	0.1544	0.1482	0.1674
0.150125	0.1975	0.1439	0.128	0.1405	0.1228	0.1324	0.1986	0.1354	0.13	0.1351
0.017889	0.143	0.15	0.1516	0.2055	0.153	0.1437	0.1484	0.1358	0.1503	0.1476
	0.1487	0.147	0.161	0.1993	0.1545	0.1504	0.1476	0.153	0.1993	0.1533
	0.1437	0.1446	0.145	0.139	0.1397	0.1601	0.1384	0.1478	0.1445	0.1404
	0.1458	0.1449	0.1422	0.1377	0.1488	0.1508	0.1467	0.1566	0.1523	0.1428
	0.1439	0.152	0.1548	0.1329	0.1433	0.1428	0.151	0.2164	0.1524	0.1409

Picual	0.1419	0.1664	0.2121	0.1398	0.1582	0.148	0.1398	0.15	0.1465	0.1402
29:15:1	0.1425	0.1473	0.1533	0.1456	0.1426	0.1486	0.1448	0.1578	0.1486	0.2099
logsid,logsig	0.1511	0.1379	0.1381	0.1494	0.1377	0.14	0.1401	0.2083	0.1478	0.144
60:20:20	0.1422	0.1377	0.1482	0.1332	0.209	0.1455	0.1541	0.1397	0.209	0.1409
0.151533	0.1487	0.1588	0.1465	0.1348	0.1436	0.1597	0.1458	0.152	0.1454	0.1849
0.019641	0.147	0.1473	0.145	0.1468	0.1413	0.1393	0.1647	0.1453	0.1472	0.1557
	0.1429	0.1421	0.1383	0.1499	0.1396	0.1318	0.1401	0.1394	0.144	0.129
	0.1465	0.1526	0.1489	0.1483	0.1428	0.1403	0.1433	0.1507	0.1572	0.1419
	0.1496	0.2216	0.1619	0.1476	0.142	0.1523	0.1465	0.1471	0.1497	0.1536
	0.1391	0.1301	0.2196	0.207	0.1442	0.1473	0.1406	0.1597	0.1456	0.141

Picual	0.14	0.1357	0.1303	0.1359	0.1461	0.1413	0.1315	0.1367	0.2086	0.1467
29:10:1	0.1459	0.1384	0.1496	0.2083	0.1477	0.1465	0.144	0.1496	0.1534	0.1341
logsid,logsig	0.2108	0.1364	0.1449	0.147	0.1477	0.1953	0.1416	0.1462	0.2108	0.1414
60:20:20	0.1374	0.1468	0.1439	0.1404	0.1356	0.1381	0.1391	0.1346	0.1406	0.1386
0.150159	0.1552	0.1531	0.1474	0.1429	0.1514	0.1529	0.1609	0.1452	0.1541	0.1516
0.020934	0.2187	0.142	0.1492	0.1486	0.1553	0.1521	0.1522	0.1466	0.1511	0.1548
	0.2018	0.1417	0.1507	0.1336	0.2018	0.1509	0.1392	0.1407	0.1491	0.1443
	0.1447	0.1372	0.2071	0.1467	0.1459	0.1435	0.1407	0.2071	0.1405	0.1323
	0.1439	0.1361	0.1334	0.1999	0.1326	0.1392	0.1422	0.1377	0.1441	0.1363
	0.1423	0.1278	0.1402	0.1411	0.1389	0.1386	0.1349	0.1428	0.1501	0.1415

Picual	0.1418	0.1336	0.1334	0.1386	0.1958	0.141	0.1391	0.1278	0.1445	0.1342
29:5:1	0.1355	0.1419	0.1569	0.1498	0.146	0.1434	0.1402	0.2114	0.148	0.1395
logsid,logsig	0.1493	0.1422	0.1357	0.1412	0.1404	0.1436	0.1428	0.1408	0.1423	0.1321
60:20:20	0.1492	0.1461	0.1446	0.2213	0.1449	0.2213	0.1601	0.1562	0.1514	0.1449
0.14959	0.1394	0.1409	0.1434	0.1392	0.1378	0.1369	0.1359	0.1269	0.1361	0.1374
0.019758	0.1441	0.139	0.1529	0.15	0.1491	0.1388	0.1432	0.1473	0.1463	0.1626
	0.1423	0.1494	0.2154	0.1469	0.1471	0.1459	0.1403	0.1456	0.1474	0.1625
	0.1527	0.1467	0.1454	0.1462	0.1397	0.15	0.1533	0.142	0.1476	0.2096
	0.1498	0.1411	0.1514	0.1477	0.1397	0.1598	0.1521	0.2104	0.2104	0.1413
	0.1383	0.146	0.1407	0.1379	0.1508	0.147	0.1405	0.1363	0.155	0.1468

Picual	0.1388	0.1404	0.201	0.1429	0.1442	0.1504	0.1434	0.201	0.1454	0.136
29:3:1	0.1403	0.1454	0.1365	0.1423	0.1399	0.2129	0.138	0.1463	0.1369	0.133
logsid,logsig	0.1525	0.2123	0.1386	0.1396	0.1428	0.2123	0.1374	0.1437	0.1422	0.146
60:20:20	0.1444	0.1447	0.1337	0.1409	0.1374	0.1361	0.1565	0.1348	0.1398	0.1416
0.151479	0.1534	0.1535	0.1677	0.1486	0.1523	0.1517	0.1594	0.143	0.1485	0.1434
0.023448	0.2178	0.1511	0.15	0.1498	0.2178	0.218	0.1474	0.1472	0.1528	0.1421
	0.1255	0.1217	0.1306	0.1584	0.1881	0.1338	0.1303	0.1228	0.1301	0.1321
	0.1573	0.1464	0.1518	0.1466	0.149	0.148	0.1405	0.1503	0.2098	
	0.1414	0.1481	0.1471	0.1519	0.1376	0.2042	0.1399	0.1431	0.1402	0.1473
	0.1407	0.1447	0.1349	0.1579	0.1424	0.1345	0.1324	0.1974	0.1311	0.1404

Picual	0.1385	0.1468	0.2035	0.2035	0.1439	0.1427	0.137	0.2035	0.1523	0.1463
29:2:1	0.1322	0.1387	0.1408	0.1443	0.1368	0.1408	0.2666	0.1594	0.1453	0.1442
logsid,logsig	0.2089	0.2089	0.2089	0.144	0.1371	0.1363	0.1343	0.2089	0.1822	0.2089
60:20:20	0.1413	0.1519	0.142	0.1406	0.1389	0.1407	0.149	0.2128	0.2128	0.1432
0.157715	0.1602	0.1292	0.1323	0.1904	0.1355	0.2065	0.1228	0.1251	0.1312	0.1258
0.029724	0.1371	0.1467	0.1389	0.1454	0.1451	0.1386	0.1443	0.1297	0.1413	0.1337
	0.1405	0.1468	0.1436	0.1416	0.1865	0.2107	0.1553	0.1442	0.1474	0.1488
	0.1412	0.2067	0.1545	0.2067	0.1403	0.2052	0.2067	0.1398	0.1557	0.2067
	0.2065	0.2065	0.1452	0.1471	0.1446	0.1501	0.144	0.1599	0.1442	0.2098
	0.1327	0.1409	0.14	0.1558	0.1426	0.1344	0.1338	0.1442	0.1381	0.1437

Picual	0.1474	0.1353	0.138	0.1357	0.1355	0.1493	0.1486	0.2049	0.1358	0.1344
29:1	0.1429	0.1508	0.1509	0.1399	0.1339	0.1361	0.1411	0.1395	0.1387	0.1425
logsid,logsig	0.1457	0.1366	0.1367	0.1397	0.1409	0.139	0.1992	0.1401	0.1323	0.1308
60:20:20	0.1382	0.1541	0.1501	0.1555	0.1431	0.1473	0.148	0.152	0.1512	0.1467
0.143948	0.1412	0.1437	0.1412	0.14	0.1431	0.1471	0.148	0.1454	0.1433	0.142
0.010358	0.1431	0.1573	0.15	0.1403	0.1405	0.1473	0.1355	0.1346	0.1435	0.1468
	0.146	0.14	0.1484	0.1402	0.1429	0.1357	0.1411	0.144	0.1424	0.149
	0.1501	0.1342	0.1491	0.1459	0.1533	0.1416	0.1432	0.1461	0.147	0.1426
	0.1386	0.1455	0.1438	0.1406	0.1507	0.1434	0.1431	0.1417	0.1486	0.1558
	0.1559	0.132	0.1352	0.1455	0.1311	0.1377	0.1349	0.1411	0.1333	0.1312

Souri	0.0835	0.1608	0.0833	0.0973	0.0834	0.0835	0.0823	0.085	0.0895	0.0857
29:1	0.0827	0.084	0.0893	0.0829	0.0791	0.0832	0.083	0.0866	0.0817	0.0822
logsid,logsig	0.0898	0.0853	0.0805	0.0896	0.0867	0.0871	0.1154	0.0862	0.0833	0.0835
34:33:33	0.0846	0.085	0.0805	0.0858	0.0932	0.0877	0.087	0.1039	0.088	0.0944
0.089055	0.0894	0.0851	0.0911	0.0839	0.0902	0.0933	0.0862	0.0843	0.0966	0.0912
0.011477	0.0888	0.0905	0.1576	0.0875	0.0929	0.0881	0.0941	0.09	0.094	0.0841
	0.0913	0.0827	0.0888	0.0836	0.0852	0.0854	0.0915	0.0839	0.095	0.0857
	0.0842	0.0944	0.0852	0.0854	0.0861	0.1003	0.0854	0.089	0.0888	0.0828
	0.0841	0.0961	0.0878	0.0872	0.0856	0.0825	0.085	0.0838	0.0812	0.0819
	0.0924	0.0886	0.1033	0.0897	0.0845	0.0898	0.0855	0.086	0.0838	0.0866

Souri	0.0841	0.0865	0.0893	0.0897	0.0844	0.0872	0.0808	0.0804	0.084	0.0854
29:1	0.0793	0.0875	0.0836	0.0854	0.083	0.0927	0.0788	0.0771	0.0857	0.0835
logsid,logsig	0.082	0.08	0.0861	0.084	0.0827	0.0845	0.082	0.0832	0.0868	0.0837
40:30:30	0.0791	0.0849	0.0876	0.0811	0.0823	0.0808	0.0864	0.0869	0.0958	0.0862
0.086089	0.0837	0.0854	0.0803	0.0821	0.0819	0.0828	0.0891	0.0823	0.0828	0.0818
0.008941	0.0865	0.0837	0.0882	0.0917	0.0888	0.0897	0.0902	0.0867	0.087	0.0876
	0.0954	0.1004	0.0924	0.0889	0.0919	0.0878	0.0848	0.0885	0.0888	0.0886
	0.0771	0.0845	0.082	0.0842	0.0769	0.0788	0.0817	0.0825	0.0972	0.0868
	0.0841	0.0878	0.0853	0.0891	0.0845	0.0815	0.0843	0.0827	0.0894	0.0834
	0.089	0.0863	0.0833	0.083	0.0861	0.0838	0.0822	0.0859	0.1643	0.0869

Souri	0.0835	0.0835	0.0861	0.0784	0.0825	0.0808	0.0819	0.0776	0.08	0.082
29:1	0.0853	0.0831	0.0869	0.0825	0.0834	0.0881	0.084	0.0897	0.0837	0.0839
logsid,logsig	0.0814	0.0799	0.0783	0.0767	0.0778	0.0787	0.0782	0.0787	0.0834	0.0793
60:20:20	0.0827	0.0772	0.0839	0.089	0.0912	0.0827	0.0826	0.0797	0.0791	0.0804
0.083483	0.0764	0.0802	0.0782	0.082	0.0744	0.0748	0.0774	0.0782	0.0747	0.0764
0.0094	0.0836	0.0834	0.0801	0.0813	0.0808	0.081	0.0809	0.0843	0.0837	0.0812
	0.0779	0.0784	0.0822	0.082	0.0776	0.0777	0.0784	0.0782	0.0809	0.0765
	0.0844	0.0928	0.1192	0.0837	0.0869	0.0816	0.0882	0.0834	0.0812	0.0859
	0.0851	0.0834	0.0841	0.0929	0.0853	0.0799	0.0883	0.0855	0.0837	0.0874
	0.0925	0.1596	0.0852	0.0863	0.0857	0.0844	0.0844	0.086	0.0848	0.0859

Souri	0.0813	0.0803	0.083	0.08	0.0796	0.0788	0.0796	0.0807	0.08	0.0821
29:1	0.0784	0.0807	0.0788	0.0787	0.0761	0.0785	0.0784	0.0785	0.0762	0.0797
logsid,logsig	0.0903	0.0812	0.0847	0.0853	0.085	0.081	0.0858	0.0816	0.0838	0.0831
80:10:10	0.081	0.0778	0.0788	0.0769	0.0774	0.0805	0.0798	0.0785	0.0767	0.0775
0.082472	0.0893	0.0949	0.0891	0.0866	0.088	0.0881	0.0891	0.0899	0.0871	0.0906
0.00875	0.08	0.08	0.0794	0.0793	0.0787	0.078	0.0774	0.08	0.0792	0.0866
	0.074	0.0733	0.0737	0.071	0.0809	0.073	0.0701	0.0743	0.0747	0.0746
	0.0845	0.0789	0.0798	0.0776	0.0807	0.0777	0.0822	0.0785	0.0775	0.0768
	0.152	0.0903	0.0886	0.0892	0.0899	0.0909	0.0895	0.0913	0.0909	0.0885
	0.0848	0.0801	0.0859	0.0854	0.0831	0.0804	0.0834	0.0857	0.0923	0.0838

Souri	0.0796	0.0829	0.0792	0.081	0.0801	0.0862	0.0784	0.0845	0.0826	0.0788
29:1	0.0777	0.0765	0.0806	0.0778	0.0828	0.0884	0.0908	0.0755	0.0773	0.0803
logsid,logsig	0.0853	0.083	0.0818	0.0855	0.0865	0.0841	0.0866	0.0891	0.0887	0.0846
60:20:20	0.0837	0.0855	0.083	0.0827	0.0846	0.0829	0.081	0.0841	0.0813	0.0828
0.082686	0.082	0.0914	0.0853	0.1572	0.0836	0.0817	0.0818	0.0851	0.0803	0.0817
0.008204	0.0767	0.08	0.0815	0.0796	0.0776	0.0764	0.0766	0.0783	0.0766	0.0801
	0.0814	0.0841	0.0852	0.0831	0.0817	0.0834	0.0825	0.0789	0.0805	0.0843
	0.0823	0.0823	0.0797	0.0876	0.0797	0.0801	0.082	0.0839	0.0836	0.0866
	0.0815	0.0826	0.0807	0.0799	0.0851	0.0838	0.0835	0.0808	0.0807	0.0793

	0.0803	0.0831	0.0774	0.0771	0.0804	0.0833	0.0819	0.0782	0.0766	0.0782
--	--------	--------	--------	--------	--------	--------	--------	--------	--------	--------

Souri	0.0833	0.0809	0.0806	0.0809	0.0792	0.0832	0.0815	0.0818	0.0803	0.083
29:1	0.0817	0.0782	0.077	0.0767	0.0863	0.0821	0.0774	0.0791	0.0779	0.0795
logsig,tansig	0.078	0.0813	0.0841	0.0807	0.0777	0.0807	0.0823	0.0816	0.0786	0.0793
60:20:20	0.1632	0.0871	0.0845	0.0833	0.0834	0.0883	0.0843	0.0809	0.2154	0.0888
0.091686	0.0786	0.0799	0.0807	0.0805	0.184	0.0814	0.0805	0.0829	0.1601	0.0827
0.028017	0.0943	0.0832	0.1024	0.1665	0.0845	0.1062	0.0836	0.0865	0.0868	0.082
	0.0813	0.0961	0.0827	0.082	0.164	0.2152	0.0866	0.0831	0.0824	0.0939
	0.0802	0.0828	0.1565	0.0773	0.082	0.0811	0.0805	0.0801	0.1566	0.0791
	0.0781	0.0778	0.0967	0.0769	0.0775	0.0768	0.0796	0.076	0.0735	0.0912
	0.0918	0.087	0.0889	0.083	0.0972	0.09	0.0866	0.1033	0.0856	0.0862

Souri	0.085	0.0854	0.0847	0.0866	0.0855	0.0848	0.086	0.0859	0.0884	0.1552
29:1	0.0837	0.0863	0.0822	0.0824	0.0865	0.0868	0.0919	0.0861	0.0854	0.0851
tansig,logsig	0.0799	0.0852	0.1309	0.081	0.0802	0.0815	0.0801	0.0825	0.0857	0.0804
60:20:20	0.0815	0.0799	0.0844	0.0822	0.0807	0.0842	0.0865	0.0819	0.0848	0.0857
0.085099	0.0817	0.0822	0.0821	0.0806	0.084	0.106	0.083	0.0823	0.0846	0.0888
0.012711	0.0798	0.0824	0.0842	0.0759	0.0823	0.0783	0.0791	0.0811	0.0809	0.0789
	0.0791	0.0787	0.0757	0.0784	0.0791	0.0815	0.0795	0.0785	0.0819	0.0775
	0.0828	0.0778	0.0805	0.0809	0.0839	0.0804	0.0795	0.0792	0.0828	0.0793
	0.0789	0.0868	0.0814	0.0791	0.0816	0.0815	0.0853	0.0827	0.0867	0.0818
	0.0866	0.0867	0.0865	0.0881	0.0852	0.0889	0.085	0.0856	0.0839	0.1693

Souri	0.0834	0.0825	0.0871	0.0838	0.0838	0.0822	0.0859	0.0809	0.0798	0.0807
29:1	0.0814	0.08	0.0929	0.0856	0.0841	0.0803	0.1036	0.0798	0.0821	0.083
tansig,tansig	0.0809	0.0815	0.0801	0.0821	0.0792	0.0824	0.0817	0.0995	0.2334	0.0807
60:20:20	0.0805	0.0799	0.0822	0.0779	0.0822	0.0807	0.0818	0.08	0.0834	0.0956
0.092715	0.0763	0.0751	0.0769	0.0777	0.0773	0.0746	0.0766	0.0826	0.2691	0.0759
0.041258	0.1413	0.0788	0.0841	0.0828	0.1939	0.0794	0.0835	0.0832	0.0811	0.0794
	0.0792	0.0842	0.0789	0.0776	0.076	0.077	0.0761	0.0821	0.1151	0.0794
	0.08	0.0856	0.0848	0.0834	0.2258	0.0829	0.0871	0.0828	0.0849	0.0796
	0.0825	0.0812	0.0806	0.3636	0.085	0.0799	0.0802	0.0893	0.083	0.0852
	0.0835	0.1292	0.0843	0.1046	0.0816	0.1019	0.0837	0.0841	0.0843	0.0831

Souri	0.0782	0.0809	0.079	0.0804	0.0752	0.077	0.0804	0.0763	0.0747	0.0805
29:1	0.089	0.0947	0.0926	0.0963	0.0953	0.093	0.0933	0.0918	0.0889	0.0887
logsig,pure line	0.0832	0.0897	0.085	0.0855	0.0809	0.0856	0.0868	0.0801	0.0819	0.0879
60:20:20	0.0913	0.0801	0.0827	0.0877	0.0855	0.0857	0.0869	0.0903	0.0861	0.0878
0.089161	0.0897	0.088	0.0871	0.0843	0.0918	0.0835	0.0942	0.0877	0.0889	0.0871
0.027447	0.0965	0.0807	0.0932	0.0912	0.0827	0.0848	0.0891	0.0869	0.0895	0.0859
	0.0897	0.0866	0.099	0.091	0.0935	0.0849	0.0862	0.0848	0.0882	0.0921
	0.093	0.0848	0.0854	0.0987	0.0889	0.0824	0.0842	0.0914	0.0858	0.085

	0.0825	0.077	0.0788	0.0742	0.0763	0.0751	0.0794	0.0733	0.0781	0.0826
	0.0938	0.0924	0.3546	0.0924	0.0919	0.0934	0.0945	0.088	0.0922	0.0903

Souri	0.1609	0.1609	0.1609	0.1609	0.1609	0.1609	0.1609	0.1609	0.1609	0.1609
29:1	0.1592	0.1592	0.1592	0.1592	0.1592	0.1592	0.1592	0.1592	0.1592	0.1592
pure line,logsig	0.1617	0.1617	0.4483	0.1617	0.1617	0.1617	0.1617	0.1617	0.1617	0.1617
60:20:20	0.163	0.163	0.163	0.163	0.163	0.163	0.163	0.163	0.163	0.163
0.163276	0.1634	0.1634	0.1634	0.1634	0.1634	0.1634	0.1634	0.1634	0.1634	0.1634
0.028885	0.1593	0.1593	0.1593	0.1593	0.1593	0.1593	0.1593	0.1593	0.1593	0.1593
	0.1593	0.1593	0.1593	0.1593	0.1593	0.1593	0.1593	0.1593	0.1593	0.1593
	0.1551	0.1551	0.1551	0.1551	0.1551	0.1551	0.1551	0.1551	0.1551	0.1551
	0.1624	0.1624	0.1624	0.1624	0.1624	0.1624	0.1624	0.1624	0.1624	0.1624
	0.1598	0.1598	0.1598	0.1598	0.1598	0.1598	0.1598	0.1598	0.1598	0.1598

Souri	0.0776	0.0776	0.0778	0.0779	0.0774	0.078	0.0777	0.0777	0.0779	0.0777
29:1	0.08	0.0799	0.0798	0.0799	0.08	0.08	0.0801	0.0796	0.0797	0.0802
pure line,pure line	0.0805	0.7248	0.0801	0.0811	0.08	0.0801	0.0801	0.0802	0.0803	0.0807
60:20:20	0.0876	0.0891	0.0863	0.0875	0.0861	0.0864	0.0864	0.0863	0.0867	0.0862
0.088256	0.081	0.0808	0.0809	0.0808	0.0807	0.0807	0.0808	0.0812	0.0812	0.081
0.064359	0.0802	0.0921	0.0803	0.0803	0.0802	0.0803	0.0805	0.0801	0.0802	0.0801
	0.0805	0.0805	0.0804	0.0805	0.0807	0.0805	0.0804	0.0805	0.0807	0.0803
	0.0819	0.0818	0.0812	0.0821	0.0821	0.0811	0.0813	0.0818	0.0818	0.0811
	0.0845	0.084	0.084	0.0839	0.0842	0.0843	0.0842	0.084	0.0843	0.0852
	0.0846	0.0847	0.0847	0.0847	0.0843	0.0851	0.0839	0.0847	0.0845	0.0842

Souri	0.0849	0.0978	0.0922	0.0883	0.09	0.0894	0.089	0.0899	0.0932	0.0897
29:1	0.0792	0.0904	0.1012	0.0912	0.1094	0.0862	0.0851	0.0866	0.0829	0.0969
tansig, pure line	0.0829	0.0855	0.0927	0.0988	0.0894	0.0879	0.0917	0.0836	0.0911	0.0844
60:20:20	0.0929	0.0997	0.0874	0.0913	0.0945	0.0858	0.0952	0.0929	0.0926	0.0833
0.089571	0.083	0.081	0.0792	0.0859	0.0814	0.0877	0.083	0.0758	0.0878	0.0817
0.006457	0.0886	0.0904	0.0933	0.0817	0.0967	0.0907	0.0873	0.0889	0.1132	0.0856
	0.1093	0.0852	0.0883	0.0881	0.0825	0.0888	0.0889	0.0884	0.0921	0.0912
	0.0971	0.1038	0.0866	0.099	0.082	0.088	0.0823	0.0922	0.0903	0.0996
	0.0858	0.0869	0.0898	0.0892	0.0928	0.0942	0.0847	0.0849	0.0861	0.0903
	0.0987	0.0912	0.0808	0.0833	0.0855	0.0959	0.0876	0.0855	0.0906	0.0896

Souri	0.0852	0.0903	0.0888	0.0878	0.0853	0.0835	0.0844	0.0873	0.0864	0.0888
29:29:1	0.0839	0.0834	0.1524	0.0819	0.079	0.0758	0.0845	0.0796	0.0762	0.0825
logsig,logsig	0.0835	0.0826	0.0888	0.0876	0.0856	0.0867	0.0876	0.0847	0.0838	0.0898
60:20:20	0.0834	0.0867	0.1668	0.0845	0.0884	0.0866	0.0853	0.0819	0.1668	0.0808
0.088941	0.0803	0.0873	0.0836	0.0858	0.0845	0.081	0.0852	0.0803	0.0837	0.078
0.019109	0.0909	0.1649	0.0876	0.09	0.09	0.0895	0.0816	0.0865	0.0868	0.0917
	0.0703	0.0823	0.0747	0.0787	0.0821	0.0816	0.0782	0.0799	0.081	0.0818

	0.0828	0.0824	0.0848	0.0821	0.08	0.0852	0.0802	0.0797	0.0858	0.0782
	0.0843	0.0801	0.0839	0.0855	0.0837	0.0928	0.0839	0.1614	0.0874	0.0765
	0.0841	0.0886	0.0875	0.0908	0.1618	0.0869	0.0859	0.0889	0.0921	0.0881

Souri	0.0894	0.0849	0.096	0.0828	0.0869	0.0904	0.0879	0.0843	0.0908	0.086
29:20:1	0.0875	0.0857	0.1641	0.0764	0.0884	0.0854	0.0854	0.0834	0.0848	0.079
logsid,logsig	0.0846	0.0847	0.0851	0.0855	0.0833	0.0828	0.1626	0.0846	0.0937	0.0881
60:20:20	0.0762	0.0728	0.085	0.0848	0.0718	0.0763	0.0793	0.0825	0.0846	0.083
0.089311	0.0837	0.0885	0.0829	0.1616	0.0892	0.0883	0.083	0.1616	0.1616	0.0895
0.020189	0.0864	0.1576	0.0835	0.0818	0.0772	0.0824	0.0833	0.0806	0.0839	0.0799
	0.0829	0.0855	0.0926	0.0844	0.0819	0.086	0.0875	0.0851	0.0865	0.0898
	0.0874	0.0857	0.0878	0.0822	0.1577	0.0854	0.0856	0.0836	0.0843	0.0803
	0.0841	0.0825	0.084	0.0804	0.0789	0.0855	0.0811	0.0767	0.0796	0.0862
	0.0847	0.0786	0.0819	0.0797	0.0783	0.0789	0.0829	0.0755	0.0833	0.0888

Souri	0.0871	0.0832	0.0867	0.0846	0.0902	0.0853	0.0863	0.1023	0.0832	0.0819
29:15:1	0.1591	0.0944	0.0905	0.0837	0.0923	0.084	0.0868	0.0878	0.089	0.0897
logsid,logsig	0.0805	0.0826	0.0795	0.0943	0.0764	0.0842	0.079	0.0826	0.0848	0.0816
60:20:20	0.0808	0.0829	0.0854	0.0859	0.0835	0.0824	0.0795	0.0852	0.0831	0.0854
0.089519	0.0802	0.0844	0.081	0.0801	0.1627	0.0781	0.0807	0.0828	0.0783	0.0784
0.016645	0.0893	0.0889	0.0892	0.091	0.0941	0.0926	0.1308	0.1607	0.0898	0.0892
	0.0873	0.0862	0.0877	0.0821	0.0862	0.0847	0.0916	0.0886	0.0829	0.0873
	0.0842	0.0828	0.0834	0.0823	0.0857	0.0849	0.0803	0.0857	0.0822	0.0912
	0.0828	0.0826	0.1398	0.0828	0.0831	0.0864	0.0819	0.0794	0.0861	0.0831
	0.0942	0.0886	0.0874	0.157	0.09	0.0945	0.09	0.0896	0.0864	0.0889

Souri	0.0902	0.09	0.0894	0.0849	0.0921	0.0992	0.1495	0.0881	0.0864	0.0873
29:10:1	0.0799	0.0802	0.0762	0.1541	0.0806	0.0807	0.0816	0.2227	0.0846	0.1541
logsid,logsig	0.0846	0.0837	0.0855	0.0793	0.0851	0.0824	0.0872	0.2832	0.085	0.0894
60:20:20	0.0844	0.1612	0.083	0.0823	0.0884	0.0825	0.0791	0.0816	0.0817	0.0823
0.09319	0.0886	0.0838	0.0845	0.0866	0.0918	0.0883	0.0896	0.0892	0.0876	0.0868
0.03097	0.0885	0.0821	0.0825	0.0799	0.0822	0.0836	0.0825	0.0862	0.0812	0.0863
	0.0832	0.0822	0.1596	0.0825	0.0864	0.0822	0.0812	0.0824	0.0797	0.0833
	0.08	0.0801	0.0814	0.08	0.1574	0.0781	0.0838	0.0831	0.0814	0.0797
	0.0838	0.1652	0.0826	0.0884	0.088	0.0844	0.0841	0.0818	0.0855	0.0822
	0.0816	0.0853	0.0852	0.1572	0.0782	0.0846	0.078	0.076	0.0769	0.0868

Souri	0.0814	0.0834	0.1603	0.2656	0.0833	0.1603	0.0856	0.1603	0.0839	0.084
29:5:1	0.0862	0.0874	0.0904	0.0877	0.0874	0.0928	0.0929	0.0898	0.0858	0.086
logsid,logsig	0.0819	0.0808	0.082	0.0835	0.0826	0.0795	0.0807	0.1447	0.0834	0.0811
60:20:20	0.0837	0.0792	0.0863	0.0855	0.0791	0.1549	0.082	0.1549	0.1013	0.0873
0.093799	0.0893	0.0879	0.0876	0.0865	0.0851	0.0882	0.0823	0.0867	0.0841	0.0856
0.02824	0.0834	0.0823	0.0799	0.0854	0.0839	0.0787	0.082	0.0827	0.0798	0.1632

	0.0847	0.081	0.0815	0.0849	0.0861	0.0836	0.0834	0.0817	0.0789	0.0866
	0.0864	0.0849	0.0882	0.0856	0.0838	0.0875	0.0823	0.0843	0.0863	0.0857
	0.0829	0.082	0.0833	0.0813	0.1591	0.0869	0.0855	0.1591	0.1591	0.0809
	0.0815	0.086	0.0912	0.085	0.0862	0.0813	0.0826	0.0888	0.091	0.0853

Souri	0.0829	0.1575	0.0798	0.0842	0.0773	0.0822	0.0815	0.0816	0.0812	0.0796
29:3:1	0.0836	0.0814	0.0793	0.0857	0.0825	0.0869	0.0791	0.0796	0.1618	0.0819
logsid,logsig	0.0873	0.0892	0.0883	0.0867	0.0886	0.1594	0.1594	0.0826	0.1594	0.1594
60:20:20	0.1603	0.0818	0.0819	0.0812	0.0789	0.082	0.081	0.0845	0.08	0.0801
0.098012	0.0787	0.085	0.0838	0.0838	0.082	0.081	0.081	0.0856	0.0859	0.1623
0.031726	0.163	0.163	0.0816	0.082	0.163	0.0742	0.0835	0.0747	0.0796	0.0768
	0.0832	0.085	0.165	0.0845	0.165	0.091	0.0871	0.1634	0.082	0.165
	0.0778	0.0791	0.0811	0.082	0.0814	0.1537	0.0841	0.0807	0.0812	0.0807
	0.0804	0.0764	0.0764	0.0813	0.1577	0.0813	0.0887	0.0754	0.1577	0.1577
	0.0856	0.0842	0.162	0.084	0.0891	0.0804	0.0836	0.0841	0.0893	0.0808

Souri	0.0842	0.1549	0.0815	0.078	0.1169	0.0776	0.1549	0.0794	0.0774	0.1549
29:2:1	0.0886	0.095	0.083	0.1568	0.0822	0.0823	0.08	0.0913	0.1568	0.1568
logsid,logsig	0.086	0.1269	0.1598	0.1598	0.1588	0.085	0.0878	0.0817	0.0852	0.1464
60:20:20	0.0839	0.0821	0.0853	0.1592	0.1591	0.0818	0.0885	0.0797	0.082	0.0872
0.102203	0.0891	0.0853	0.0886	0.1676	0.0888	0.0836	0.1676	0.0885	0.1206	0.0913
0.031892	0.0843	0.0813	0.1584	0.0788	0.0824	0.0847	0.0846	0.077	0.0826	0.1583
	0.1674	0.0891	0.1674	0.0898	0.0853	0.0881	0.0898	0.0928	0.0863	0.1674
	0.0824	0.0816	0.0814	0.0839	0.0865	0.0856	0.0821	0.0827	0.1006	0.0843
	0.0862	0.1576	0.0828	0.1576	0.0798	0.0902	0.1352	0.0807	0.0785	0.1576
	0.0795	0.0781	0.0818	0.0785	0.0833	0.0768	0.0773	0.0769	0.0821	0.0832

Souri	0.082	0.0828	0.0851	0.1559	0.0827	0.0815	0.0827	0.085	0.0864	0.0852
29:1	0.0758	0.0772	0.0761	0.0874	0.0794	0.0773	0.0741	0.0761	0.0766	0.0758
logsid,logsig	0.0841	0.0888	0.0856	0.0842	0.0823	0.0873	0.0824	0.0833	0.082	0.0829
60:20:20	0.0844	0.0848	0.086	0.0852	0.1629	0.0872	0.0866	0.0898	0.0859	0.0851
0.085473	0.0787	0.0789	0.0836	0.0828	0.0782	0.0774	0.1594	0.0778	0.0757	0.0808
0.015958	0.081	0.08	0.0778	0.0801	0.0798	0.084	0.08	0.078	0.082	0.0766
	0.0785	0.0745	0.0794	0.1608	0.0776	0.0759	0.08	0.0796	0.0782	0.0791
	0.0888	0.0815	0.0808	0.0816	0.0911	0.08	0.0796	0.1015	0.0808	0.0811
	0.0796	0.084	0.0917	0.0999	0.0822	0.0821	0.0807	0.0823	0.0833	0.0805
	0.0855	0.0887	0.0907	0.0842	0.0805	0.0815	0.0832	0.0813	0.0921	0.0844

FA set

Picual	0.1355	0.1401	0.1448	0.1439	0.1396	0.1417	0.1444	0.1425	0.1444	0.1425
29:1	0.1347	0.1356	0.1336	0.1339	0.1335	0.136	0.1386	0.1365	0.1357	0.1337
logsid,logsig	0.1419	0.1381	0.1365	0.2064	0.1355	0.1447	0.137	0.1329	0.1359	0.1358
34:33:33	0.2073	0.1393	0.1403	0.1375	0.1395	0.1417	0.1396	0.14	0.1361	0.1379

0.14279	0.1491	0.1494	0.1496	0.1499	0.1483	0.1485	0.1442	0.1506	0.1491	0.1456
0.013125	0.1395	0.1442	0.1414	0.1427	0.1416	0.1418	0.1438	0.1434	0.1463	0.1435
	0.1446	0.1443	0.1469	0.1434	0.1418	0.1413	0.1438	0.1418	0.1463	0.1446
	0.1418	0.1405	0.1398	0.1387	0.1415	0.1369	0.1399	0.139	0.1405	0.2231
	0.1395	0.1417	0.143	0.1388	0.1465	0.1396	0.1432	0.14	0.1437	0.1433
	0.1337	0.1366	0.1312	0.1376	0.134	0.1333	0.1356	0.1393	0.1338	0.1365

Picual	0.1505	0.1434	0.137	0.1465	0.1419	0.1391	0.1497	0.1409	0.1385	0.1424
29:1	0.1362	0.1368	0.1362	0.1327	0.1456	0.1404	0.136	0.1358	0.1359	0.1342
logsig,logsig	0.1375	0.2031	0.1355	0.1341	0.1363	0.137	0.1362	0.134	0.1362	0.1335
40:30:30	0.2067	0.1351	0.1438	0.1372	0.1338	0.1362	0.1398	0.1349	0.135	0.1456
0.14251	0.1364	0.1398	0.1345	0.1387	0.1358	0.1384	0.1448	0.1393	0.135	0.1361
0.010891	0.1462	0.1394	0.1384	0.1508	0.1409	0.1404	0.1441	0.1512	0.1439	0.1477
	0.1491	0.1389	0.1425	0.1403	0.1446	0.1475	0.156	0.147	0.139	0.1371
	0.1432	0.142	0.1439	0.1414	0.1459	0.1791	0.1429	0.1388	0.1468	0.1387
	0.1505	0.1483	0.1379	0.1427	0.1433	0.1471	0.1404	0.1388	0.1424	0.1447
	0.1463	0.1413	0.1385	0.1362	0.1411	0.1384	0.1464	0.1406	0.1474	0.141

Picual	0.1258	0.1295	0.1272	0.1298	0.1316	0.13	0.1356	0.1289	0.1329	0.1257
29:1	0.1334	0.1375	0.1444	0.1354	0.1369	0.1367	0.1411	0.1365	0.1395	0.1387
logsig,logsig	0.129	0.1272	0.1326	0.1399	0.1266	0.1299	0.1367	0.1358	0.1301	0.131
60:20:20	0.1374	0.1419	0.1367	0.1356	0.147	0.1369	0.1358	0.137	0.138	0.3904
0.137747	0.1459	0.145	0.1379	0.1465	0.1506	0.1411	0.1449	0.1399	0.1439	0.1411
0.026074	0.1328	0.1265	0.1327	0.1327	0.1344	0.1342	0.1364	0.132	0.1361	0.1301
	0.135	0.1347	0.1333	0.1324	0.1374	0.1344	0.1359	0.1323	0.1337	0.1371
	0.1332	0.1323	0.1347	0.1336	0.1348	0.1439	0.1404	0.135	0.1468	0.1344
	0.1269	0.1389	0.1298	0.1331	0.1338	0.1369	0.1267	0.1278	0.1312	0.1268
	0.141	0.1312	0.1382	0.1306	0.1329	0.1323	0.1282	0.1408	0.1365	0.1385

Picual	0.1382	0.1324	0.1327	0.1354	0.1287	0.1342	0.1314	0.1315	0.1342	0.1344
29:1	0.135	0.1383	0.1376	0.1349	0.1413	0.1333	0.1351	0.2254	0.1369	0.137
logsig,logsig	0.1382	0.1348	0.1365	0.1327	0.1334	0.1386	0.1325	0.1333	0.1265	0.1293
80:10:10	0.1495	0.1416	0.1393	0.1406	0.1396	0.1462	0.1469	0.1388	0.1477	0.1429
0.137319	0.1411	0.1492	0.1464	0.1392	0.1426	0.1456	0.1454	0.1468	0.1447	0.1436
0.011212	0.1334	0.1351	0.1412	0.1299	0.1337	0.1417	0.1445	0.1399	0.1342	0.1484
0.011711	0.1432	0.1459	0.1435	0.1368	0.1511	0.1395	0.1445	0.1411	0.1434	0.1374
	0.1196	0.1217	0.1277	0.1271	0.1315	0.1346	0.1254	0.1214	0.124	0.1173
	0.1345	0.1289	0.1294	0.137	0.1306	0.1313	0.134	0.1371	0.1317	0.1298
	0.1383	0.1355	0.1299	0.1432	0.1377	0.135	0.1324	0.1325	0.131	0.132

Picual	0.1453	0.1436	0.1481	0.1414	0.1419	0.1463	0.1484	0.1512	0.153	0.1416
29:1	0.1384	0.1387	0.1445	0.1379	0.1418	0.1418	0.1416	0.1354	0.1359	0.1372
logsig,logsig	0.1311	0.1401	0.1336	0.1363	0.1365	0.1398	0.1366	0.1429	0.1305	0.1423

60:20:20	0.1428	0.1414	0.1408	0.1477	0.1498	0.1392	0.1426	0.1506	0.1457	0.1507
0.137631	0.1404	0.1474	0.1348	0.138	0.1341	0.1366	0.1403	0.133	0.1356	0.1343
0.006843	0.1311	0.1426	0.1294	0.1357	0.1361	0.1422	0.1298	0.1333	0.1368	0.1414
	0.1301	0.129	0.1365	0.1347	0.1305	0.1311	0.134	0.1339	0.1324	0.1323
	0.1309	0.1373	0.1431	0.1301	0.1375	0.1344	0.1315	0.1302	0.1331	0.1344
	0.1255	0.126	0.1287	0.1272	0.1262	0.1248	0.1257	0.1261	0.1264	0.1275
	0.1393	0.1417	0.1374	0.156	0.1395	0.14	0.1427	0.1429	0.1451	0.1395

Picual	0.3675	0.1387	0.1386	0.1376	0.1407	0.4063	0.1424	0.1402	0.1413	0.1347
29:1	0.1451	0.1425	0.1448	0.1396	0.1389	0.1381	0.138	0.2642	0.1408	0.1365
logsig,tansig	0.3572	0.1359	0.2408	0.1365	0.3663	0.1365	0.1399	0.137	0.14	0.1398
60:20:20	0.1373	0.2181	0.1379	0.1369	0.1382	0.1355	0.2817	0.1403	0.1396	0.1386
0.16599	0.1552	0.1504	0.1469	0.1447	0.153	0.1473	0.2666	0.1462	0.153	0.1537
0.064744	0.1322	0.1314	0.13	0.2807	0.1402	0.1297	0.136	0.1329	0.1311	0.1341
	0.1292	0.2738	0.1364	0.4007	0.1339	0.1399	0.1338	0.1362	0.1358	0.133
	0.1436	0.1442	0.1536	0.148	0.1377	0.3249	0.1407	0.1401	0.1431	0.1416
	0.1369	0.1396	0.1361	0.1579	0.1336	0.1385	0.1356	0.1377	0.1374	0.1421
	0.1442	0.2577	0.1442	0.1403	0.3133	0.1405	0.1397	0.1406	0.1427	0.2244

Picual	0.1399	0.1355	0.143	0.1381	0.1326	0.1358	0.4343	0.1388	0.1428	0.1344
29:1	0.1374	0.1366	0.1431	0.1454	0.1395	0.143	0.1422	0.1367	0.1432	0.1472
tansig,logsig	0.1302	0.1306	0.133	0.1283	0.1297	0.1296	0.1339	0.1383	0.1297	0.1258
60:20:20	0.1352	0.13	0.1332	0.1314	0.144	0.1332	0.1331	0.1368	0.1321	0.1302
0.14119	0.137	0.1358	0.136	0.1469	0.1386	0.1422	0.1365	0.1354	0.1388	0.132
0.03003	0.1409	0.1386	0.1413	0.1404	0.1521	0.1429	0.1421	0.1432	0.1432	0.1463
	0.1385	0.1418	0.1388	0.1433	0.1423	0.1369	0.1406	0.1459	0.143	0.1377
	0.1379	0.1424	0.1414	0.1454	0.1374	0.1433	0.1399	0.1365	0.1449	0.1442
	0.1348	0.1344	0.1388	0.14	0.1341	0.1297	0.1304	0.1354	0.1367	0.1451
	0.1371	0.1362	0.1395	0.1389	0.14	0.1388	0.1443	0.1353	0.1359	0.1435

Picual	0.1393	0.1372	0.1402	0.1397	0.1356	0.1385	0.5425	0.1349	0.1446	0.142
29:1	0.1443	0.3691	0.4891	0.3792	0.1414	0.1366	0.1434	0.1468	0.1394	0.4108
tansig,tansig	0.1419	0.1524	0.1417	0.1411	0.1412	0.1389	0.1461	0.1457	0.1426	0.141
60:20:20	0.1343	0.1389	0.3174	0.1429	0.1401	0.1415	0.4584	0.136	0.1321	0.9159
0.189862	0.1384	0.1338	0.1442	0.1335	0.1384	0.14	0.1413	0.1426	0.1416	0.1432
0.124924	0.1331	0.1324	0.2071	0.2085	0.4593	0.1367	0.1374	0.1406	0.2664	0.1358
	0.3717	0.1405	0.1451	0.142	0.4492	0.1399	0.1421	0.1404	0.1477	0.1478
	0.4759	0.141	0.1432	0.3124	0.1468	0.1396	0.1401	0.5068	0.1397	0.1465
	0.1376	0.1337	0.1348	0.1426	0.1348	0.1408	0.1316	0.1385	0.1329	0.1362
	0.2975	0.1337	0.1356	0.1377	0.1376	0.1352	0.1353	0.2494	0.1317	0.1316

Picual	0.1407	0.1336	0.1418	0.1435	0.1366	0.1409	0.1414	0.1362	0.1443	0.144
29:1	0.1352	0.1314	0.1306	0.132	0.1309	0.1352	0.13	0.1306	0.1405	0.1262

logsig,pure line	0.1235	0.1246	0.1239	0.1243	0.1323	0.1275	0.1203	0.1214	0.1289	0.131
60:20:20	0.1462	0.1433	0.1492	0.1451	0.1465	0.1466	0.1425	0.1438	0.141	0.1514
0.13774	0.1387	0.1459	0.1411	0.1404	0.1425	0.1375	0.1441	0.1418	0.1447	0.1425
0.006386	0.1348	0.1318	0.1376	0.133	0.1363	0.1401	0.1381	0.1397	0.1378	0.1348
	0.1346	0.1348	0.1342	0.1421	0.1354	0.1349	0.1387	0.1308	0.1321	0.1332
	0.1428	0.1454	0.1347	0.1371	0.1403	0.1468	0.1405	0.1394	0.1384	0.1417
	0.1429	0.1437	0.1425	0.1418	0.1416	0.1388	0.1416	0.1429	0.1474	0.1433
	0.1362	0.1293	0.1427	0.1353	0.1341	0.1404	0.1398	0.1401	0.1328	0.1368

Picual	0.1533	0.1533	0.1531	0.1533	0.153	0.1529	0.1529	0.1533	0.1533	0.1533
29:1	0.1471	0.1471	0.1479	0.1471	0.1471	0.1471	0.1471	0.1471	0.1471	0.1471
pure line,logsig	0.1507	0.1507	0.1507	0.1507	0.1507	0.1507	0.1506	0.1507	0.1507	0.1507
60:20:20	0.1508	0.1508	0.1508	0.1508	0.1508	0.1508	0.1505	0.1505	0.1508	0.1508
0.147276	0.1461	0.1461	0.1461	0.1461	0.1461	0.1461	0.1461	0.146	0.1461	0.1461
0.004267	0.1398	0.1398	0.1398	0.1398	0.1399	0.1398	0.1398	0.1397	0.1397	0.1397
	0.1451	0.1451	0.1451	0.1451	0.1451	0.1451	0.1451	0.1451	0.1451	0.1451
	0.1508	0.1512	0.1508	0.1509	0.1517	0.1508	0.1509	0.1509	0.1509	0.1509
	0.1485	0.1485	0.1485	0.1485	0.1479	0.1485	0.1484	0.1483	0.1485	0.1485
	0.1406	0.1406	0.1406	0.1407	0.1406	0.1407	0.1406	0.1406	0.1406	0.1406

Picual	0.1457	0.1457	0.1457	0.1457	0.1457	0.1457	0.1457	0.1457	0.1457	0.1457
29:1	0.1527	0.1527	0.1527	0.1527	0.1527	0.1525	0.1527	0.1527	0.1527	0.1527
pure line,pure line	0.1536	0.1536	0.1537	0.1537	0.1537	0.1536	0.1536	0.1536	0.1536	0.1536
60:20:20	0.1517	0.1517	0.1517	0.1516	0.1518	0.1517	0.1518	0.1517	0.1517	0.1517
0.147076	0.1423	0.1423	0.1423	0.1423	0.1423	0.1423	0.1423	0.1423	0.1423	0.1423
0.004942	0.1394	0.1394	0.1394	0.1394	0.1394	0.1394	0.1394	0.1394	0.1394	0.1394
	0.1458	0.1458	0.1458	0.1458	0.1458	0.1458	0.1458	0.1458	0.1458	0.1458
	0.1399	0.1399	0.1399	0.1399	0.1399	0.1399	0.1399	0.1436	0.1399	0.1399
	0.1498	0.1498	0.1498	0.1495	0.1498	0.1498	0.1498	0.1498	0.1498	0.1498
	0.1495	0.1495	0.1495	0.1495	0.1495	0.1495	0.1495	0.1495	0.1495	0.1495

Picual	0.1389	0.1376	0.1349	0.1465	0.1432	0.1398	0.1426	0.1414	0.1402	0.139
29:1	0.1402	0.1433	0.1365	0.1363	0.146	0.1364	0.1365	0.1432	0.1357	0.1367
tansig, pure line	0.1424	0.1457	0.1435	0.1424	0.1423	0.1426	0.1383	0.1438	0.1448	0.1335
60:20:20	0.1385	0.1343	0.1314	0.1318	0.1358	0.1357	0.1324	0.1386	0.129	0.1373
0.140191	0.1348	0.1357	0.1443	0.1355	0.1327	0.1366	0.1553	0.1351	0.1335	0.1353
0.004415	0.1433	0.1421	0.1379	0.1388	0.1458	0.1353	0.138	0.142	0.1418	0.1412
	0.1433	0.1456	0.1439	0.1437	0.1455	0.1433	0.143	0.1437	0.1417	0.1449
	0.141	0.1406	0.1383	0.137	0.1361	0.1348	0.1427	0.1369	0.1409	0.14
	0.1429	0.1464	0.143	0.139	0.1412	0.145	0.1385	0.1518	0.1409	0.1406
	0.1484	0.1437	0.1442	0.1411	0.1417	0.1378	0.1426	0.1419	0.1386	0.1389

Picual	0.127	0.1266	0.1259	0.1262	0.1274	0.1274	0.1307	0.127	0.1503	0.1311
--------	-------	--------	--------	--------	--------	--------	--------	-------	--------	--------

29:29:1	0.1333	0.1361	0.1349	0.1534	0.134	0.1376	0.1362	0.1561	0.1404	0.1342
logsid,logsig	0.1388	0.1418	0.21	0.1388	0.1388	0.1392	0.1411	0.146	0.1535	0.1437
60:20:20	0.132	0.1379	0.1347	0.136	0.153	0.1341	0.1387	0.1482	0.1349	0.1402
0.1386	0.1457	0.1345	0.1572	0.1464	0.1354	0.1353	0.1449	0.1555	0.1387	0.1354
0.012492	0.1413	0.1384	0.139	0.1362	0.1359	0.1401	0.1363	0.1337	0.1444	0.1498
	0.1334	0.1313	0.1284	0.1286	0.1299	0.1309	0.1265	0.1316	0.204	0.1322
	0.133	0.1388	0.1236	0.1257	0.1252	0.1242	0.1292	0.1276	0.144	0.1338
	0.1401	0.1464	0.1415	0.1508	0.1422	0.1446	0.1387	0.1422	0.1419	0.1408
	0.1302	0.1463	0.1337	0.1284	0.1324	0.1364	0.1382	0.1398	0.1336	0.1286

Picual	0.1492	0.135	0.132	0.1348	0.1361	0.1396	0.1406	0.1326	0.1396	0.1426
29:20:1	0.1409	0.136	0.1388	0.1373	0.1416	0.1378	0.1423	0.1431	0.1382	0.1392
logsid,logsig	0.1429	0.1338	0.1396	0.1332	0.1356	0.1353	0.1379	0.1337	0.1367	0.1537
60:20:20	0.1335	0.1507	0.1448	0.139	0.1348	0.1336	0.1391	0.1357	0.1417	0.1371
0.139522	0.1389	0.1434	0.1429	0.1476	0.1377	0.1381	0.1422	0.1388	0.1364	0.1947
0.01152	0.1315	0.1567	0.1342	0.1319	0.2206	0.1504	0.1391	0.1348	0.1479	0.1353
	0.1368	0.1346	0.1386	0.1466	0.1414	0.1383	0.1404	0.1534	0.1382	0.1348
	0.1362	0.1277	0.1301	0.1343	0.1321	0.1307	0.1298	0.1419	0.1308	0.1352
	0.1329	0.1392	0.138	0.1401	0.1476	0.1378	0.1346	0.1308	0.1335	0.1516
	0.1316	0.1324	0.1314	0.1311	0.1335	0.1411	0.1443	0.1319	0.1307	0.1334

Picual	0.1401	0.1366	0.1414	0.1389	0.1354	0.1446	0.1407	0.137	0.1434	0.1374
29:15:1	0.149	0.1426	0.146	0.1441	0.1432	0.1376	0.1415	0.1388	0.1401	0.1483
logsid,logsig	0.1338	0.1322	0.1285	0.147	0.1365	0.1303	0.1288	0.1321	0.1294	0.1341
60:20:20	0.1423	0.1468	0.1407	0.1447	0.1383	0.14	0.2106	0.2106	0.1377	0.1398
0.142296	0.1371	0.128	0.1532	0.1298	0.1262	0.1377	0.1342	0.1284	0.1417	0.2042
0.01611	0.1481	0.1507	0.2087	0.1492	0.1387	0.143	0.1557	0.141	0.1422	0.1408
	0.1501	0.1329	0.1394	0.1312	0.1374	0.132	0.1384	0.1323	0.1312	0.1378
	0.1345	0.1353	0.1364	0.147	0.1446	0.1343	0.1386	0.1488	0.137	0.1407
	0.1353	0.1349	0.2011	0.1358	0.1321	0.1372	0.1421	0.148	0.1446	0.1322
	0.1385	0.1406	0.1384	0.135	0.1331	0.1358	0.1364	0.1488	0.1376	0.1327

Picual	0.1384	0.1407	0.1468	0.1468	0.1454	0.142	0.1401	0.1432	0.1403	0.1396
29:10:1	0.1337	0.1444	0.1249	0.1266	0.1364	0.1237	0.1241	0.1305	0.1239	0.1234
logsid,logsig	0.1472	0.1423	0.1378	0.1352	0.1529	0.1436	0.1457	0.1517	0.2071	0.1404
60:20:20	0.1379	0.1402	0.1497	0.1397	0.1405	0.1408	0.1386	0.1382	0.1443	0.1453
0.139055	0.1365	0.1346	0.1429	0.1422	0.1357	0.135	0.1356	0.131	0.1314	0.1414
0.009634	0.1309	0.1512	0.1305	0.1343	0.1471	0.1451	0.1445	0.1339	0.1389	0.15
	0.1371	0.1421	0.1401	0.1483	0.1356	0.1474	0.1505	0.1473	0.1351	0.139
	0.1301	0.1316	0.1396	0.1306	0.1342	0.1296	0.1314	0.1311	0.131	0.1323
	0.1324	0.137	0.1319	0.1439	0.1293	0.1386	0.1281	0.1413	0.1327	0.1429
	0.1353	0.14	0.1413	0.1452	0.1371	0.1363	0.14	0.1385	0.1424	0.1406

Picual	0.1449	0.2099	0.1396	0.1441	0.1425	0.1538	0.1398	0.1407	0.1409	0.1436
29:5:1	0.1389	0.1437	0.1371	0.2052	0.1345	0.1351	0.1363	0.1441	0.1408	0.1602
logsig,logsig	0.1351	0.1326	0.1284	0.1346	0.1257	0.1343	0.135	0.1311	0.1351	0.128
60:20:20	0.1287	0.1368	0.139	0.1274	0.1269	0.1265	0.1958	0.1397	0.1289	0.1452
0.144342	0.1428	0.2168	0.1428	0.1385	0.138	0.1402	0.1386	0.2168	0.1449	0.1387
0.024988	0.1326	0.1331	0.141	0.1416	0.139	0.1357	0.1358	0.2128	0.1368	0.1349
	0.1344	0.1525	0.1435	0.1388	0.1285	0.1311	0.1358	0.1283	0.1271	0.1366
	0.139	0.1517	0.1411	0.1451	0.1485	0.1414	0.146	0.1402	0.143	0.147
	0.1286	0.13	0.1343	0.1302	0.1329	0.1274	0.1289	0.2982	0.1323	0.136
	0.1341	0.1408	0.1383	0.2081	0.1519	0.1363	0.134	0.1338	0.142	0.1446

Picual	0.128	0.1255	0.1345	0.1377	0.1321	0.1391	0.1689	0.129	0.1254	0.1283
29:3:1	0.1319	0.2121	0.1421	0.1385	0.1355	0.1443	0.1354	0.1334	0.1331	0.1326
logsig,logsig	0.1356	0.13	0.1375	0.1293	0.1279	0.133	0.1316	0.1289	0.1313	0.1289
60:20:20	0.1383	0.131	0.2081	0.1496	0.1349	0.1306	0.1431	0.1287	0.1276	0.2081
0.139088	0.1406	0.1409	0.1476	0.1312	0.1316	0.1428	0.1426	0.1324	0.1302	0.1318
0.017931	0.1333	0.1328	0.133	0.1339	0.1435	0.1348	0.1505	0.1309	0.1389	0.1298
	0.1259	0.1237	0.2106	0.1245	0.1259	0.1256	0.1532	0.1353	0.1282	0.1278
	0.1432	0.1349	0.1346	0.1361	0.1361	0.1484	0.1398	0.1345	0.1356	0.1363
	0.1588	0.1471	0.1383	0.1337	0.1435	0.1395	0.2114	0.1367	0.1353	0.1358
	0.128	0.1335	0.1384	0.1305	0.1384	0.1399	0.1327	0.1289	0.1352	0.1285

Picual	0.141	0.2198	0.1338	0.1378	0.1365	0.1363	0.1368	0.1398	0.1375	0.1365
29:2:1	0.1454	0.1479	0.1536	0.1502	0.1529	0.2128	0.1492	0.1647	0.1451	0.1605
logsig,logsig	0.1379	0.1489	0.1431	0.1392	0.1488	0.1486	0.1683	0.1443	0.1488	0.1409
60:20:20	0.1472	0.1689	0.1421	0.1573	0.1439	0.1411	0.1505	0.141	0.1414	0.1468
0.146523	0.134	0.1388	0.1404	0.1347	0.1453	0.1322	0.1498	0.1339	0.1319	0.1392
0.018646	0.1368	0.1406	0.1849	0.1483	0.1396	0.1434	0.1518	0.1387	0.1344	0.1489
	0.1366	0.1305	0.1394	0.1286	0.1342	0.1304	0.1366	0.1988	0.1329	0.1337
	0.1427	0.134	0.1621	0.2112	0.137	0.1333	0.1353	0.1424	0.1367	0.1377
	0.1339	0.1376	0.1358	0.1339	0.1332	0.2029	0.1453	0.1353	0.1344	0.1312
	0.1487	0.2159	0.1411	0.1414	0.1422	0.1468	0.1437	0.1404	0.1466	0.1532

Picual	0.1318	0.1339	0.1333	0.1367	0.1301	0.1336	0.132	0.1331	0.1329	0.1358
29:1	0.1358	0.1362	0.1387	0.145	0.1442	0.1395	0.1406	0.1385	0.1398	0.1401
logsig,logsig	0.1495	0.1439	0.1423	0.1414	0.1452	0.1404	0.1463	0.1427	0.141	0.1439
60:20:20	0.1403	0.1444	0.1365	0.1384	0.1387	0.1427	0.1377	0.1495	0.1382	0.1377
0.13976	0.1394	0.1379	0.1354	0.1376	0.1372	0.1327	0.1324	0.1373	0.1349	0.1372
0.018673	0.1369	0.1338	0.1333	0.1294	0.1351	0.1414	0.1312	0.1295	0.1369	0.1312
	0.1373	0.1392	0.1344	0.1405	0.1398	0.1363	0.1416	0.137	0.1414	0.3188
	0.1354	0.14	0.1371	0.1495	0.1401	0.1468	0.1405	0.1524	0.1389	0.1398
	0.1375	0.1327	0.142	0.1445	0.1325	0.1339	0.1361	0.1337	0.1359	0.135
	0.1344	0.1382	0.134	0.1361	0.1311	0.1374	0.1352	0.1334	0.1395	0.1331

Souri	0.0801	0.0804	0.0804	0.081	0.0799	0.0798	0.08	0.0806	0.081	0.079
29:1	0.0757	0.0764	0.0755	0.0763	0.0762	0.076	0.0762	0.0768	0.0755	0.0778
logsid,logsig	0.0827	0.0818	0.0811	0.0814	0.0813	0.081	0.0809	0.0807	0.0818	0.0808
34:33:33	0.0812	0.0813	0.0815	0.1632	0.0825	0.0803	0.0808	0.0808	0.0815	0.0814
0.084286	0.0821	0.0808	0.0821	0.0811	0.0822	0.0836	0.0833	0.0821	0.0824	0.0826
0.01741	0.0794	0.0798	0.0788	0.0794	0.0798	0.0796	0.0791	0.0797	0.0804	0.079
	0.0794	0.0796	0.0795	0.0802	0.08	0.0793	0.0802	0.0794	0.1594	0.0795
	0.0802	0.0793	0.0795	0.0801	0.0796	0.0792	0.0792	0.0806	0.1614	0.0794
	0.0813	0.0805	0.0807	0.0805	0.0803	0.0802	0.0815	0.082	0.0809	0.0806
	0.0815	0.0819	0.0815	0.0867	0.0819	0.1563	0.0826	0.0838	0.1563	0.0827

Souri	0.0779	0.0789	0.0784	0.0793	0.08	0.1545	0.0791	0.0781	0.0798	0.0785
29:1	0.0801	0.0808	0.0807	0.0804	0.0802	0.0795	0.0801	0.0844	0.0792	0.0806
logsid,logsig	0.0803	0.0815	0.08	0.1598	0.0817	0.0797	0.0806	0.0804	0.0812	0.0814
40:30:30	0.0818	0.0812	0.159	0.081	0.0832	0.0805	0.0805	0.0814	0.0822	0.0816
0.083411	0.0846	0.0851	0.0846	0.0869	0.0842	0.0855	0.0847	0.0851	0.0851	0.0843
0.01331	0.081	0.0796	0.0794	0.0799	0.0798	0.0781	0.0799	0.0799	0.0786	0.0796
	0.082	0.0833	0.0826	0.0829	0.0835	0.0826	0.0832	0.083	0.083	0.0827
	0.0814	0.0799	0.0813	0.0805	0.081	0.0803	0.0808	0.0805	0.0806	0.0806
	0.082	0.0819	0.0818	0.0826	0.0822	0.0817	0.0861	0.0833	0.0822	0.082
	0.0771	0.0781	0.08	0.0791	0.0788	0.0797	0.0779	0.0778	0.0781	0.0776

Souri	0.0783	0.0783	0.0788	0.0773	0.0787	0.078	0.0785	0.0822	0.0788	0.0783
29:1	0.0824	0.082	0.0827	0.0838	0.0825	0.0824	0.0826	0.0824	0.0815	0.0824
logsid,logsig	0.0778	0.0782	0.0788	0.0788	0.0789	0.0781	0.0777	0.0779	0.079	0.0788
60:20:20	0.0793	0.0794	0.0783	0.0794	0.0788	0.0799	0.079	0.0781	0.0798	0.0783
0.082391	0.0847	0.084	0.0846	0.0846	0.0859	0.0837	0.0841	0.0838	0.0845	0.0836
0.011299	0.0797	0.0799	0.0785	0.0801	0.0816	0.0791	0.079	0.08	0.0794	0.0798
	0.0855	0.086	0.0862	0.0879	0.0865	0.0864	0.0867	0.086	0.0865	0.0855
	0.0781	0.0766	0.0766	0.0776	0.0764	0.0772	0.0772	0.0784	0.0769	0.0777
	0.0819	0.0818	0.0847	0.0817	0.0805	0.0809	0.081	0.0832	0.159	0.0821
	0.0802	0.0806	0.0793	0.0801	0.0802	0.0807	0.0803	0.1581	0.0798	0.0803

Souri	0.0782	0.0747	0.159	0.0768	0.0779	0.0773	0.077	0.0793	0.0757	0.0754
29:1	0.0829	0.0831	0.0832	0.0837	0.0832	0.0838	0.085	0.0822	0.0848	0.0845
logsid,logsig	0.1744	0.0805	0.0805	0.0827	0.0804	0.0846	0.0819	0.0805	0.0811	0.0812
80:10:10	0.0791	0.0793	0.0796	0.079	0.0781	0.0797	0.1655	0.0803	0.0785	0.0788
0.08318	0.0774	0.0769	0.0783	0.0773	0.0765	0.0788	0.0766	0.0772	0.0783	0.0782
0.017872	0.0826	0.0824	0.0825	0.0819	0.0834	0.0824	0.0829	0.0827	0.0826	0.0823
	0.0786	0.0767	0.0781	0.0775	0.0783	0.0774	0.0772	0.0779	0.078	0.0782
	0.0893	0.0911	0.09	0.09	0.0888	0.1069	0.0923	0.0893	0.0911	0.0895
	0.0723	0.1638	0.0734	0.0714	0.0718	0.0716	0.0716	0.072	0.0715	0.0711
	0.0737	0.0745	0.072	0.074	0.0727	0.0749	0.0744	0.0748	0.0723	0.0734

Souri	0.0769	0.0775	0.078	0.0778	0.0771	0.0769	0.0772	0.0773	0.0768	0.0773
29:1	0.0778	0.0779	0.0784	0.0779	0.0785	0.0773	0.0784	0.0784	0.0779	0.0806
logsig,logsig	0.0821	0.0838	0.0824	0.0825	0.083	0.083	0.0833	0.083	0.0829	0.0833
60:20:20	0.0828	0.0841	0.0836	0.0834	0.0828	0.0822	0.0832	0.0817	0.0841	0.0862
0.082382	0.0816	0.0824	0.0851	0.0823	0.0824	0.0818	0.0819	0.0828	0.0826	0.0835
0.011515	0.0796	0.078	0.0779	0.0783	0.079	0.0777	0.0768	0.0786	0.0782	0.1628
	0.0866	0.0827	0.0832	0.0824	0.0824	0.0817	0.0822	0.0824	0.0829	0.0825
	0.0773	0.0792	0.0777	0.0778	0.0789	0.078	0.0787	0.0788	0.0778	0.0786
	0.079	0.0789	0.0796	0.08	0.079	0.158	0.0795	0.0793	0.0797	0.08
	0.0837	0.0838	0.0862	0.0832	0.0849	0.0834	0.0844	0.0834	0.084	0.0838

Souri	0.0735	0.0716	0.071	0.0723	0.0721	0.0732	0.0731	0.0719	0.0728	0.0707
29:1	0.079	0.0799	0.0788	0.0793	0.0791	0.2252	0.0813	0.0807	0.08	0.0813
logsig,tansig	0.0798	0.0807	0.1632	0.081	0.0811	0.0797	0.1632	0.0793	0.0795	0.0797
60:20:20	0.082	0.0826	0.0836	0.0818	0.0819	0.0845	0.0823	0.0824	0.0822	0.0823
0.089704	0.0808	0.0809	0.0814	0.0808	0.0828	0.0814	0.0813	0.0874	0.0809	0.0809
0.029275	0.0798	0.0803	0.08	0.08	0.0803	0.0793	0.0808	0.1634	0.0806	0.0797
	0.0781	0.0775	0.078	0.163	0.077	0.0779	0.1723	0.0787	0.0783	0.082
	0.0797	0.0795	0.0784	0.1561	0.0796	0.0775	0.1561	0.0772	0.0775	0.1561
	0.0761	0.0753	0.1573	0.078	0.076	0.0755	0.0753	0.0749	0.0757	0.0754
	0.0833	0.0831	0.0843	0.1591	0.0841	0.0837	0.1591	0.0841	0.084	0.0832

Souri	0.0831	0.0836	0.0823	0.0824	0.0837	0.1204	0.0827	0.0833	0.0825	0.0824
29:1	0.0777	0.0764	0.0778	0.0768	0.0785	0.0771	0.0769	0.0774	0.0777	0.0783
tansig,logsig	0.0839	0.0859	0.0869	0.0855	0.0845	0.0836	0.085	0.0848	0.0847	0.0849
60:20:20	0.0768	0.0785	0.0781	0.0791	0.0793	0.0771	0.0813	0.0773	0.0768	0.0766
0.088612	0.0764	0.074	0.0756	0.0743	0.0737	0.075	0.0762	0.0743	0.075	0.1678
0.034068	0.1766	0.0808	0.0803	0.0819	0.0806	0.0813	0.0805	0.0807	0.0831	0.0805
0.190817	0.0791	0.0777	0.0788	0.0771	0.0884	0.0776	0.3427	0.0784	0.0773	0.0771
	0.0827	0.0826	0.0832	0.0822	0.0824	0.0839	0.0819	0.0824	0.0814	0.0819
	0.0859	0.0843	0.0859	0.0848	0.085	0.0858	0.0849	0.0848	0.1621	0.0849
	0.0806	0.0813	0.0822	0.0808	0.0819	0.0809	0.1601	0.082	0.2226	0.0814

Souri	0.0776	0.0778	0.0786	0.078	0.0788	0.0779	0.0783	0.0793	0.0782	0.1564
29:1	0.1523	0.0718	0.0742	0.0729	0.0758	0.0723	0.0724	0.0722	0.0935	0.0712
tansig,tansig	0.083	0.1922	0.0795	0.0796	0.0821	0.0808	0.0815	0.0805	0.0824	0.0809
60:20:20	0.0813	0.0817	0.0797	0.27	0.0797	0.0794	0.0795	0.08	0.0799	0.0808
0.089167	0.0773	0.0793	0.0776	0.0783	0.0767	0.1583	0.0771	0.0773	0.0772	0.0771
0.032406	0.2322	0.0811	0.0821	0.0821	0.0815	0.0805	0.0813	0.082	0.0825	0.0815
0.186384	0.0805	0.0793	0.0808	0.0806	0.0799	0.0787	0.0787	0.0792	0.0792	0.0786
	0.0825	0.0819	0.1604	0.0829	0.0826	0.0825	0.0815	0.0815	0.0824	0.0821
	0.1731	0.0849	0.0823	0.083	0.0853	0.0829	0.0822	0.0827	0.0824	0.0824
	0.1652	0.0786	0.0801	0.0782	0.0778	0.0776	0.0797	0.079	0.0785	0.078

Souri	0.0812	0.0805	0.0812	0.0804	0.0807	0.0805	0.081	0.0797	0.081	0.0806
29:1	0.0762	0.0756	0.0741	0.0757	0.0745	0.0753	0.0746	0.0758	0.0756	0.0748
logsig,pure line	0.0749	0.0749	0.0765	0.0759	0.0755	0.0754	0.0758	0.0753	0.0762	0.075
60:20:20	0.0833	0.0837	0.0834	0.0849	0.085	0.0838	0.0842	0.0839	0.0833	0.0849
0.077948	0.071	0.0712	0.0704	0.0709	0.0711	0.0705	0.071	0.0722	0.0718	0.0755
0.004224	0.082	0.0822	0.083	0.0818	0.0824	0.0828	0.0813	0.0817	0.0813	0.0815
0.090619	0.0709	0.0728	0.0732	0.072	0.072	0.0725	0.0723	0.0701	0.0715	0.0717
	0.0799	0.0811	0.0807	0.081	0.0805	0.0809	0.0801	0.0815	0.0805	0.0808
	0.0806	0.0796	0.0806	0.0837	0.0815	0.0806	0.0808	0.081	0.0812	0.0817
	0.0767	0.0757	0.0767	0.0765	0.0771	0.0765	0.0766	0.0773	0.0769	0.0771

Souri	0.0926	0.0928	0.0926	0.0926	0.0926	0.0926	0.0926	0.0926	0.0925	0.0926
29:1	0.0942	0.0942	0.0942	0.0941	0.0942	0.0942	0.0941	0.0942	0.0942	0.0942
pure line,logsig	0.0893	0.0893	0.0893	0.0894	0.0893	0.0893	0.0893	0.0893	0.0893	0.0893
60:20:20	0.0864	0.0864	0.0865	0.0865	0.0865	0.0865	0.0865	0.0865	0.0865	0.0865
0.089604	0.0873	0.0873	0.0873	0.0873	0.0872	0.0873	0.0873	0.0873	0.0872	0.0873
0.00305	0.0935	0.0935	0.0935	0.0935	0.0935	0.0935	0.0935	0.0935	0.0935	0.0935
0.098753	0.0885	0.0883	0.0883	0.0884	0.0884	0.0884	0.0883	0.0883	0.0884	0.0883
	0.0894	0.0894	0.0895	0.0894	0.0895	0.0895	0.0894	0.0894	0.0895	0.0895
	0.0842	0.0842	0.0842	0.0844	0.0842	0.0842	0.0842	0.0842	0.0842	0.0842
	0.0905	0.0907	0.0907	0.0907	0.0907	0.0907	0.0906	0.0907	0.0907	0.0905

Souri	0.0923	0.0923	0.0923	0.0923	0.0923	0.0923	0.0923	0.0923	0.0924	0.0924
29:1	0.0937	0.0937	0.0938	0.0937	0.0936	0.0937	0.0937	0.0937	0.0937	0.0934
pure line,pure line	0.0852	0.0852	0.0852	0.0853	0.0852	0.0852	0.0852	0.0852	0.0852	0.0855
60:20:20	0.0916	0.0916	0.0916	0.0916	0.0916	0.0916	0.0916	0.0916	0.0916	0.0916
0.087874	0.0872	0.0872	0.0872	0.0872	0.0872	0.0872	0.0872	0.0872	0.0872	0.0872
0.003342	0.0868	0.0867	0.0868	0.0868	0.0868	0.0868	0.0868	0.0868	0.0868	0.0868
0.097899	0.0855	0.0855	0.0855	0.0855	0.0854	0.0855	0.0855	0.0855	0.0855	0.0855
	0.0847	0.0847	0.0847	0.0847	0.0847	0.0847	0.0847	0.0847	0.085	0.0847
	0.0882	0.0882	0.0882	0.0882	0.0882	0.0882	0.0881	0.0882	0.0882	0.0882
	0.0835	0.0836	0.0835	0.0835	0.0835	0.0835	0.0835	0.0835	0.0835	0.0835

Souri	0.0865	0.0872	0.0863	0.087	0.0875	0.0855	0.086	0.0869	0.0858	0.0857
29:1	0.0729	0.0737	0.0731	0.0747	0.0737	0.0738	0.0725	0.0738	0.0733	0.0732
tansig, pure line	0.079	0.0785	0.078	0.0782	0.0782	0.0784	0.0783	0.0787	0.0788	0.078
60:20:20	0.0807	0.0808	0.0807	0.0797	0.0794	0.0809	0.0802	0.0805	0.0812	0.081
0.079425	0.078	0.0787	0.0792	0.0794	0.0781	0.0783	0.077	0.0775	0.0789	0.0787
0.003366	0.0768	0.0765	0.0778	0.0774	0.0786	0.0783	0.0772	0.0766	0.0774	0.0758
0.089524	0.0803	0.0812	0.0823	0.0813	0.0824	0.0803	0.082	0.0812	0.0823	0.081
	0.0778	0.0773	0.0776	0.0786	0.0772	0.0778	0.0766	0.0784	0.0775	0.0771
	0.0791	0.0793	0.0775	0.0789	0.0781	0.0786	0.0784	0.0783	0.0792	0.0786

	0.0825	0.0821	0.082	0.0818	0.0833	0.0821	0.0828	0.082	0.0813	0.0819
--	--------	--------	-------	--------	--------	--------	--------	-------	--------	--------

Souri	0.0794	0.0783	0.0786	0.0784	0.0816	0.0802	0.0789	0.1613	0.0816	0.0787
29:29:1	0.0828	0.0823	0.0819	0.0835	0.0822	0.0807	0.081	0.0828	0.0814	0.0816
logsid,logsig	0.0817	0.0795	0.0795	0.0879	0.0791	0.0795	0.0793	0.08	0.0815	0.0796
60:20:20	0.0795	0.0783	0.0795	0.0789	0.0787	0.0815	0.078	0.081	0.1541	0.0785
0.085193	0.0825	0.161	0.0781	0.083	0.0782	0.0783	0.0808	0.0786	0.0786	0.0827
0.017659	0.0796	0.0802	0.0796	0.0878	0.0813	0.0792	0.0845	0.08	0.1629	0.0794
0.138171	0.0807	0.0796	0.166	0.0814	0.0816	0.0813	0.0829	0.0799	0.08	0.0818
	0.0807	0.0819	0.083	0.085	0.0806	0.0814	0.0829	0.0831	0.0798	0.0812
	0.0832	0.0851	0.084	0.0837	0.0843	0.0846	0.0843	0.0847	0.0828	0.0872
	0.0809	0.0795	0.0819	0.0788	0.0813	0.0804	0.0792	0.079	0.082	0.0885

Souri	0.08	0.084	0.0796	0.0798	0.0799	0.0797	0.0792	0.0802	0.083	0.0845
29:20:1	0.0808	0.0821	0.0798	0.0806	0.0801	0.0801	0.08	0.0812	0.0801	0.0812
logsid,logsig	0.0811	0.1505	0.082	0.0793	0.0795	0.0808	0.0796	0.0784	0.0806	0.0782
60:20:20	0.0834	0.0828	0.0835	0.0847	0.0824	0.0858	0.083	0.0833	0.0866	0.0832
0.083202	0.0798	0.0808	0.0811	0.0796	0.0825	0.0805	0.0807	0.0801	0.0792	0.0787
0.010608	0.0787	0.0785	0.0787	0.0787	0.0876	0.0824	0.0791	0.0833	0.0781	0.0821
0.115027	0.0778	0.0757	0.0784	0.0777	0.0765	0.0783	0.0768	0.0786	0.0768	0.077
	0.0843	0.0871	0.1565	0.0848	0.0823	0.0837	0.0816	0.0827	0.0832	0.0875
	0.0895	0.0861	0.0893	0.0883	0.0865	0.0896	0.0867	0.0867	0.09	0.0883
	0.0812	0.0797	0.0848	0.0826	0.08	0.082	0.0853	0.0796	0.0801	0.0818

Souri	0.0831	0.0839	0.0816	0.0812	0.0825	0.0847	0.0841	0.088	0.0817	0.0818
29:15:1	0.0785	0.163	0.0756	0.0799	0.0776	0.0799	0.0759	0.0776	0.0756	0.0795
logsid,logsig	0.0889	0.0843	0.0828	0.0849	0.0863	0.084	0.0848	0.0831	0.0858	0.0838
60:20:20	0.0748	0.0794	0.0785	0.0762	0.075	0.0788	0.08	0.0758	0.0777	0.0803
0.081381	0.0775	0.0793	0.0768	0.0766	0.0813	0.0792	0.0765	0.0772	0.0805	0.0779
0.008815	0.0796	0.0798	0.0796	0.0791	0.0813	0.0779	0.079	0.0809	0.0785	0.081
0.107825	0.0797	0.0805	0.0848	0.0787	0.0805	0.0828	0.0793	0.0804	0.0796	0.0812
	0.0795	0.0803	0.0801	0.0835	0.0823	0.0807	0.0792	0.0806	0.0816	0.081
	0.0842	0.0881	0.0843	0.0847	0.0854	0.0829	0.0816	0.0862	0.0815	0.0851
	0.0788	0.0764	0.0764	0.0787	0.0763	0.0786	0.0768	0.0783	0.0794	0.0777

Souri	0.0769	0.077	0.0757	0.075	0.0797	0.0755	0.0761	0.1609	0.0757	0.0757
29:10:1	0.0807	0.082	0.0823	0.083	0.0817	0.0813	0.0801	0.081	0.0914	0.0816
logsid,logsig	0.0749	0.0784	0.1141	0.0765	0.0754	0.0781	0.0787	0.0752	0.0763	0.0761
60:20:20	0.076	0.0716	0.0722	0.0761	0.0739	0.075	0.0747	0.0749	0.0731	0.072
0.082443	0.0837	0.0855	0.084	0.0843	0.0844	0.0833	0.0822	0.0824	0.0836	0.0825
0.009575	0.0837	0.083	0.0851	0.0829	0.0838	0.0845	0.0833	0.0881	0.0906	0.0839
0.111167	0.082	0.0856	0.0811	0.0831	0.081	0.0807	0.0836	0.0806	0.0807	0.0808
	0.0824	0.0814	0.0882	0.0832	0.0822	0.082	0.0843	0.0838	0.0827	0.0838

	0.0833	0.0834	0.0815	0.0829	0.0872	0.0831	0.0831	0.0826	0.0826	0.0834
	0.0851	0.0845	0.0858	0.0837	0.0855	0.084	0.0831	0.087	0.0852	0.0928

Souri	0.0779	0.0785	0.0796	0.0799	0.0775	0.0801	0.0775	0.0768	0.0899	0.0767
29:5:1	0.0815	0.0825	0.0814	0.0814	0.083	0.0813	0.0808	0.0816	0.0831	0.0819
logsid,logsig	0.1589	0.0841	0.0848	0.0829	0.0869	0.084	0.0833	0.0835	0.0857	0.083
60:20:20	0.0808	0.0811	0.0815	0.0804	0.0787	0.0783	0.0811	0.1625	0.0791	0.0806
0.085517	0.0711	0.0706	0.0722	0.0723	0.1561	0.0702	0.1561	0.0697	0.0712	0.0706
0.018999	0.0753	0.0752	0.0768	0.0759	0.075	0.081	0.0753	0.0753	0.0745	0.1531
0.142515	0.0821	0.0821	0.1627	0.0817	0.0838	0.086	0.086	0.0825	0.0839	0.0841
	0.0792	0.081	0.08	0.0795	0.0797	0.0792	0.0796	0.0799	0.0796	0.0788
	0.0854	0.0866	0.0861	0.0866	0.0893	0.0872	0.0857	0.086	0.0863	0.0884
	0.0835	0.0833	0.0838	0.083	0.0829	0.0843	0.085	0.0854	0.084	0.0859

Souri	0.077	0.0799	0.0778	0.0792	0.0813	0.0782	0.087	0.0797	0.077	0.0766
29:3:1	0.0849	0.0856	0.0846	0.0854	0.0851	0.0843	0.0871	0.0841	0.0851	0.0873
logsid,logsig	0.163	0.0785	0.0806	0.0799	0.0818	0.0789	0.0785	0.0811	0.0799	0.0791
60:20:20	0.0852	0.0869	0.1675	0.1675	0.1675	0.1675	0.1675	0.0844	0.0861	0.0881
0.090302	0.0809	0.0822	0.0823	0.0828	0.0832	0.0819	0.0833	0.1586	0.1587	0.118
0.023908	0.0796	0.0803	0.0827	0.0802	0.081	0.0808	0.08	0.0818	0.1639	0.081
	0.0828	0.0825	0.0851	0.0827	0.0829	0.085	0.0849	0.0829	0.0828	0.0821
	0.0837	0.0825	0.0839	0.0814	0.0829	0.0817	0.0841	0.083	0.0829	0.0818
	0.0833	0.0849	0.0842	0.0867	0.085	0.088	0.083	0.0857	0.0843	0.0837
	0.0831	0.0822	0.0827	0.0816	0.0803	0.0813	0.0823	0.081	0.0842	0.0812

Souri	0.0829	0.0836	0.1582	0.0843	0.0839	0.0847	0.0828	0.0839	0.0821	0.0826
29:2:1	0.0766	0.1594	0.0776	0.0789	0.0778	0.0764	0.0767	0.0767	0.0806	0.0785
logsid,logsig	0.0861	0.1576	0.0868	0.0888	0.0884	0.0877	0.0848	0.0886	0.089	0.0872
60:20:20	0.0846	0.0841	0.1592	0.087	0.0834	0.1592	0.0826	0.0825	0.0845	0.0831
0.088275	0.0803	0.078	0.0791	0.0773	0.1546	0.0797	0.0789	0.081	0.0794	0.0773
0.023679	0.0799	0.0788	0.08	0.0803	0.079	0.0801	0.0809	0.0793	0.08	0.0805
	0.0837	0.0833	0.083	0.0842	0.0813	0.0825	0.0842	0.0832	0.0832	0.0842
	0.0809	0.0817	0.0816	0.0836	0.0819	0.0813	0.0817	0.0828	0.0851	0.081
	0.0759	0.0775	0.0762	0.0783	0.0756	0.2146	0.0782	0.0761	0.0761	0.0779
	0.081	0.1607	0.0816	0.0821	0.0823	0.0826	0.0819	0.0819	0.0825	0.0823

Souri	0.0839	0.0816	0.0835	0.0816	0.0828	0.0818	0.082	0.0816	0.0813	0.0821
29:1	0.0756	0.0745	0.0748	0.0765	0.0746	0.0763	0.0749	0.0779	0.0761	0.0759
logsid,logsig	0.084	0.0843	0.085	0.0817	0.0838	0.0824	0.0828	0.0838	0.0842	0.0841
60:20:20	0.0834	0.0836	0.084	0.0874	0.0833	0.0841	0.0825	0.083	0.0848	0.0844
0.082439	0.0808	0.0762	0.0773	0.0775	0.0786	0.078	0.0779	0.0773	0.0774	0.0775
0.013331	0.0827	0.0797	0.0806	0.0813	0.0803	0.0805	0.0802	0.0853	0.0801	0.0807
	0.0759	0.075	0.0768	0.0761	0.1767	0.0757	0.0758	0.0756	0.075	0.0756

	0.0839	0.0844	0.0868	0.0837	0.0837	0.0859	0.0839	0.083	0.0848	0.0851
	0.0769	0.078	0.1673	0.0774	0.0765	0.0779	0.0775	0.077	0.0771	0.0782
	0.0823	0.0828	0.0824	0.0833	0.084	0.0834	0.0821	0.0837	0.0846	0.0823

Appendix C. ANN software

Matlab code for ANN training and testing

```

function e=ANN(data)
p=data(:,2:30); %-----select input -----
t=data(:,1); %-----select tagets-----
p=p';
t=t';
for k=1:10
    [trainV,val,test] = dividevec(p,t,0.20,0.20); %-----Divide data to traing validating and testing
    net=newff(minmax(p),[29, 1],{'logsig','logsig'},'trainlm','learngdm','mse');%-Define network structure and transfer functions
    for j=1:10
        net.trainParam.show = NaN; %-----define stopping criteria
        net.trainParam.epochs = 100;
        net.trainParam.goal = 0;
        net.trainParam.max_fail = 5;
        net.trainParam.mem_reduc = 1;
        net.trainParam.min_grad = 1e-10;
        [net,tr]=train(net,trainV.P,trainV.T,[],[],val);%-----train network
        a = sim(net,test.P,[],[],test.T);%-----simulate results with testing set
        e(k,j)=std(test.T-a);%-----calculate standard error
        net=init(net);%-----initiate weights
    end
    clear tarinV val test %-----clear sets
end

```

Appendix D. Statistical Analysis software

SPSS code for simple linear regression

6. REGRESSION
7. /SELECT= Variety_Code EQ 1
8. /MISSING LISTWISE
9. /STATISTICS COEFF OUTS R ANOVA
10. /CRITERIA=PIN(.05) POUT(.10)
11. /NOORIGIN
12. /DEPENDENT Oil_amount
13. /METHOD=ENTER AVG_FD1 AVG_FD2 AVG_FD3 AVG_FD4 AVG_FD5 AVG_RatioElong
AVG_Av#G AVG_Var#G AVG_DefectArea AVG_Mean_Gr
14. AVG_SD_Gr AVG_Smooth_Gr AVG_3rd_Moment AVG_Uniformity_Gr AVG_Entropy_Gr
AVG_Mean_Hue AVG_SD_Hue AVG_Smooth_Hue
15. AVG_3rd_Moment_Hue AVG_Uniformity_Hue AVG_Entropy_Hue .

SPSS code for factor analysis

FACTOR

/VARIABLES Area length width Eccentricity EquiveD Compctness MaxDist LengthVec
AVG_FD1 AVG_FD2 AVG_FD3 AVG_FD4 AVG_FD5

```

AVG_RatioElong AVG_Av#G AVG_Var#G AVG_DefectArea AVG_Mean_Gr AVG_SD_Gr
AVG_Smooth_Gr AVG_3rd_Moment AVG_Uniformity_Gr
AVG_Entropy_Gr AVG_Mean_Hue AVG_SD_Hue AVG_Smooth_Hue AVG_3rd_Moment_Hue
AVG_Uniformity_Hue AVG_Entropy_Hue /MISSING
LISTWISE /ANALYSIS Area length width Eccentricity EquiveD Compctness MaxDist LengthVec
AVG_FD1 AVG_FD2 AVG_FD3 AVG_FD4
AVG_FD5 AVG_RatioElong AVG_Av#G AVG_Var#G AVG_DefectArea AVG_Mean_Gr
AVG_SD_Gr AVG_Smooth_Gr AVG_3rd_Moment
AVG_Uniformity_Gr AVG_Entropy_Gr AVG_Mean_Hue AVG_SD_Hue AVG_Smooth_Hue
AVG_3rd_Moment_Hue AVG_Uniformity_Hue
AVG_Entropy_Hue
/SELECT=Variety_Code(1)
/PRINT INITIAL EXTRACTION ROTATION FSCORE
/PLOT EIGEN
/CRITERIA MINEIGEN(1) ITERATE(25)
/EXTRACTION PC
/CRITERIA ITERATE(25)
/ROTATION EQUAMAX
/SAVE REG(ALL)
/METHOD=CORRELATION .

```

Appendix E. Raw data – example

Side	Variety	Picking date	Picture date	Pic No	Olive No	Wet Weight	Dry Weight	Oil%	Area	length	width	Eccentricity
1	Picual	11/25/2007	11/26/2007	p1	1	4458	1838	3030	156954	516	397	0.641877
1	Picual	11/25/2007	11/26/2007	p1	2	6155	1952	3004	194168	570	440	0.632148
1	Picual	11/25/2007	11/26/2007	p1	3	4141	1614	2913	150042	497	383	0.658908
1	Picual	11/25/2007	11/26/2007	p1	4	6144	2057	3481	193208	566	447	0.63384
1	Picual	11/25/2007	11/26/2007	p1	5	6235	2340	3562	196590	578	430	0.659247
1	Picual	11/25/2007	11/26/2007	p1	6	5728	2092	3254	186550	537	461	0.565788
1	Picual	11/25/2007	11/26/2007	p1	7	5900	2130	3152	183657	581	405	0.711967
1	Picual	11/25/2007	11/26/2007	p1	8	5218	1951	3429	172392	528	417	0.620221
1	Picual	11/25/2007	11/26/2007	p1	9	5634	2040	3325	178145	537	423	0.630589
1	Picual	11/25/2007	11/26/2007	p1	10	5231	2052	3397	168725	542	405	0.651191
1	Picual	11/25/2007	11/26/2007	p2	1	3560	1387	2737	133591	493	344	0.721486
1	Picual	11/25/2007	11/26/2007	p2	2	5044	1697	2970	163289	522	404	0.624328
1	Picual	11/25/2007	11/26/2007	p2	3	5530	1964	3282	191440	575	426	0.670392
1	Picual	11/25/2007	11/26/2007	p2	4	3487	1436	3206	129111	430	374	0.505476
1	Picual	11/25/2007	11/26/2007	p2	5	7509	2481	3275	224674	642	463	0.688205
1	Picual	11/25/2007	11/26/2007	p2	6	2954	1122	2501	112997	455	322	0.721791
1	Picual	11/25/2007	11/26/2007	p2	7	6795	2515	3441	212926	609	449	0.668252
1	Picual	11/25/2007	11/26/2007	p2	8	2601	986	1988	106867	444	317	0.719175
1	Picual	11/25/2007	11/26/2007	p2	9	5068	1912	3050	168223	551	396	0.699014
1	Picual	11/25/2007	11/26/2007	p2	10	5977	2112	3120	192157	588	413	0.709864
1	Picual	11/25/2007	11/26/2007	p3	1	2881	1343	3211	114004	436	341	0.60267
1	Picual	11/25/2007	11/26/2007	p3	2	4428	1680	3466	153394	485	403	0.589897
1	Picual	11/25/2007	11/26/2007	p3	3	5440	1753	3055	178042	532	424	0.626101
1	Picual	11/25/2007	11/26/2007	p3	4	6309	1926	3370	199735	593	425	0.701194
1	Picual	11/25/2007	11/26/2007	p3	5	3805	1524	2664	138416	478	373	0.632253
1	Picual	11/25/2007	11/26/2007	p3	6	5404	1895	3325	175119	549	424	0.656102
1	Picual	11/25/2007	11/26/2007	p3	7	4779	1645	3114	164869	535	393	0.679028

Appendix F. Abbreviation

Feature	Description
Area	Number of relevant pixels
length	Length of olive bounding box
width	Width of olive bounding box
Eccentricity	L1/L2: Ellipse (same second moment as the region) centers distance (L1) by Long Axis (L2) (~1 – Circle; ~0 - Area Line).
EquiveD	Diameter of same area circle
Compctness	Shape - Perimeter/Area^2
MaxDist	maximum distance from center to edge
LengthVec	Length vector - The distance vector length
AVG_FD1	Average of first FFT coefficient - Average Radius
AVG_FD2	Average second FFT coefficient - Bendingness
AVG_FD3	Average of third FFT coefficient - Elongation
AVG_FD4	Average of forth FFT coefficient
AVG_FD5	Average of fifth FFT coefficient
AVG_RatioElong	(FD(1)-2*(FD(3)))/(FD(1)+2*(FD(3)))
AVG_Av#G	Average of average green value (RGB matrix)
AVG_Var#G	Average of variance of green value (RGB matrix)
AVG_DefectArea	Average ratio between defect area and non defect area
AVG_Mean_Gr	Texture - Average intensity (GrayImage).
AVG_SD_Gr	Texture - Standard deviation – measure of average contrast
AVG_Smooth_Gr	Texture - $R = 1 - 1/(1 + \sigma^2)$
AVG_3rd_Moment	Texture - Measure of the skewness of the histogram
AVG_Uniformity_Gr	Texture - $U = \sum_{i=0}^{L-1} p^2(z_i)$
AVG_Entropy_Gr	Measure of randomness
AVG_Mean_Hue	Texture - Average Hue (HSI image).
AVG_SD_Hue	Texture - Standard deviation of Hue – measure of average contrast
AVG_Smooth_Hue	Texture - $R = 1 - 1/(1 + \sigma^2)$
AVG_3rd_Moment_Hue	Texture - Measure of the skewness of the histogram
AVG_Uniformity_Hue	Texture - $U = \sum_{i=0}^{L-1} p^2(z_i)$
AVG_Entropy_Hue	Measure of randomness

Appendix G. Weights and biases of best networks

<i>Picual</i>								
b {1}	IW{1,1}						b {2}	IW{2,1}
-6.0932	-2.0721	-1.6912	-0.8199	-0.4488	-0.5418	-1.8642	-0.9825	0.2503
4.9475	1.0352	1.8347	-1.7986	0.8853	0.8539	-0.5668		1.0746
2.7631	-1.1154	-0.2931	1.4823	-0.2121	-0.6618	0.4917		-2.8869
-0.4899	0.0059	-0.0554	2.2734	1.8107	-0.9295	-0.3884		1.731
2.8674	1.7311	0.7148	-1.285	-0.6023	1.884	0.547		-0.8116
2.4101	1.0456	0.4536	-2.5146	-1.5493	1.475	1.0224		0.7395
-4.6786	-1.6526	0.8024	2.0093	0.2807	0.2213	0.5387		-1.4601
-3.0847	-1.7504	-1.3981	-0.8538	1.3867	-1.8806	0.0497		-0.8415
2.949	-0.4463	-0.0677	0.6909	-0.7095	0.1881	-0.0708		-2.1652
1.873	1.0389	0.2672	0.239	3.2063	1.044	-2.499		0.6868
-5.1063	1.9423	-0.4895	-0.4705	-0.8287	0.1987	0.6561		2.6349
-0.0713	-0.6322	-0.0833	-1.2979	-1.7785	0.1407	0.6591		1.7236
-0.6575	-2.1103	-1.2974	-0.774	0.4164	0.3891	0.6121		1.1374
0.2422	-2.8836	0.0423	0.0191	0.0398	1.5668	0.5342		0.8969
-0.8349	1.4827	0.2197	0.3057	-0.288	-2.0683	-0.2373		1.6436
2.8793	1.2141	1.3943	2.5086	0.6691	0.5158	-0.6208		1.9884
-0.9564	-2.9163	0.9716	0.456	0.1191	-1.7869	-0.1809		-0.5993
0.3743	0.5888	-0.4825	0.1663	0.7368	1.5136	1.7571		0.7426
0.4703	-0.7941	-0.7249	-3.1453	0.7224	1.573	1.0918		-0.7979
-1.1538	0.1885	-0.9439	-1.8404	-0.648	-3.1058	0.0744		-1.4307
0.1654	-2.7215	0.1459	2.3059	1.9116	0.1218	1.6986		-0.4776
4.3406	1.488	0.4943	-1.2172	0.3097	1.9666	0.6136		1.0331
2.7626	1.2032	1.1915	3.7022	0.5724	0.1507	-0.6158		-1.7004
2.0466	-5.0663	0.7191	3.5149	1.8974	-1.894	-0.5571		-0.2235
-4.0963	-1.48	-0.6577	0.4339	-0.1461	-0.1489	0.4163		2.0612
-3.5516	-0.6423	0.5165	0.5413	-0.6763	-2.5143	-0.2158		1.2399
4.7268	-0.9873	1.1078	1.2223	0.5375	3.2482	-1.0678		-0.2725
5.2316	0.5703	0.3508	0.4966	-0.0607	-3.2947	-0.003		1.6094
-4.7073	0.2051	0.3313	-1.89	0.9411	-0.4422	-0.0755		-1.6044

<i>Souri</i>							
b {1}	IW{1,1}					b {2}	IW{2,1}
0.1276	0.1276	-1.0494	-0.8239	-0.8739	-0.3739	-0.3742	0.1959
-0.7385	-0.7385	-0.2365	1.1193	-0.8785	-0.4952		0.3577
0.4216	0.4216	-0.9539	0.3613	0.3137	-0.5405		-1.3392
-0.5861	-0.5861	1.2921	-0.875	-0.052	0.7525		-0.8535
0.2424	0.2424	-1.7647	1.0876	-0.972	-1.7264		0.1106
-0.0264	-0.0264	-2.4694	0.7328	1.2326	-0.5417		0.238
-1.2128	-1.2128	2.4935	1.6848	1.0509	0.3075		0.3939
-0.2491	-0.2491	1.706	-0.377	0.7522	-0.6105		-0.2279
1.3477	1.3477	0.7004	0.054	0.2548	0.1238		0.4248
-0.316	-0.316	0.2553	-0.4872	-0.9892	-0.174		0.4427
0.6108	0.6108	0.0854	0.5066	0.9637	-1.2882		-0.1065
1.3519	1.3519	-1.7049	-0.4634	0.5482	-0.0312		-0.0919
0.0762	0.0762	0.6036	0.9872	-2.3506	0.765		0.0937
-2.9953	-2.9953	-0.6708	-0.9627	-0.6976	0.6826		-0.1007
-0.3276	-0.3276	2.4297	-1.0228	0.2394	-1.264		-0.058
0.1017	0.1017	1.906	1.3507	0.2022	-0.1358		0.3064
0.1427	0.1427	1.4628	-0.4411	-1.1404	0.4968		-0.1931
1.1385	1.1385	-2.1433	-1.6361	-0.19	-0.3427		0.392
1.4239	1.4239	-1.8148	0.3408	-0.3932	-0.1077		-0.0062
-2.535	-2.535	-3.3745	-0.0184	-0.2996	-0.1519		-0.2648
-2.2005	-2.2005	-1.7132	0.6247	-0.7648	0.1542		0.1676
-0.5308	-0.5308	1.1264	0.7171	1.2646	0.1264		-0.4278
-0.0208	-0.0208	-0.01	-0.0841	0.7683	-0.0632		1.084
-0.1241	-0.1241	0.3946	1.4573	0.6946	-0.2014		0.1931
-0.1375	-0.1375	0.0754	2.1866	1.056	0.1207		0.2462
0.6689	0.6689	0.9055	-1.8391	0.7023	0.5165		0.3427
-0.9189	-0.9189	0.6693	0.6203	-0.5911	0.0824		0.5694
4.2034	4.2034	-0.6604	-0.2468	-1.0488	0.5155		0.1391
0.3869	0.3869	-0.8549	-0.133	-1.3829	-0.3119		-0.7057

תוכן עניינים

1. מבוא.....	12
1.1 תאור הבעיה.....	12
1.2 יעדים.....	13
1.3 מבנה התזה.....	14
2. סקר ספרות.....	15
2.1 תעשיית שמן הזית.....	15
2.2 מודלים לחיזוי בחקלאות.....	20
2.3 רשותות נוירוניות מלאכותיות.....	23
2.4 הקטנת מימד.....	27
2.5 ראייה ממוחשבת.....	28
2.6 החזר תהודה מגנטית ברזולוציה נמוכה.....	31
3. שיטה.....	34
3.1 איסוף נתונים.....	34
3.2 ניתוח הנתונים.....	36
3.3 מודלים לחיזוי.....	37
3.4 ניתוח רגישות.....	38
4. תוצאות.....	40
4.1 ניתוח הנתונים.....	40
4.2 מודלים לחיזוי.....	61
4.3 ניתוח רגישות.....	68
4.4 מודל חיזוי אופטימלי.....	75
5. דיוון.....	79
6. סיכום ומחקר המשך.....	82
6.1 סיכום.....	82
6.2 מחקר המשך.....	83
7.ביבליוגרפיה.....	85
8. נספחים.....	91
נספה A רגרסיה רבת משתנים.....	91
נספה B רשותות נוירוניות מלאכותיות.....	91
נספה C תוכנית רשותות נוירוניות.....	112
נספה D תוכנית ניתוח סטטיסטי.....	112

113.....	נספח E נתונים גולמיים – דוגמא
114.....	נספח F ראשיתיבות
114.....	נספח G משקלים והטיות של הרשותות הטובות ביותר

תקציר

יצור שמן הזית הופך לתעשייה צומחת וברת קיימת. התכונות הבריאות המשויכות לשמן הזית יוצרים ביקושים גוברים בכל רחבי העולם. יצור עיל יותר יוכל להגדיל באופן משמעותי את הכנסתיהם של המגדלים המעורכיות ביותר מ-10 מיליארד יורו בשנה. אחת הדרכים ליעול היצור היא ע"י הגדלת תפוקת השמן לזרת ליחידת קרקע. שיפור כזה יושג ע"י מציאת זמן המסיק האופטימלי של העצים במטע. מחקר זה מתמקד בפיתוח מודלים לקביעת מועד המסיק האופטימלי של זיתים ע"י מיקסום תכולת השמן. כמות השמן בזיתים מזנים "סורי" ו"פיקואל" נקבעה על פי תכונת שהתקבלו מתוך ניתוח תמנותיהם בעזרת אלגוריתמים שפותחו ע"י ליין (2002).

שמונה דגימות של ארבע מאות זיתים נקטו מידיו שבוע לאורך עונת הבשלה. הזיתים צולמו משני צידיהם ע"י מצלמה דיגיטלית צבעונית, ותכולת השמן בהם נקבע ע"י מכשיר למדידת החזר תהודה מגנטית ברזולוציה גבוהה (LR-NMR). 29 פרמטרים הנוגרים מוגדל, צורה, צבע ומרקם הזיתים הופקו מתוך תמנות הזיתים באמצעות פרוצדורות ב- Matlab. המתאם הפנימי בין הפרמטרים שהופקו ובין תכולת השמן חושב, וניתוה גורמים (FA) שמש ליצירת סט גורמים חדש ובלתי מחווק. מתוך ניתוח הגורמים נמצא שבשני הזנים הפרמטרים הקשורים למרקם הזית הינם באותה מקום בשני בהשפעתם על תכולת השמן ואילו פרמטרים הקשורים בצורת הזית הינם בעלי ההשפעה הנמוכה ביותר על תכולת השמן.

שני מודלים שונים לקביעת כמות השמן בזית רגרסיה ליניארית ועל בסיס רשותות עצביות. המודלים התקבלו ע"י שימוש בסט אימון שנבחר באופן אקראי מתוך סט הפרמטרים המקורי ומתוך סט הגורמים החדש. לאחר מכן המודלים נבחנו בעזרת שאר הנתונים על מנת להעריך את דיוקם עם נתונים חדשים.

רגישות המודל לשינויים ביחס בין סט האימון לסט הבדיקה, שינוי בטופולוגיה הרשת ושינויים בפונקציות המעבר נבחנה, והמודל הטוב ביותר, שהיא שונה בין שני הזנים נבחר. המודל המבוסס על רשותות עצביות היה מדויק יותר מהמודל המבוסס על הרגרסיה הליניארית והציג רמת מתאם ליניארית של 0.81 ו- 0.87 עם כמות השמן של זיתי הפיקואל והסורי בהתאם.

**אוניברסיטת בן גוריון בנגב
הפקולטה למדעי ההנדסה
המחלקה להנדסת תעשייה וניהול**

מודלים לחיזוי כמות זמן זית מבוססי ראייה ממוחשבת

МОГЕШ ЧАЛК МДРИШОТ ХОВОХА ЛКВЛТА ТОАР МАСТЕР ЛМДУИМ БАНДОСТ ТУШИИХ

מאת: תומר רם

יוני 2009

מנחים: פרופ' יעל אידן, פרופ' זאב וייסמן

תאריך	מחבר
תאריך	מנחה
תאריך	מנחה
תאריך	יושב ראש ועדת הוראה

**אוניברסיטת בן גוריון בנגב
הפקולטה למדעי ההנדסה
המחלקה להנדסת תעשייה וניהול**

מודלים לחיזוי כמות שמן זית מבוססי ראייה ממוחשבת

מוגש כחלק מדרישות החובה לקבלת תואר מאסטר למדעים בהנדסת תעשייה

מאת: תומר רם

יוני 2009

מנחים: פרופ' יעל אידן, פרופ' זאב וייסמן